

QFT as a set of ODEs: higher dimensions

Fabiana De Cesare, Manuel Loparco

*Istituto Nazionale di Fisica Nucleare, Sezione di Torino, and
Department of Physics, University of Turin,
Via P. Giuria 1, 10125, Turin, Italy*

E-mail: fabiana.decesare@unito.it, manuel.loparco@gmail.com

ABSTRACT: Correlation functions of local operators in Quantum Field Theory (QFT) in Anti-de Sitter space (AdS) are completely fixed by the QFT data: the set of scaling dimensions Δ_i and OPE coefficients C_{ijk} of the boundary operators, and the bulk-boundary (BOE) coefficients $b_i^{\hat{\Phi}}$ encoding how bulk fields decompose into boundary operators. In this work, we generalize the ordinary differential equations (ODEs) that govern the variation of the QFT data under a bulk relevant deformation, originally derived for AdS₂ [1], to the cases of AdS₃ and AdS₄. We demonstrate that these flow equations natively capture the mechanism of merger-annihilation when a boundary operator hits marginality, as well as level repulsion when different Δ_i 's approach each other. Furthermore, we address the practical implementation of the framework: we propose substituting the ODE for the OPE coefficients with the crossing equation for greater efficiency, and we observe that Padé approximants dramatically improve the convergence of the sums over boundary operators, at least in free theories. Altogether, these advances lay the groundwork for the future application of the flow equations to the study of strongly coupled QFTs in AdS and their flat space limits.

Contents

1	Introduction	2
2	Preliminaries	6
2.1	Geometry	6
2.2	Operator expansions	9
2.3	Conformal blocks	13
2.4	Local blocks	18
3	Derivation of the flow equations	20
3.1	Flow of scaling dimensions	20
3.2	Flow of BOE coefficients	26
3.3	Closing the system with crossing	30
3.4	Convergence of sums in the flow equations	31
4	Checks in free theories	33
4.1	Flow of scaling dimensions	33
4.2	Flow of BOE coefficients	37
4.3	OPE coefficients from crossing	38
5	The (un)reasonable effectiveness of Padé	42
5.1	Quick intro to Padé approximants	42
5.2	Padé for exponential convergence in free theory	43
5.3	Proposal for Padé in interacting theories	46
6	Merger-annihilation and level repulsion	47
6.1	Merger-annihilation	47
6.2	Level repulsion	49
7	Discussion	52
7.1	Beyond our assumptions	53
7.2	Flow equations with no coupling	55
7.3	Open questions	56
7.4	Possible applications	57
A	Derivation of blocks	58
A.1	Bulk-bulk	58
A.2	Bulk-boundary-boundary	59
A.3	Bulk-bulk-boundary	62

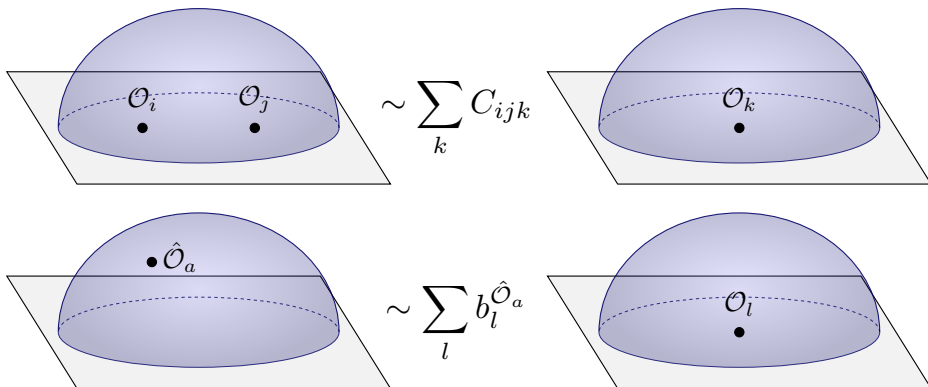
B	Details about the derivation of the flow equations	64
B.1	Flow of scaling dimensions	64
B.2	Flow of BOE coefficients	66
C	Some properties of $\frac{dC_{ijk}}{d\lambda}$	69
D	Universal asymptotics of QFT data	72
D.1	Asymptotics of BOE coefficients	73
D.2	Asymptotics of OPE coefficients	75
E	QFT data of free scalar and free tensor	77
E.1	Free scalar theory	77
E.2	Free tensor theory	78

1 Introduction

Many phenomena of Nature are believed to be described by strongly coupled quantum field theories (QFTs). Despite this, non-perturbative methods to compute observables in such theories remain scarce. The lattice approach [2], based on the discretization of spacetime, is the method that has yielded the most results, regarding for example the spectrum of many strongly coupled QFTs. However, it suffers from fundamental shortcomings, such as the sign problem and the inability to capture real-time dynamics. Hamiltonian truncation [3] and the numerical S-matrix bootstrap [4] are two approaches that work directly in the continuum and can capture Lorentzian dynamics, but they come with their own limitations: Hamiltonian truncation often exhibits slow convergence with the UV cutoff, and the 2-to-2 S-matrix bootstrap primarily yields bounds on Wilson coefficients rather than precise spectra¹. In the absence of supersymmetry, conformal symmetry, integrability, or a strong-weak holographic duality, we are not left with many alternatives.

In [1], a program was initiated towards a new non-perturbative framework in the continuum. Let us describe the basic idea².

Consider placing a QFT on a $d + 1$ dimensional rigid hyperboloid, which we will refer to as Anti-de Sitter (AdS) space. The isometries of AdS and its conformal boundary make it an ideal playground for studying strongly coupled QFTs [15–24]. Crucially, these isometries imply the existence of a map between bulk QFT states and operators living on the boundary. These boundary operators are classified by their scaling dimensions Δ_i and their representations ρ_i under $SO(d)$ (the group of rotations preserving the boundary)³. Furthermore, the AdS isometries guarantee the existence of two types of convergent expansions: the operator product expansion (OPE) among boundary operators, and the boundary operator expansion (BOE), where a bulk operator is expanded in terms of boundary operators. Pictorially:



where the light gray surface represents the boundary of AdS and the half-spheres are foliations of AdS in radial quantization (position dependence and the sum over descendants

¹However, recently the S-matrix bootstrap has been successfully utilized as a tool to compute observables in QCD [5–12].

²The original idea presented in [1] was itself inspired by the work on ODEs for the CFT data of 1D conformal manifolds by Behan [13] and the study of the OPE in QFT by Hollands and Wald [14].

³Boundary operators may carry additional quantum numbers in the presence of global symmetries.

are suppressed). When operators carry non-trivial representations of $SO(d)$, there can be multiple OPE coefficients $C_{ijk}^{(n)}$ for a given triplet of boundary operators, and multiple BOE coefficients $b_l^{\hat{\mathcal{O}}_a(n)}$ for a given bulk-boundary pair. The OPE and BOE coefficients satisfy various non-trivial constraints, such as the crossing equations and the BOE locality sum rules [25–28].

Thanks to these convergent expansions, any correlation function of local operators in the bulk or on the boundary can be iteratively decomposed into lower-point correlators. Ultimately, all local observables are entirely determined by the set

$$\{\Delta_i, \rho_i, C_{ijk}^{(n)}, b_l^{\hat{\mathcal{O}}_a(n)}\} \quad (1.1)$$

which we refer to as the QFT data.

QFTs in AdS come in continuous families, parametrized by dimensionless variables λ_i constructed from the dimensionful couplings $\bar{\lambda}_i$ of the relevant bulk operators $\hat{\Phi}_i$ in the action and the AdS radius R , such that $\lambda_i \equiv \bar{\lambda}_i R^{d+1-\Delta_{\hat{\Phi}_i}^{\text{UV}}}$, where $\Delta_{\hat{\Phi}_i}^{\text{UV}}$ is the dimension of $\hat{\Phi}_i$ in the UV CFT. For simplicity we will work with theories deformed by a single bulk relevant scalar operator $\hat{\Phi}$, and we will work in units where $R = 1$. Under an infinitesimal variation of λ , the action changes as

$$S(\lambda + \delta\lambda) = S(\lambda) + \delta\lambda \int_{\text{AdS}} dX \hat{\Phi}(X), \quad (1.2)$$

and consequently all QFT data vary continuously with λ . In [1], computing the universal effect of the deformation (1.2) on the QFT data in AdS_2 led to the derivation of an infinite set of coupled ODEs governing their evolution.

In this paper, we generalize this framework to higher dimensions, motivated by the presence of many interesting strongly coupled QFTs in more than two dimensions. In AdS_{d+1} , our generalized ODEs take the form:

$$\begin{aligned} \frac{d\Delta_i}{d\lambda} &= \sum_l b_l^{\hat{\Phi}} C_{lii}^{(0)} \mathcal{I}(\Delta_l), \\ \frac{db_i^{\hat{\Phi}}}{d\lambda} &= \sum_l \sum_j b_l^{\hat{\Phi}} b_j^{\hat{\Phi}} C_{lij} \mathcal{J}_{\Delta_i}(\Delta_l, \Delta_j), \end{aligned} \quad (1.3)$$

where \mathcal{I} and \mathcal{J} are regulated integrals of conformal blocks, with explicit forms (3.21) and (3.46), Δ_i can be the scaling dimension of any boundary operator carrying a traceless symmetric representation of $SO(d)$, and $C_{lii}^{(0)}$ is the $n = 0$ OPE coefficient in the basis defined in (2.36)⁴. Crucially, the sums run over all scalar boundary operators excluding the identity⁵.

We call these the *flow equations*. Their practical applicability will rely heavily on the efficient numerical convergence of the sums in (1.3). When utilizing standard conformal

⁴When \mathcal{O}_i is a scalar, there is only one OPE coefficient and we omit the superscript.

⁵Excluding the identity is equivalent to subtracting the vacuum expectation value of the deforming operator $\langle \hat{\Phi} \rangle$ at each infinitesimal increment of λ . We are effectively choosing a scheme where $b_1^{\hat{\Phi}}(\lambda) \equiv 0$.

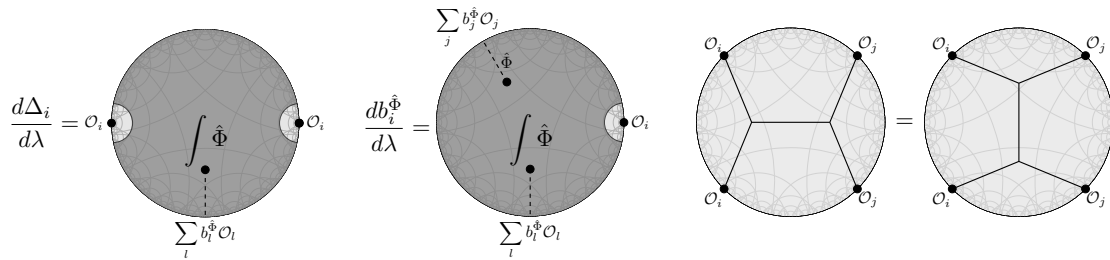


Figure 1. Pictorial representation of the flow equations. In this work, the crossing equations take the place of the ODE involving the derivative of the OPE coefficients.

blocks, the sums do not generically converge. One known resolution is to instead use local blocks [25–27], a basis which possesses the physical analytic structure of a correlator block by block, altering the expressions of \mathcal{I} and \mathcal{J} to (3.34) and (3.51) respectively. The updated sums are then absolutely convergent. In this work, we introduce an alternative method to render the sums of standard blocks convergent by employing Padé approximants. We discuss this in section 5, where we show that the rate of convergence is drastically improved with respect to the local blocks method, at least in free theory.

In AdS_{d+1} with $d+1 < 5$, the flow equations close when supplemented with the crossing equations for a four-point function of the form $\langle \mathcal{O}_i \mathcal{O}_i \mathcal{O}_j \mathcal{O}_j \rangle$ ⁶. In AdS_3 , there is a single OPE coefficient for a triplet of boundary operators, so the crossing equations read (the notation is introduced in section 3.3).

$$\sum_m \left(C_{mij}^2 \mathcal{F}_{i,j,m}^t(\eta, \bar{\eta}) - C_{im} C_{mjj} \mathcal{F}_{i,j,m}^s(\eta, \bar{\eta}) \right) = \mathcal{F}_{i,j,1}^s(\eta, \bar{\eta}). \quad (1.4)$$

In AdS_4 , instead, considering a scalar \mathcal{O}_i and a traceless symmetric tensor \mathcal{O}_j , crossing reads

$$\sum_m \left(\sum_{a,b} C_{mij}^{(a)} C_{mij}^{(b)} \mathcal{F}_{i,j,m;I}^{t(a,b)}(v, u) - C_{mii} \sum_c C_{mjj}^{(c)} \mathcal{F}_{i,j,m;I}^{s(c)}(u, v) \right) = \mathcal{F}_{i,j,1;I}^{s(c)}(u, v). \quad (1.5)$$

We propose to use crossing rather than the generalization of the ODE involving $\frac{dC_{ijk}}{d\lambda}$ in [1] because the integrated blocks \mathcal{K} entering in that equation are only known through integral representations which are expensive to evaluate numerically, an issue that scales poorly in higher dimensions⁷. Notice that solving crossing in this context is instead a relatively cheap numerical problem, in particular it is simpler than in the context of the conformal bootstrap: the spectrum, obtained by integrating (1.3) over an infinitesimal $\delta\lambda$, is an input, and the OPE coefficients are the only unknowns.

Let us now explain in what sense equations (1.3) and (1.5) can provide a new non-perturbative method to extract observables of strongly coupled QFTs.

⁶In AdS_{d+1} with $d > 4$ mixed symmetry representations appear in the OPE expansion, hence one would have to derive the ODE for $\frac{d\Delta_i}{d\lambda}$ for operators carrying such representations in order to close the equations.

⁷We nevertheless discuss some properties of $\frac{dC_{ijk}}{d\lambda}$ in higher dimensions in appendix C.

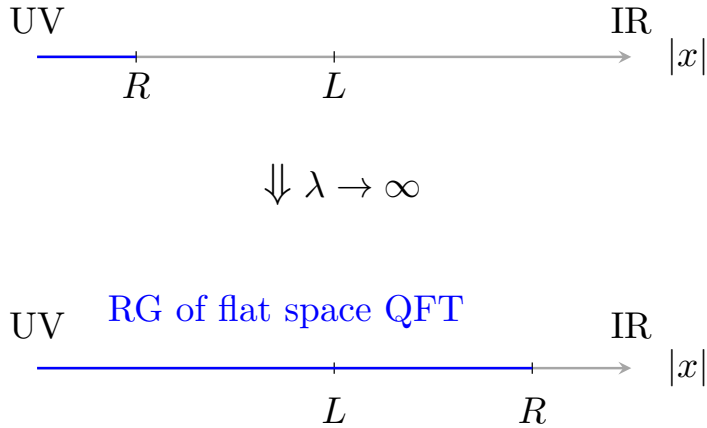


Figure 2. As the dimensionless coupling $\lambda \equiv \bar{\lambda} R^{d+1-\Delta_{\Phi}^{\text{UV}}}$ grows, more of the flat space RG flow is revealed and imprinted on the QFT data. Here L is a characteristic length scale of the QFT, R is the AdS radius, and $|x|$ is the length scale at which we probe the theory.

Consider a QFT in AdS defined as a relevant deformation of a conformal field theory (CFT) with conformal boundary conditions:

$$S_{\text{QFT}}(\lambda) = S_{\text{CFT}} + \lambda \int_{\text{AdS}} \hat{\Phi}(X). \quad (1.6)$$

If the starting CFT is solvable (for example it is a free theory, or a 2D minimal model) its QFT data is known, or can be computed algorithmically. Then, this data furnishes the initial conditions of the ODEs. Because the coupling is measured in units of the AdS radius, increasing λ by integrating the ODEs effectively evolves the data toward the flat space regime. When $\lambda \gg 1$, the radius of AdS is much larger than the characteristic length scales of the theory, and the QFT data becomes sensitive to the flat space renormalization group (RG) flow (see figure 2 for a pictorial representation).

In this regime, the ratios of the lightest scaling dimensions are expected to asymptote to the mass ratios of the stable particles in the flat space QFT:

$$\lim_{\lambda \rightarrow \infty} \frac{\Delta_i(\lambda)}{\Delta_1(\lambda)} = \frac{m_i}{m_1} \quad (1.7)$$

and specific combinations of OPE coefficients are expected to yield the flat space S-matrix [29–38]. Thus, finding the asymptotic solutions of the ODEs resolves the spectrum and dynamics of the flat space QFT.

We note that the concrete applicability of this non-perturbative method will rely on the development of efficient numerical algorithms that can implement the ODEs for interacting theories, while keeping the errors originating from the truncation of the sums in (1.3) and (1.5) under control. We envision that to be the main next step to be taken by this program.

Outline We begin with section 2, where we review the geometry of AdS and the classification of boundary operators in 3D and 4D. Then, we present the explicit form of standard

conformal blocks and local blocks for bulk-boundary-boundary and bulk-bulk-boundary correlation functions, which we will need to derive the flow equations (1.3).

In section 3 we present the derivation of the flow equations (1.3), which require the careful treating of divergences and the renormalization of boundary operators.

In section 4 we present checks of the flow equations in free theories, involving both scalar and spinning operators. We compare the performance of regular conformal blocks, local blocks and Padé approximants of both and find that Padé approximants of standard blocks converge fastest. We also present some rudimentary implementation of the crossing equations.

In section 5 we discuss the details of the Padé procedure, we explain why it works so well in free theory and compare analytic estimates of the error from theorems by Stahl with the errors observed in 4 and find agreement. We then discuss possible generalizations to the interacting case.

In section 6 we show that the mechanisms of level repulsion and merger-annihilation are implied by the flow equations, and derive some detailed features of these phenomena.

In section 7 we discuss how to move beyond some of our assumptions and outline some future directions and open questions.

Mathematica notebook We attach to our ArXiv submission a Mathematica notebook where checks of the flow equations and the implementation of crossing from section 4 can be reproduced.

Summary of assumptions Throughout most of this paper we assume we are working with a unitary and local QFT in AdS_{d+1} with irrelevant boundary operators $\Delta_i > d$ and one relevant deformation in the bulk with UV scaling dimension $\Delta_{\hat{\Phi}}^{\text{UV}} < d + 1$. We will assume the theory is parity invariant unless stated otherwise, and we will assume the convergence of the OPE and BOE and the absence of degeneracies. Finally, we assume that in the UV CFT there is no scalar $\hat{\mathcal{O}}$ in the OPE of $\hat{\Phi} \times \hat{\Phi}$ with $\Delta_{\hat{\mathcal{O}}}^{\text{UV}} < 2\Delta_{\hat{\Phi}}^{\text{UV}} - d - 1$. We will move past some of these assumptions in section 7.

2 Preliminaries

2.1 Geometry

We define $d + 1$ dimensional Euclidean Anti-de Sitter space (for brevity AdS_{d+1}) through its embedding in $\mathbb{R}^{1,d+1}$. Points in embedding space belonging to AdS will be denoted as $X^A = (X^0, X^a, X^{d+1}) \in \mathbb{R}^{1,d+1}$ where $a = 1, \dots, d$, and they satisfy

$$-(X^0)^2 + \delta_{ab}X^aX^b + (X^{d+1})^2 = -R^2, \quad X^0 > 0, \quad (2.1)$$

where $X^0 > 0$ restricts us to one of the two branches of the hyperboloid.

Points at the conformal boundary of AdS are embedding space lightrays, which we denote as $P^A \in \mathbb{R}^{1,d+1}$, satisfying

$$-(P^0)^2 + \delta_{ab}P^aP^b + (P^{d+1})^2 = 0, \quad P^0 > 0, \quad (2.2)$$

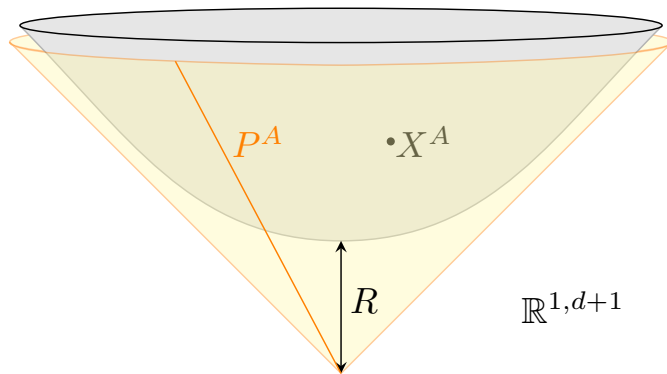


Figure 3. A representation of AdS (in gray) and the lightcone (in yellow) in embedding space $\mathbb{R}^{1,d+1}$. Points in the bulk of AdS are denoted by X^A . Lightrays, which are in one-to-one correspondence with points on the boundary of AdS, are indicated as P^A . R is the radius of AdS. We slightly vertically displaced AdS from the lightcone for visualization purposes.

with the identification $P^A \sim \lambda P^A$ with $\lambda > 0$. The group of isometries preserving one branch of the hyperboloid is $SO^+(1, d+1)$, and it acts linearly on embedding space vectors. This implies in particular that all invariant cross ratios can be constructed from contractions of vectors P^A and X^A with the embedding metric $\eta_{AB} = \text{diag}(-1, 1, \dots, 1)$ and with the Levi-Civita symbol $\epsilon_{A_1 \dots A_{d+2}}$. We give a pictorial representation of the embedding space setup in figure 3.

2.1.1 Poincaré half-plane coordinates

We will frequently use Poincaré half-plane coordinates to chart AdS:

$$\begin{aligned} X^0 &= \frac{1 + z^2 + \mathbf{x}^2}{2z}, & X^a &= \frac{\mathbf{x}^a}{z}, & X^{d+1} &= \frac{1 - z^2 - \mathbf{x}^2}{2z}, \\ P^0 &= \frac{1 + \mathbf{x}^2}{2}, & P^a &= \mathbf{x}^a, & P^{d+1} &= \frac{1 - \mathbf{x}^2}{2}. \end{aligned} \quad (2.3)$$

where we set $R = 1$, as will be done for most of this paper. The metric then reads

$$ds^2 = \frac{dz^2 + d\mathbf{x}^2}{z^2}, \quad z > 0, \quad \mathbf{x}^i \in \mathbb{R}^d, \quad (2.4)$$

where $z \rightarrow 0$ is the limit to the conformal boundary.

2.1.2 Poincaré ball coordinates

Alternatively, AdS can be represented as a ball. We can find the Poincaré ball coordinates by constructing the stereographic projection from $X^A = (-1, \mathbf{0}, 0)$

$$\mathbf{y}^a \equiv \frac{X^a}{1 + X^0}, \quad u \equiv \frac{X^{d+1}}{1 + X^0}. \quad (2.5)$$

The hyperboloid constraint (2.1) then forces $\mathbf{y}^2 + u^2 < 1$, thus defining a $d+1$ dimensional ball B^{d+1} , with metric

$$ds^2 = \frac{4(du^2 + d\mathbf{y}^2)}{(1 - u^2 - \mathbf{y}^2)^2}, \quad \mathbf{y}^2 + u^2 < 1. \quad (2.6)$$

2.1.3 Boundary operators

The geometry of AdS also dictates how we should organize states in the Hilbert space of our QFT, and in turn the way in which we should organize boundary operators. The two cases of interest to us, AdS₃ and AdS₄, benefit from a separate treatment. The discussion for AdS₄ straightforwardly generalizes to traceless symmetric tensors in higher dimensions.

AdS₃ The group of isometries in the 3D case is $SO(3,1)$. Its associated Lie algebra, when complexified, decomposes as follows

$$\mathfrak{so}(1,3)_{\mathbb{C}} \cong \mathfrak{sl}(2, \mathbb{C}) \oplus \mathfrak{sl}(2, \mathbb{C}) \quad (2.7)$$

To make use of this fact, it is convenient to switch to complex coordinates

$$\mathbf{z} = \mathbf{x}^1 + i\mathbf{x}^2, \quad \bar{\mathbf{z}} = \mathbf{x}^1 - i\mathbf{x}^2, \quad (2.8)$$

so that the associated metric becomes

$$ds^2 = \frac{dz^2 + dzd\bar{z}}{z^2}. \quad (2.9)$$

Each boundary operator is then labeled by the eigenvalues h and \bar{h} of the two Cartans associated to the two copies of $\mathfrak{sl}(2, \mathbb{C})$, respectively L_0 and \bar{L}_0 , realized as differential operators as

$$L_0 = -z\partial_z, \quad \bar{L}_0 = -\bar{z}\partial_{\bar{z}}. \quad (2.10)$$

As is usually done, we will call h and \bar{h} the holomorphic and antiholomorphic weights. They are related to the scaling dimension Δ and the $SO(2)$ spin J as

$$h \equiv \frac{\Delta + J}{2}, \quad \bar{h} \equiv \frac{\Delta - J}{2}. \quad (2.11)$$

We will denote an operator with weights (h_i, \bar{h}_i) as $\mathcal{O}_i(\mathbf{z}, \bar{\mathbf{z}})$. It behaves under scalings and rotations as

$$\begin{aligned} \mathcal{O}_i(\lambda\mathbf{z}, \lambda\bar{\mathbf{z}}) &= \lambda^{-h_i - \bar{h}_i} \mathcal{O}_i(\mathbf{z}, \bar{\mathbf{z}}), \\ \mathcal{O}_i(e^{i\theta}\mathbf{z}, e^{-i\theta}\bar{\mathbf{z}}) &= e^{-i\theta(h_i - \bar{h}_i)} \mathcal{O}_i(\mathbf{z}, \bar{\mathbf{z}}). \end{aligned} \quad (2.12)$$

To relate these operators to their counterparts in cartesian coordinates, it suffices to know that

$$\mathcal{O}_i(\mathbf{z}, \bar{\mathbf{z}}) = \mathcal{O}_i^{\overbrace{z z \dots z}^{J_i}}(\mathbf{z}, \bar{\mathbf{z}}). \quad (2.13)$$

One can then change coordinates through (2.8). Notice that in complex coordinates it is manifest that $\mathcal{O}_i^{z z \dots z}$ and $\mathcal{O}_i^{\bar{z} \bar{z} \dots \bar{z}}$ are the only two independent components of an irreducible tensor: every mixed component would be proportional to a trace.

The action of parity on the coordinates is

$$(z, \mathbf{x}^1, \mathbf{x}^2) \xrightarrow{\mathcal{P}} (z, \mathbf{x}^1, -\mathbf{x}^2) \quad (2.14)$$

thus sending $\mathbf{z} \leftrightarrow \bar{\mathbf{z}}$. On operators, this has the effect of exchanging the holomorphic weights $(h_i, \bar{h}_i) \rightarrow (\bar{h}_i, h_i)$. We will denote the operator with weights (\bar{h}_i, h_i) as $\mathcal{O}_{\bar{i}}(\mathbf{z}, \bar{\mathbf{z}})$.

AdS₄ In four dimensions, boundary operators are organized into irreducible representations of $SO(4, 1)$, which we classify by the scaling dimension Δ and the $SO(3)$ spin J . We will thus consider traceless symmetric tensors with J indices, which we will represent in the usual index-free embedding formalism, by contracting the operator's indices with null vectors $Z^A \in \mathbb{C}^5$

$$\mathcal{O}_i^{(J)}(P, Z) \equiv Z_{A_1} \cdots Z_{A_J} \mathcal{O}_i^{A_1 \cdots A_J}(P). \quad (2.15)$$

In this form, scaling dimension and spin are encoded in the behavior of the operator under rescalings of P^A and Z^A

$$\begin{aligned} \mathcal{O}_i^{(J)}(\lambda P, Z) &= \lambda^{-\Delta_i} \mathcal{O}_i^{(J)}(P, Z), \\ \mathcal{O}_i^{(J)}(P, \alpha Z) &= \alpha^J \mathcal{O}_i^{(J)}(P, Z). \end{aligned} \quad (2.16)$$

The operator with indices can be retrieved through the action of a differential operator

$$\mathcal{O}_i^{A_1 \cdots A_J}(P) = \frac{1}{(\frac{1}{2})_J J!} D_{Z_{A_1}} \cdots D_{Z_{A_J}} \mathcal{O}_i^{(J)}(P, Z) \quad (2.17)$$

where $(a)_n \equiv \frac{\Gamma(a+n)}{\Gamma(a)}$ is the Pochhammer symbol and

$$D_{Z_A} \equiv \frac{1}{2} \partial_{Z_A} + (Z \cdot \partial_Z) \partial_{Z_A} - \frac{1}{2} Z_A (\partial_Z \cdot \partial_Z). \quad (2.18)$$

Sometimes it will be useful to consider the pullback to local coordinates

$$\mathcal{O}_i^{a_1 \cdots a_J}(\mathbf{x}) = \frac{\partial P_{A_1}}{\partial \mathbf{x}_{a_1}} \cdots \frac{\partial P_{A_J}}{\partial \mathbf{x}_{a_J}} \mathcal{O}_i^{A_1 \cdots A_J}(P), \quad (2.19)$$

and we will at times employ complex auxiliary null vectors $\mathbf{z}^a \in \mathbb{C}^3$ to contract indices in local coordinates

$$\mathcal{O}_i^{(J)}(\mathbf{x}, \mathbf{z}) \equiv \mathbf{z}_{a_1} \cdots \mathbf{z}_{a_J} \mathcal{O}_i^{a_1 \cdots a_J}(\mathbf{x}) \quad (2.20)$$

The explicit relation between Z^A and \mathbf{z}^a is

$$Z^0 = \mathbf{x} \cdot \mathbf{z}, \quad Z^a = \mathbf{z}^a, \quad Z^4 = -\mathbf{x} \cdot \mathbf{z}. \quad (2.21)$$

Sometimes we will need to strip off indices directly in local coordinates. That is done through the action of the differential operators

$$D_{\mathbf{z}_a} \equiv \frac{1}{2} \partial_{\mathbf{z}_a} + (Z \cdot \partial_Z) \partial_{\mathbf{z}_a} - \frac{1}{2} \mathbf{z}_a (\partial_Z \cdot \partial_Z). \quad (2.22)$$

2.2 Operator expansions

The main advantage of placing a QFT on AdS is the presence of a boundary on which the group of isometries acts like the conformal group. Moreover, in radial quantization, symmetries map the foliation surfaces into one another. On the conformal boundary, the edges of the foliation surfaces appear as spheres, which under dilatations can be shrunk down to points (see figure 4 for a pictorial representation). These facts ensure the existence of a map between states defined on the radial foliation surfaces and local operators on the boundary,

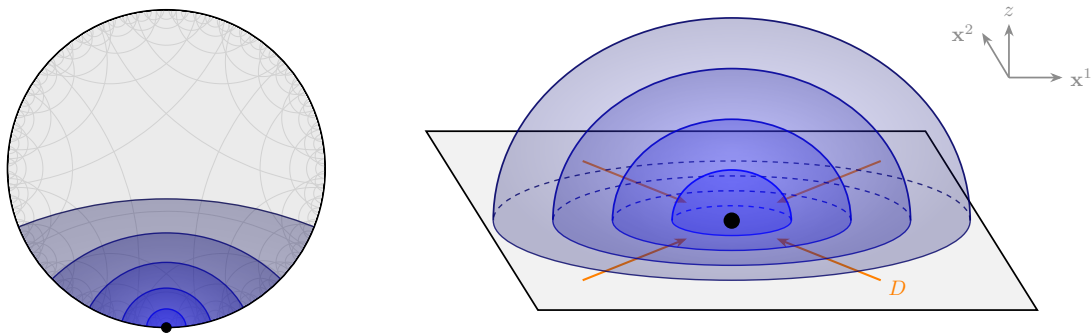


Figure 4. Radial quantization slices of AdS, represented on the left in the ball coordinates (2.6) and on the right in half-plane coordinates (2.3). The AdS isometries relate different slices to one another. In half-plane coordinates, it is clear that boundary dilatations relate to one another the spheres defined by the intersection between the slices and the boundary.

which themselves can be classified in terms of Unitary Irreducible Representations (UIRs) of the conformal group.

Here we will discuss two immediate consequences of the state-operator map for QFTs in AdS: the expansion of local bulk fields into a sum of local boundary operators – the boundary operator expansion, or BOE – and the expansion of a product of two boundary operators into a sum of boundary operators – the operator product expansion, or OPE. First, let us discuss how we normalize boundary operators.

2.2.1 Two-point functions and normalizations

To begin, we need to define the normalization of our boundary operators. This is done by choosing a convention for the numerical factor appearing in the two-point function.

AdS₃ We choose to normalize AdS₃ boundary operators as follows⁸

$$\langle \mathcal{O}_i(\mathbf{z}_1, \bar{\mathbf{z}}_1) \mathcal{O}_j(\mathbf{z}_2, \bar{\mathbf{z}}_2) \rangle = \frac{\delta_{h_i, h_j} \delta_{\bar{h}_i, \bar{h}_j}}{\mathbf{z}_{12}^{2h} \bar{\mathbf{z}}_{12}^{2\bar{h}}} \quad (2.24)$$

where, as in the rest of the paper, we use $\mathbf{z}_{ij} \equiv \mathbf{z}_i - \mathbf{z}_j$. Equivalently, we can write

$$\langle \mathcal{O}_i(\mathbf{z}_1, \bar{\mathbf{z}}_1) \mathcal{O}_j(\mathbf{z}_2, \bar{\mathbf{z}}_2) \rangle = \frac{\delta_{\Delta_i, \Delta_j} \delta_{J_i, J_j}}{|\mathbf{z}_{12}|^{2\Delta}} \left(\frac{\mathbf{z}_{12}}{\bar{\mathbf{z}}_{12}} \right)^{J_i}. \quad (2.25)$$

From the two-point function it is immediate to see that complex conjugation relates an operator with holomorphic weights (h, \bar{h}) to one with weights (\bar{h}, h) .

⁸Notice that in this normalization, the two-point function in cartesian coordinates reads

$$\langle \mathcal{O}_i^{a_1 \dots a_J}(\mathbf{x}_1) \mathcal{O}_j^{b_1 \dots b_J}(\mathbf{x}_2) \rangle = \delta_{\Delta_i, \Delta_j} \frac{1}{(-2)^{J_i}} \frac{\mathcal{I}^{a_1 \dots a_J, b_1 \dots b_J}(\mathbf{x}_{12})}{(\mathbf{x}_{12}^2)^{\Delta_i}}, \quad (2.23)$$

where $\mathbf{x}^2 \equiv \delta_{ab} \mathbf{x}^a \mathbf{x}^b$ and $\mathcal{I}^{a_1 \dots a_J, b_1 \dots b_J}(\mathbf{x})$ is the symmetric traceless tensor structure constructed from the product of J fundamental inversion tensors $I^{ab}(\mathbf{x}) = \delta^{ab} - 2 \frac{\mathbf{x}^a \mathbf{x}^b}{\mathbf{x}^2}$. To map this to complex coordinates, we use $I^{zz}(\mathbf{z}, \bar{\mathbf{z}}) = -2\mathbf{z}/\bar{\mathbf{z}}$, $I^{\bar{z}\bar{z}}(\mathbf{z}, \bar{\mathbf{z}}) = -2\bar{\mathbf{z}}/\mathbf{z}$, and that mixed components vanish.

AdS₄ In four dimensions, we adopt the index-free embedding formalism and normalize boundary two-point functions as

$$\langle \mathcal{O}_i^{(J_i)}(P_1, Z_1) \mathcal{O}_j^{(J_j)}(P_2, Z_2) \rangle = \delta_{\Delta_i, \Delta_j} \delta_{J_i, J_j} \frac{H_{1,2}^{J_i}}{P_{12}^{\Delta_i + J_i}}, \quad P_{ij} \equiv -2P_i \cdot P_j \quad (2.26)$$

where $H_{1,2}$ is the invariant structure from [39]

$$H_{i,j} \equiv (Z_i \cdot Z_j)(P_i \cdot P_j) - (Z_i \cdot P_j)(Z_j \cdot P_i). \quad (2.27)$$

Equation (2.26) is also the form of two-point functions of symmetric traceless tensors in higher dimensions.

2.2.2 Operator Product Expansion and three-point functions

A powerful property of CFTs is the existence of a convergent and associative OPE. This is the fundamental fact that allows for the description of all local observables in terms of the CFT data, and it also holds for boundary operators in the context of QFT in AdS.

For two scalar operators, when the distance between their insertion points is smaller than their distance to any other operator insertion, the OPE takes the form

$$\mathcal{O}_i(\mathbf{x}_1) \mathcal{O}_j(\mathbf{x}_2) = \sum_k \frac{C_{ijk}}{(\mathbf{x}_{12}^2)^{\frac{\Delta_{ijk}}{2}}} \mathcal{C}_{a_1 \dots a_{J_k}}(\mathbf{x}_{12}, \partial_2) \mathcal{O}_k^{a_1 \dots a_{J_k}}(\mathbf{x}_2) \quad (2.28)$$

where C_{ijk} are called OPE coefficients, and the sum over descendants, encoded in the differential operator \mathcal{C} , is fully fixed by symmetry.

As a consequence of the OPE, three-point functions of primary scalar operators take the universal form

$$\langle \mathcal{O}_i(\mathbf{x}_1) \mathcal{O}_j(\mathbf{x}_2) \mathcal{O}_k(\mathbf{x}_3) \rangle = \frac{C_{ijk}}{(\mathbf{x}_{12}^2)^{\frac{\Delta_{ijk}}{2}} (\mathbf{x}_{13}^2)^{\frac{\Delta_{ikj}}{2}} (\mathbf{x}_{23}^2)^{\frac{\Delta_{jki}}{2}}}, \quad (2.29)$$

where unitarity fixes $C_{ijk} \in \mathbb{R}$ and we are using the notation $\Delta_{ijk} \equiv \Delta_i + \Delta_j - \Delta_k$.

For operators carrying spin, a separate treatment of AdS₃ and AdS₄ is in order.

AdS₃ If we classify boundary operators in AdS₃ by their holomorphic weights, each three-point function still depends on a single OPE coefficient [40]

$$\begin{aligned} \langle \mathcal{O}_i(z_1, \bar{z}_1) \mathcal{O}_j(z_2, \bar{z}_2) \mathcal{O}_k(z_3, \bar{z}_3) \rangle &= \frac{C_{ijk}}{z_{12}^{h_{ijk}} \bar{z}_{12}^{\bar{h}_{ijk}} z_{13}^{h_{ikj}} \bar{z}_{13}^{\bar{h}_{ikj}} z_{23}^{h_{jki}} \bar{z}_{23}^{\bar{h}_{jki}}} \\ &= \frac{C_{ijk}}{|z_{12}|^{\Delta_{ijk}} |z_{13}|^{\Delta_{ikj}} |z_{23}|^{\Delta_{jki}}} \left(\frac{z_{12}}{\bar{z}_{12}} \right)^{\frac{J_{ijk}}{2}} \left(\frac{z_{13}}{\bar{z}_{13}} \right)^{\frac{J_{ikj}}{2}} \left(\frac{z_{23}}{\bar{z}_{23}} \right)^{\frac{J_{jki}}{2}} \end{aligned} \quad (2.30)$$

where $h_{ijk} \equiv h_i + h_j - h_k$ and $J_{ijk} \equiv J_i + J_j - J_k$.

If we take a complex conjugate on each side of (2.30), we get

$$C_{ijk} = (C_{\bar{i}\bar{j}\bar{k}})^* . \quad (2.31)$$

In a parity invariant theory, we can make further statements on these OPE coefficients. Consider the action of parity on an operator

$$\mathcal{P}\mathcal{O}_i(\mathbf{z}, \bar{\mathbf{z}})\mathcal{P}^{-1} = p_i\mathcal{O}_{\bar{i}}(\bar{\mathbf{z}}, \mathbf{z}), \quad p_i = \pm 1, \quad (2.32)$$

where $p_i = +$ for a parity even operator and $p_i = -1$ for a parity odd one. Importantly, notice that parity swaps both $\mathbf{z} \leftrightarrow \bar{\mathbf{z}}$ and $h_i \leftrightarrow \bar{h}_i$.

If we act with parity, defined as in (2.14), on both sides of (2.30), introducing the identity $\mathbb{1} = \mathcal{P}^{-1}\mathcal{P}$ in between operators, we get the equality

$$C_{ijk} = p_i p_j p_k C_{\bar{i}\bar{j}\bar{k}}. \quad (2.33)$$

If one or all three operators are parity even, we have $C_{ijk} = C_{\bar{i}\bar{j}\bar{k}}$. If exactly two of them are parity even, $C_{ijk} = -C_{\bar{i}\bar{j}\bar{k}}$.

AdS₄ Three-point functions of traceless symmetric boundary operators in AdS₄ depend on multiple independent OPE coefficients associated to different tensor structures. For a complete classification, see [39]. For the current purposes, we will need to study the case where we have two identical operators of spin J and one parity even scalar operator and the case in which we have two parity even scalars and one spin J operator. The complete decomposition for the first case includes $J + 1$ independent OPE coefficients [39]

$$\langle \mathcal{O}_i^{(J)}(P_1, Z_1)\mathcal{O}_i^{(J)}(P_2, Z_2)\mathcal{O}_l(P_3) \rangle = \sum_{n=0}^J \tilde{C}_{iil}^{(n)} \frac{V_{1,23}^n V_{2,31}^n H_{1,2}^{J-n}}{P_{12}^{\frac{2\Delta_i - \Delta_l + 2J}{2}} P_{13}^{\frac{\Delta_l}{2}} P_{23}^{\frac{\Delta_l}{2}}} \quad (2.34)$$

where

$$V_{k,ij} \equiv \frac{(Z_k \cdot P_i)(P_j \cdot P_k) - (Z_k \cdot P_j)(P_i \cdot P_k)}{P_i \cdot P_j}, \quad (2.35)$$

and $H_{i,j}$ was defined in (2.27). We wrote tildes on the OPE coefficients because there is an alternative yet equivalent basis for the decomposition in (2.34), which will be better suited to our purposes:

$$\langle \mathcal{O}_i^{(J)}(P_1, Z_1)\mathcal{O}_i^{(J)}(P_2, Z_2)\mathcal{O}_l(P_3) \rangle = H_{1,2}^J \sum_{n=0}^J C_{iil}^{(n)} \frac{\mathcal{H}_n(\tau)}{P_{12}^{\frac{2\Delta_i - \Delta_l + 2J}{2}} P_{13}^{\frac{\Delta_l}{2}} P_{23}^{\frac{\Delta_l}{2}}} \quad (2.36)$$

where \mathcal{H}_n are a special kind of Jacobi polynomials

$$\mathcal{H}_n(\tau) = {}_2F_1\left(-n, n + \frac{1}{2}; 2\tau\right), \quad \tau \equiv \frac{V_{1,23}V_{2,13}}{H_{1,2}} \quad (2.37)$$

The reasoning for using this basis becomes clear when deriving the spinning bulk-boundary-boundary conformal blocks, which we do in detail in appendix A.2.

When instead we have only one operator with spin, there is only one OPE coefficient

$$\langle \mathcal{O}_i^{(J)}(P_1, Z_1)\mathcal{O}_j(P_2)\mathcal{O}_l(P_3) \rangle = C_{ijl} \frac{V_{1,23}^J}{P_{12}^{\frac{\Delta_{ijl} + J}{2}} P_{23}^{\frac{\Delta_{jli} - J}{2}} P_{13}^{\frac{\Delta_{ilj} + J}{2}}}. \quad (2.38)$$

Once again, the discussion in this paragraph generalizes straightforwardly to traceless symmetric operators in higher dimensions.

2.2.3 Boundary Operator Expansion

Radial quantization implies the existence of another kind of operator expansion, which involves bulk operators. In fact, any bulk local operator in AdS_{d+1} can be expanded into a sum of boundary operators. For scalars, the explicit expansion reads [25]

$$\hat{\Phi}(z, \mathbf{x}) = \sum_l b_l^{\hat{\Phi}} z^{\Delta_l} \sum_{n=0}^{\infty} \frac{(-1)^n}{n! 2^{2n} (\Delta_l - \frac{d-2}{2})_n} z^{2n} \square^n \mathcal{O}_l(\mathbf{x}) \quad (2.39)$$

where $\square \equiv \delta^{ab} \frac{\partial}{\partial x^a} \frac{\partial}{\partial x^b}$ and $(a)_n \equiv \frac{\Gamma(a+n)}{\Gamma(a)}$ are Pochhammer symbols. Since $\hat{\Phi}$ is a scalar, the index l runs over scalar primary boundary operators, while the sum over n is the sum over descendants, which is fixed by symmetry. We call $b_l^{\hat{\Phi}}$ the BOE coefficients. They are related to the form factors of the bulk field $\hat{\Phi}$ between the vacuum and the state created by \mathcal{O}_l at the origin. Under this normalization of bulk operators, the bulk-boundary two-point function takes the form

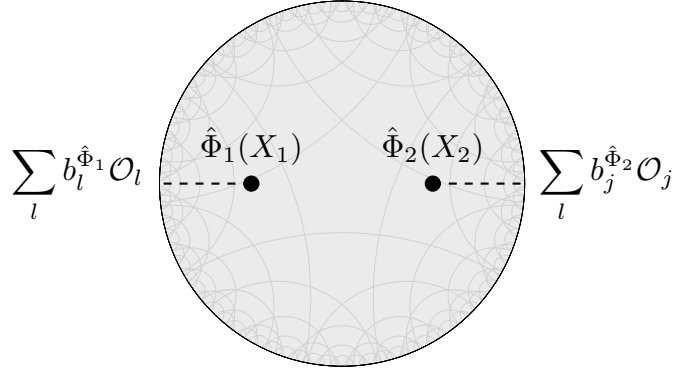
$$\langle \hat{\Phi}(z, \mathbf{x}_1) \mathcal{O}_l(\mathbf{x}_2) \rangle = b_l^{\hat{\Phi}} \left(\frac{z}{z^2 + \mathbf{x}_{12}^2} \right)^{\Delta_l}. \quad (2.40)$$

Unitarity fixes $b_l^{\hat{\Phi}} \in \mathbb{R}$.

2.3 Conformal blocks

Using the operator expansions we just discussed, we can derive compact representations for higher-point functions. In fact, iteratively applying the expansions of the previous section, one can express higher-point functions as sums of kinematic “blocks”, each of which is associated to specific representations of the AdS isometry group, and all dynamics are encoded in the QFT data. Let us discuss the various types of conformal blocks in order of complexity.

2.3.1 Bulk-bulk



Let us start from a bulk scalar two-point function. From two bulk points X_1^A and X_2^B one can construct the invariant

$$\sigma \equiv X_1 \cdot X_2 = -\frac{z_1^2 + z_2^2 + \mathbf{x}_{12}^2}{2z_1 z_2}, \quad (2.41)$$

which takes values $\sigma \leq -1$, with $\sigma = -1$ corresponding to coincident points configurations. The associated conformal blocks can be derived by applying the BOE (2.39) to both bulk fields and summing over the descendants. We do that explicitly in appendix A.1. The result is

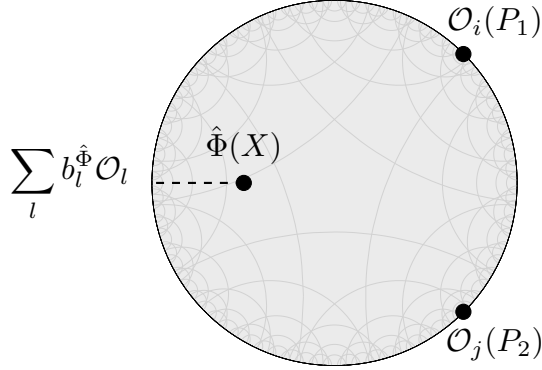
$$\langle \hat{\Phi}_1(X_1) \hat{\Phi}_2(X_2) \rangle = \sum_l b_l^{\hat{\Phi}_1} b_l^{\hat{\Phi}_2} G_{\text{BB}}^{\Delta_l}(\sigma), \quad (2.42)$$

where

$$G_{\text{BB}}^{\Delta}(\sigma) = \frac{1}{(-2-2\sigma)^{\Delta}} {}_2F_1\left(\Delta, \Delta - \frac{d-1}{2}, \frac{2}{1+\sigma}\right). \quad (2.43)$$

Notice that this decomposition is valid for scalar bulk operators in any number of dimensions.

2.3.2 Bulk-boundary-boundary



From one bulk and two boundary points we can construct one invariant cross ratio

$$\chi \equiv -\frac{1}{2} \frac{P_1 \cdot P_2}{(P_1 \cdot X)(P_2 \cdot X)} = \frac{z^2 \mathbf{x}_{12}^2}{(z^2 + (\mathbf{x} - \mathbf{x}_1)^2)(z^2 + (\mathbf{x} - \mathbf{x}_2)^2)}. \quad (2.44)$$

Scalars Let us start by considering scalar operators only. Carrying out the BOE on the bulk field (see appendix A.2), the conformal block decomposition takes the form

$$\langle \mathcal{O}_i(P_1) \mathcal{O}_j(P_2) \hat{\Phi}(X) \rangle = \frac{1}{P_{12}^{\frac{\Delta_i + \Delta_j}{2}}} \left(\frac{P_1 \cdot X}{P_2 \cdot X} \right)^{\frac{\Delta_j - \Delta_i}{2}} \sum_l b_l^{\hat{\Phi}} C_{ijl} G_{\text{Bbb}}^{\Delta_l, \Delta_j, \Delta_i}(\chi) \quad (2.45)$$

where

$$G_{\text{Bbb}}^{\Delta_l, \Delta_j, \Delta_i}(\chi) = \chi^{\frac{\Delta_l}{2}} {}_2F_1\left(\frac{\Delta_{lij}}{2}, \frac{\Delta_{lji}}{2}, \Delta_l - \frac{d-2}{2}; \chi\right), \quad (2.46)$$

where once again, this result is valid in any number of dimensions.

We will also need the block decomposition for the case in which the two boundary operators are identical and carry a traceless symmetric spin J representation of $SO(d)$. To derive it, we expand the bulk field to the boundary, reducing the correlator to a sum of CFT three-point functions. Here the dimension matters: for AdS_3 , we must use (2.30), while for AdS_4 (2.36). The result in AdS_4 easily generalizes to any number of dimensions.

AdS₃ In this case, the blocks are essentially the same as the scalar case with an overall tensor structure. When we have two identical spin J_i boundary operators, the decomposition takes the form

$$\langle \mathcal{O}_i(\mathbf{z}_1, \bar{\mathbf{z}}_1) \mathcal{O}_i(\mathbf{z}_2, \bar{\mathbf{z}}_2) \hat{\Phi}(z, \mathbf{z}_3, \bar{\mathbf{z}}_3) \rangle = \frac{1}{|\mathbf{z}_{12}|^{2\Delta_i}} \left(\frac{\bar{\mathbf{z}}_{12}}{\mathbf{z}_{12}} \right)^{J_i} \sum_l b_l^{\hat{\Phi}} C_{lii} G_{\text{Bbb}}^{\Delta_l, \Delta_i, \Delta_i}(\chi) \quad (2.47)$$

where $G_{\text{Bbb}}^{\Delta_l, \Delta_i, \Delta_i}(\chi)$ is (2.46) with $d = 2$ and $\Delta_j \rightarrow \Delta_i$. See the detailed derivation in appendix A.2.

AdS₄ In 4D (and higher) there are multiple OPE coefficients when two operators have spin. Explicitly, the decomposition reads

$$\langle \mathcal{O}_i^{(J)}(P_1, Z_1) \mathcal{O}_i^{(J)}(P_2, Z_2) \hat{\Phi}(X) \rangle = \frac{(H_{1,2})^J}{P_{12}^{\Delta_i+J}} \sum_l b_l^{\hat{\Phi}} \sum_{n=0}^J C_{iil}^{(n)} \mathcal{H}_n(v) G_{\text{Bbb}}^{\Delta_l, n}(\chi), \quad (2.48)$$

where

$$G_{\text{Bbb}}^{\Delta_l, n}(\chi) \equiv (1-\chi)^n \chi^{\frac{\Delta_l}{2}} {}_2F_1 \left(\frac{\Delta_l}{2} + n, \frac{\Delta_l}{2} + n; \Delta_l - \frac{d-2}{2}; \chi \right) \quad (2.49)$$

and \mathcal{H}_n was defined in (2.37), but now the cross ratio v is adapted to involve the bulk point X

$$v \equiv \frac{1}{\chi-1} \frac{V_{1,23} V_{2,31}}{H_{1,2}}, \quad P_3 \rightarrow X \quad (2.50)$$

The details of the derivation are in appendix A.2.

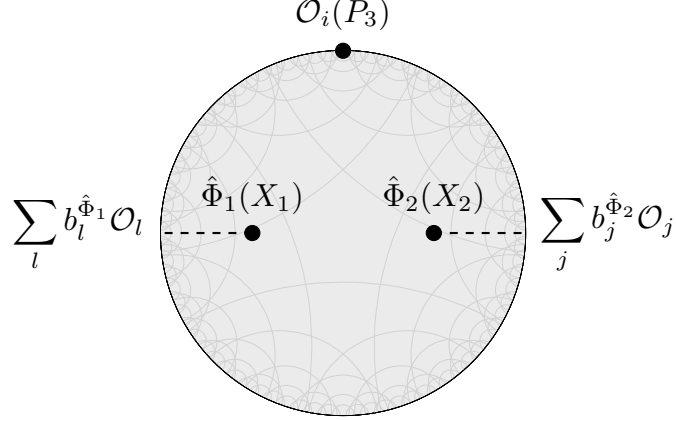
Specifically for AdS₄, we also require the bulk-boundary-boundary block involving a spinning boundary operator, a boundary scalar, and a bulk scalar, see appendix C. Using (2.38), this decomposition gives

$$\langle \mathcal{O}_i^{(J_i)}(P_1, Z_1) \mathcal{O}_j(P_2) \hat{\Phi}(X) \rangle = \frac{(V_{1,23})^{J_i}}{P_{12}^{\frac{\Delta_i+\Delta_j+J_i}{2}}} \left(\frac{P_1 \cdot X}{P_2 \cdot X} \right)^{\frac{\Delta_j-\Delta_i-J_i}{2}} \sum_l b_l^{\hat{\Phi}} C_{lij} G_{\text{Bbb}, J_i}^{\Delta_l, \Delta_i, \Delta_j}(\chi) \quad (2.51)$$

where $V_{1,23}$ is as in (2.35) but with $P_3 \rightarrow X$, and

$$G_{\text{Bbb}, J_i}^{\Delta_l, \Delta_i, \Delta_j}(\chi) = \left(-\frac{1}{2} \right)^{J_i} \chi^{\frac{\Delta_l}{2}} {}_2F_1 \left(\frac{\Delta_{lij}}{2} + J_i, \frac{\Delta_{lji}}{2} + J_i; \Delta_l - \frac{d-2}{2}; \chi \right). \quad (2.52)$$

2.3.3 Bulk-bulk-boundary



We are interested in bulk-bulk-boundary three-point functions which involve only scalars. When we have two points in the bulk and one on the boundary, there are two independent cross ratios, which we choose to be

$$\xi = \left(\frac{P_3 \cdot X_1}{P_3 \cdot X_2} \right)^2, \quad \rho = -1 - \xi - 2(X_1 \cdot X_2)\sqrt{\xi} \quad (2.53)$$

Notice that $\xi > 0$ and $\rho > 0$ ⁹. The conformal block expansion is obtained by expanding both bulk operators to the boundary. In appendix A.3 we get

$$\langle \hat{\Phi}_1(X_1) \hat{\Phi}_2(X_2) \mathcal{O}_i(P_3) \rangle = \frac{1}{(-2P_3 \cdot X_2)^{\Delta_i}} \sum_j \sum_l b_l^{\hat{\Phi}_1} b_j^{\hat{\Phi}_2} C_{lij} G_{\text{BBb}}^{\Delta_l, \Delta_j, \Delta_i}(\xi, \rho). \quad (2.54)$$

with

$$G_{\text{BBb}}^{\Delta_l, \Delta_j, \Delta_i}(\xi, \rho) = \frac{\xi^{\frac{\Delta_j - \Delta_i}{2}}}{\rho^{\frac{\Delta_{lj}}{2}}} F_4 \left(\frac{\Delta_{lj}}{2}, \frac{\Delta_{lj}}{2} - \frac{d-2}{2}; -\frac{1}{\rho}, -\frac{\xi}{\rho} \right) \quad (2.55)$$

where F_4 is an Appell function, defined through the following series representation, convergent for $\sqrt{|x|} + \sqrt{|y|} < 1$:

$$F_4 \left(\begin{matrix} a & b \\ c, & d \end{matrix}; x, y \right) \equiv \sum_{m=0}^{\infty} \sum_{n=0}^{\infty} \frac{(a)_{m+n} (b)_{m+n}}{(c)_m (d)_n m! n!} x^m y^n \quad (2.56)$$

Notice that the domain of convergence does not include all possible values of the cross ratios. For an alternative (but more complicated) representation of this conformal block which converges for all AdS configurations, see equation (A.37).

2.3.4 Boundary 4-pt

The last conformal blocks we need are those associated to four-point functions on the boundary. These are the standard CFT conformal blocks, and their explicit form depends on the number of dimensions.

⁹That is because when $X_1 \rightarrow X_2$ we have $\rho = -(1 - \sqrt{\xi})^2$ but also $\xi = 1$.

AdS₂ Four-point functions on the 1D boundary can be decomposed in blocks as follows

$$\langle \mathcal{O}_l(x_1) \mathcal{O}_i(x_2) \mathcal{O}_j(x_3) \mathcal{O}_k(x_4) \rangle = \left(\frac{x_{14}^2}{x_{13}^2} \right)^{\frac{\Delta_j - \Delta_k}{2}} \left(\frac{x_{24}^2}{x_{14}^2} \right)^{\frac{\Delta_l - \Delta_i}{2}} \frac{\mathcal{G}(\zeta)}{(x_{12}^2)^{\frac{\Delta_l + \Delta_i}{2}} (x_{34}^2)^{\frac{\Delta_j + \Delta_k}{2}}} \quad (2.57)$$

where we used the fact that in 1D four-point functions can be fixed up to a function of a single cross ratio, which we take to be $\zeta \equiv \frac{x_{12}x_{34}}{x_{13}x_{24}}$. Moreover, operators are labeled only by their scaling dimension.

The function $\mathcal{G}(\zeta)$ can be decomposed in various channels. The s -channel decomposition, defined by the pairings $(li)(jk)$, reads

$$\mathcal{G}(\zeta) = \sum_m C_{lim} C_{mjk} G_{\Delta_m}^{lijk}(\zeta) \quad (2.58)$$

where the explicit form of the block is

$$G_{\Delta_m}^{lijk}(\zeta) = \zeta^{\Delta_m} {}_2F_1 \left(\begin{matrix} \Delta_{mil}, \Delta_{mjk} \\ 2\Delta_m \end{matrix}; \zeta \right) \quad (2.59)$$

where we use $lijk$ as a shorthand for $\Delta_l, \Delta_i, \Delta_j, \Delta_k$, but we emphasize the blocks only depend on the scaling dimensions of the operators.

AdS₃ In 2D CFT, the decomposition of a four-point function of operators with generic holomorphic weights reads [40]

$$\begin{aligned} & \langle \mathcal{O}_l(\mathbf{z}_1, \bar{\mathbf{z}}_1) \mathcal{O}_i(\mathbf{z}_2, \bar{\mathbf{z}}_2) \mathcal{O}_j(\mathbf{z}_3, \bar{\mathbf{z}}_3) \mathcal{O}_k(\mathbf{z}_4, \bar{\mathbf{z}}_4) \rangle \\ &= \frac{1}{z_{12}^{h_l+h_i} z_{34}^{h_j+h_k}} \left(\frac{z_{24}}{z_{14}} \right)^{h_{li}} \left(\frac{z_{14}}{z_{13}} \right)^{h_{jk}} \frac{1}{z_{12}^{\bar{h}_l+\bar{h}_i} z_{34}^{\bar{h}_j+\bar{h}_k}} \left(\frac{\bar{z}_{24}}{\bar{z}_{14}} \right)^{\bar{h}_{li}} \left(\frac{\bar{z}_{14}}{\bar{z}_{13}} \right)^{\bar{h}_{jk}} \mathcal{G}(\eta, \bar{\eta}) \end{aligned} \quad (2.60)$$

where $h_{ij} \equiv h_i - h_j$ and we used the fact that in 2D we can fix a four-point function up to a function of two real variables, or one complex cross-ratio, which we take to be

$$\eta \equiv \frac{z_{12}z_{34}}{z_{13}z_{24}} \quad (2.61)$$

This function can then be decomposed into conformal blocks in the s -channel as follows

$$\mathcal{G}(\eta, \bar{\eta}) = \sum_m C_{lim} C_{mjk} G_{h_m, \bar{h}_m}^{lijk}(\eta, \bar{\eta}), \quad (2.62)$$

Notice that the sum is taken to run over operators labeled by (h_m, \bar{h}_m) , hence the complex conjugate operators labeled by (\bar{h}_m, h_m) must be included independently.

These blocks are known in closed form for every value of the external holomorphic weights [40]

$$G_{h_m, \bar{h}_m}^{lijk}(\eta, \bar{\eta}) = \frac{1}{2} \eta^{h_m} \bar{\eta}^{\bar{h}_m} {}_2F_1 \left(\begin{matrix} h_{mil}, h_{mjk} \\ 2h_m \end{matrix}; \eta \right) {}_2F_1 \left(\begin{matrix} \bar{h}_{mil}, \bar{h}_{mjk} \\ 2\bar{h}_m \end{matrix}; \bar{\eta} \right) \quad (2.63)$$

where $h_{ijk} \equiv h_i + h_j - h_k$.

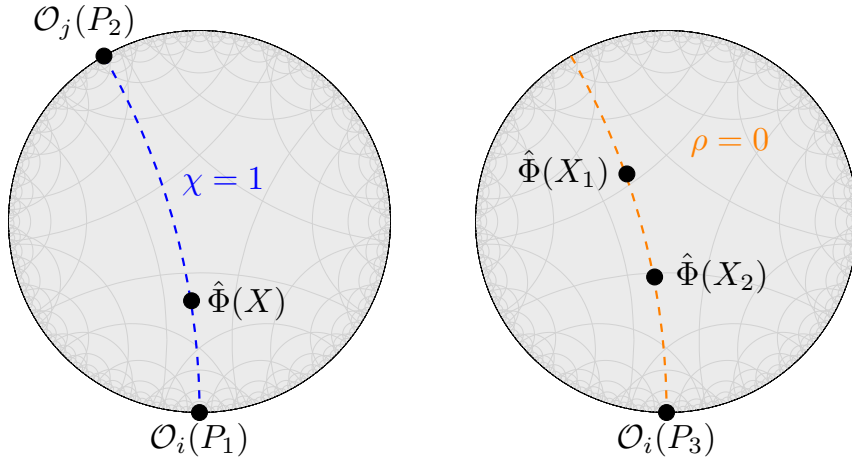


Figure 5. When a bulk operator is inserted on the geodesic connecting two other operators, the conformal block decompositions for bulk-boundary-boundary (2.45) and bulk-bulk-boundary (2.55) correlation functions fail to converge. On the left, the geodesic in the bulk-boundary-boundary case, which corresponds to configurations where the cross ratio χ (2.44) is 1. On the right, the geodesic in the bulk-bulk-boundary case, which corresponds to configurations where the cross-ratio ρ (2.53) is equal to 0 (and ξ has any value). Local blocks solve this issue.

AdS₄ In 3D CFT, the situation is significantly more complicated. Let us focus on scalar operators. The four-point function can again be fixed up to a function of two cross-ratios

$$\langle \mathcal{O}_l(\mathbf{x}_1) \mathcal{O}_i(\mathbf{x}_2) \mathcal{O}_j(\mathbf{x}_3) \mathcal{O}_k(\mathbf{x}_4) \rangle = \left(\frac{\mathbf{x}_{14}^2}{\mathbf{x}_{13}^2} \right)^{\frac{\Delta_j - \Delta_k}{2}} \left(\frac{\mathbf{x}_{24}^2}{\mathbf{x}_{14}^2} \right)^{\frac{\Delta_l - \Delta_i}{2}} \frac{\mathcal{G}(u, v)}{(\mathbf{x}_{12}^2)^{\frac{\Delta_l + \Delta_i}{2}} (\mathbf{x}_{34}^2)^{\frac{\Delta_j + \Delta_k}{2}}} \quad (2.64)$$

which we take to be

$$u = \frac{\mathbf{x}_{12}^2 \mathbf{x}_{34}^2}{\mathbf{x}_{13}^2 \mathbf{x}_{24}^2}, \quad v = \frac{\mathbf{x}_{14}^2 \mathbf{x}_{23}^2}{\mathbf{x}_{13}^2 \mathbf{x}_{24}^2}. \quad (2.65)$$

The s -channel decomposition in this case reads

$$\mathcal{G}(u, v) = \sum_m C_{lim} C_{mjk} G_{\Delta_m, J_m}^{lijk}(u, v), \quad (2.66)$$

where Δ_m and J_m are the scaling dimension and spin of the exchanged operator \mathcal{O}_m , but the blocks are not known in closed form for generic u and v .

For operators with external spin, the situation is more complicated. We refer the reader to [41–45].

2.4 Local blocks

The conformal block decomposition of correlation functions involving bulk fields fails for certain configurations of points. Specifically, the bulk-boundary-boundary and bulk-bulk-boundary blocks present singularities whenever a bulk point lies on a geodesic which joins

any two other insertion points, see figure 5. Take for example the decomposition of a bulk-boundary-boundary correlation function (2.45). At the value of the cross ratio $\chi = 1$, the blocks are singular:

$$G_{\text{Bbb}}^{\Delta_l, \Delta_i, \Delta_j}(\chi) \underset{\chi \rightarrow 1}{\sim} \begin{cases} \log(1 - \chi), & d = 2 \\ (1 - \chi)^{\frac{2-d}{2}}, & d > 2 \end{cases} \quad (2.67)$$

At the same time, the analytic domain of a physical correlation function can be argued to be the cut complex plane $\chi \in \mathbb{C} \setminus (-\infty, 0]$ [28], and so we do not expect a singularity at $\chi = 1$.

This issue is resolved by introducing *local blocks* [25, 26], a basis which is composed of elements with the correct analytic structure term by term. We are going to limit ourselves here to report their form, and for in-depth discussions we direct the reader towards [25, 26], and [28] for the subtle case of AdS₂.

2.4.1 Bulk-boundary-boundary

The decomposition in terms of bulk-boundary-boundary local blocks mirrors the one in terms of regular conformal blocks (2.45)

$$\langle \hat{\Phi}(X) \mathcal{O}_i(P_1) \mathcal{O}_j(P_2) \rangle = \frac{1}{P_{12}^{\Delta_i}} \sum_l b_l^{\hat{\Phi}} C_{ijl} G_{\text{Bbb}}^{\Delta_l, \Delta_i, \Delta_j, \alpha}(\chi) \quad (2.68)$$

where now [25, 26]

$$G_{\text{Bbb}}^{\Delta_l, \Delta_i, \Delta_j, \alpha}(\chi) = G_{\text{Bbb}}^{\Delta_l, \Delta_i, \Delta_j}(\chi) - \chi^\alpha \frac{\Gamma(\alpha + \frac{\Delta_i - \Delta_j}{2}) \Gamma(\alpha + \frac{\Delta_j - \Delta_i}{2}) \Gamma(\Delta_l - \frac{d-2}{2})}{\Gamma(1 + \alpha - \frac{\Delta_l}{2}) \Gamma(\alpha + \frac{\Delta_l}{2} - \frac{d-2}{2}) \Gamma(\frac{\Delta_{ij}}{2}) \Gamma(\frac{\Delta_{ji}}{2})} \times {}_3F_2 \left(1, \alpha + \frac{\Delta_i - \Delta_j}{2}, \alpha + \frac{\Delta_j - \Delta_i}{2}; 1 + \alpha - \frac{\Delta_l}{2}, 1 + \alpha - \frac{d - \Delta_l}{2}; \chi \right) \quad (2.69)$$

Notice the presence of an extra real parameter α , which originates from the dispersion relation between local blocks and standard conformal blocks

$$G_{\text{Bbb}}^{\Delta_l, \Delta_i, \Delta_j, \alpha}(\chi) = \chi^\alpha \int_{-\infty}^0 \frac{d\chi'}{2\pi i} \frac{1}{\chi' - \chi} \text{Disc}_{\chi' \leq 0} \left(\frac{G_{\text{Bbb}}^{\Delta_l, \Delta_i, \Delta_j}(\chi')}{\chi'^\alpha} \right) \quad (2.70)$$

The validity of this dispersion relation and the convergence of the resulting block decomposition (2.68) requires a bound on α [26, 28]:

$$\alpha > \frac{\Delta_i + \Delta_j + \Delta_{\hat{\Phi}}^{\text{UV}}}{2} \quad (2.71)$$

where $\Delta_{\hat{\Phi}}^{\text{UV}}$ is the scaling dimension of the bulk field $\hat{\Phi}$ at the UV fixed point of the bulk theory.

It can be verified that now the blocks in (2.68) are finite at $\chi = 1$. Using this particular basis will be crucial for us to have convergent sums in the flow equations (1.3).

2.4.2 Bulk-bulk-boundary

The same issue presents itself in the bulk-bulk-boundary case. The resolution is to expand one of the bulk operators to the boundary to then use the local block decomposition (2.68) for the resulting correlation function. Schematically,

$$\begin{aligned}
\langle \hat{\Phi}_1(z_1, \mathbf{x}_1) \hat{\Phi}_2(z_2, \mathbf{x}_2) \mathcal{O}_i(\mathbf{x}_3) \rangle &= \sum_j b_j^{\hat{\Phi}_2} z_2^{\Delta_j} \langle \hat{\Phi}_1(z, \mathbf{x}_1) \mathcal{O}_j(\mathbf{x}_2) \mathcal{O}_i(\mathbf{x}_3) \rangle + \dots \\
&= \sum_{l,j} b_l^{\hat{\Phi}_1} b_j^{\hat{\Phi}_2} C_{lji} z_2^{\Delta_j} \frac{1}{(\mathbf{x}_{23}^2)^{\frac{\Delta_i + \Delta_j}{2}}} \left(\frac{z_2^2 + \mathbf{x}_{23}^2}{z_2^2 + \mathbf{x}_{12}^2} \right)^{\frac{\Delta_i - \Delta_j}{2}} G_{\text{BBb}}^{\Delta_l, \Delta_j, \Delta_i, \alpha}(\chi_{(2,3)}) + \dots \quad (2.72) \\
&\equiv \frac{1}{(-2P_3 \cdot X_2)^{\Delta_i}} \sum_{l,j} b_l^{\hat{\Phi}_1} b_j^{\hat{\Phi}_2} C_{lji} G_{\text{BBb}}^{\Delta_l, \Delta_j, \Delta_i, \alpha}(\xi, \rho)
\end{aligned}$$

where the dots stand for the sum over descendants of \mathcal{O}_j , which we omit to avoid clutter. Unlike the standard conformal block case, that sum cannot be carried out explicitly here. The result reads

$$\begin{aligned}
G_{\text{BBb}}^{\Delta_l, \Delta_j, \Delta_i, \alpha}(\xi, \rho) &= - \sum_{k,m,n} \frac{(-1)^{k+n} \xi^{n - \frac{\Delta_{ij}}{2}} \rho^{-k-m-n-\alpha + \frac{\Delta_{ij}}{2}} \Gamma\left(\alpha + \frac{\Delta_{ij}}{2}\right) \Gamma\left(k + \alpha - \frac{\Delta_{ij}}{2}\right)}{n! k! \Gamma\left(1 + \alpha - \frac{\Delta_l}{2}\right) \Gamma\left(1 - \frac{d}{2} + \alpha + \frac{\Delta_l}{2}\right) \Gamma\left(\frac{\Delta_{ij} + \Delta_l}{2}\right) \Gamma\left(\frac{-\Delta_{ij} + \Delta_l}{2}\right)} \\
&\times \frac{\Gamma\left(1 - \frac{d}{2} + \Delta_l\right) \left(\alpha + \frac{\Delta_{ij}}{2}\right)_m \left(k + \alpha - \frac{\Delta_{ij}}{2}\right)_{m+n} \left(1 - \frac{d}{2} + k + \alpha - \frac{\Delta_{ij}}{2}\right)_{m+n}}{\left(1 - \frac{d}{2} + k + \alpha - \frac{\Delta_{ij}}{2}\right)_m \left(1 - \frac{d}{2} + \Delta_j\right)_n \left(1 + \alpha - \frac{\Delta_l}{2}\right)_m \left(1 - \frac{d}{2} + \alpha + \frac{\Delta_l}{2}\right)_m} \quad (2.73)
\end{aligned}$$

3 Derivation of the flow equations

Armed with the conformal block decompositions described in the previous section, we now present the derivation of our main results, which will be ODEs describing the variation of the QFT data in AdS₃ and AdS₄ under a bulk relevant deformation. We start by deriving the ODE involving the variation of the scaling dimensions Δ_i . For scalar operators, we leave the spacetime dimension generic. For spinning operators, we focus specifically on 3D and 4D, which require separate treatment. In both cases the result turns out to be closely related to the scalar case.

3.1 Flow of scaling dimensions

Scalars We begin by examining the two-point function of scalar boundary primary operators at a finite coupling λ . Assuming the spectrum contains no degeneracies and choosing a diagonal basis for the operators, this reads

$$\langle \mathcal{O}_i(\mathbf{x}_1) \mathcal{O}_j(\mathbf{x}_2) \rangle_\lambda = \frac{\delta_{ij}}{(\mathbf{x}_{12}^2)^{\Delta_i(\lambda)}}. \quad (3.1)$$

Let us now introduce an infinitesimal shift in the bulk coupling, $\lambda \rightarrow \lambda + \delta\lambda$. As we will show shortly, the correction to the two-point function in perturbation theory generically diverges. This divergence arises from integrating over the bulk deformation close to the boundary

and therefore corresponds to an IR divergence. To address this, we must renormalize the boundary theory by expressing the bare operators in terms of renormalized ones, as in¹⁰

$$\mathcal{O}_i^{(\text{bare})}(\mathbf{x}) = \sum_k \sum_{n=0}^{\infty} \mathcal{Z}_{ik;n} \square^n \mathcal{O}_k^{(\text{ren})}(\mathbf{x}), \quad (3.2)$$

where the coefficients $\mathcal{Z}_{ik;n}$ are the scalar field-strength renormalization constants, which can be written as

$$\mathcal{Z}_{ik;n} = \delta_{ik} \delta_{n,0} + \delta \mathcal{Z}_{ik;n}, \quad (3.3)$$

where $\delta \mathcal{Z}_{ik;n}$ is of order $\delta\lambda$. Because we shifted the coupling in the bulk, the physical scaling dimensions of the operators generically shift by $\delta\Delta_i$. The two-point function of the renormalized operators then reads, imposing that they are canonically normalized and that they do not mix,

$$\langle \mathcal{O}_i^{(\text{ren})}(\mathbf{x}_1) \mathcal{O}_j^{(\text{ren})}(\mathbf{x}_2) \rangle_{\lambda+\delta\lambda} = \frac{\delta_{ij}}{(\mathbf{x}_{12}^2)^{\Delta_i(\lambda)+\delta\Delta_i}}. \quad (3.4)$$

Combining these expressions and expanding for small deformations, we obtain

$$\begin{aligned} \langle \mathcal{O}_i^{(\text{bare})}(\mathbf{x}_1) \mathcal{O}_j^{(\text{bare})}(\mathbf{x}_2) \rangle_{\lambda+\delta\lambda} &= \delta_{ij} \left(\frac{1}{(\mathbf{x}_{12}^2)^{\Delta_i}} - \delta\Delta_i \frac{\log(\mathbf{x}_{12}^2)}{(\mathbf{x}_{12}^2)^{\Delta_i}} \right) \\ &+ \sum_{n=0}^{\infty} \frac{2^{2n}}{(\mathbf{x}_{12}^2)^n} \left(\frac{(\Delta_j)_n (\Delta_j - \frac{d-2}{2})_n}{(\mathbf{x}_{12}^2)^{\Delta_j}} \delta \mathcal{Z}_{ij;n} + \frac{(\Delta_i)_n (\Delta_i - \frac{d-2}{2})_n}{(\mathbf{x}_{12}^2)^{\Delta_i}} \delta \mathcal{Z}_{ji;n} \right) \\ &+ O(\delta\lambda^2). \end{aligned} \quad (3.5)$$

On the other hand, a shift in the coupling by $\delta\lambda$ corresponds to a shift in the bulk action of

$$\delta S_{\text{bulk}} = \delta\lambda \int \frac{dz d^d \mathbf{x}}{z^{d+1}} \hat{\Phi}(z, \mathbf{x}). \quad (3.6)$$

As a consequence, the change in the boundary two-point function can be computed with bulk perturbation theory in the coupling $\delta\lambda$, which, at leading order, gives

$$\langle \mathcal{O}_i^{(\text{bare})}(\mathbf{x}_1) \mathcal{O}_j^{(\text{bare})}(\mathbf{x}_2) \rangle_{\lambda+\delta\lambda} = \langle \mathcal{O}_i(\mathbf{x}_1) \mathcal{O}_j(\mathbf{x}_2) \rangle_{\lambda-\delta\lambda} \int \frac{dz d^d \mathbf{x}}{z^{d+1}} \langle \mathcal{O}_i(\mathbf{x}_1) \mathcal{O}_j(\mathbf{x}_2) \hat{\Phi}(z, \mathbf{x}) \rangle_{\lambda+\dots}, \quad (3.7)$$

where we dropped the superscript on the right-hand side because these operators are evaluated in the undeformed theory, where bare and renormalized operators coincide. Comparing this equation with (3.5), we can extract a differential equation for the scaling dimensions Δ_i , which will be the main result of this section. Before proceeding, we note that, as anticipated, the integral in (3.7) diverges as the bulk point approaches the boundary points \mathbf{x}_1 and \mathbf{x}_2 . Crucially, two types of divergences arise, which can be regulated by introducing a cutoff ϵ near the boundary insertions. First, there are power-law divergences as $\epsilon \rightarrow 0$, which are scheme-dependent and absorbable into the field-strength

¹⁰Because the bare primary operators are scalars, they can only mix with renormalized operators that are also scalars. This is why we restricted to descendants constructed by taking powers of \square .

renormalization constants in (3.5). Second, there are logarithmic divergences, which arise when $i = j$ and are instead universal. All these divergences must be perfectly canceled by the counterterms in (3.5). Imposing this, we obtain

$$\frac{d\Delta_i}{d\lambda} = \frac{\int \frac{dzd^d\mathbf{x}}{z^{d+1}} \langle \mathcal{O}_i(\mathbf{x}_1) \mathcal{O}_i(\mathbf{x}_2) \hat{\Phi}(z, \mathbf{x}) \rangle_\lambda \Big|_{\log}}{\langle \mathcal{O}_i(\mathbf{x}_1) \mathcal{O}_i(\mathbf{x}_2) \rangle_\lambda}, \quad (3.8)$$

where we have denoted with the subscript log the terms proportional to $\log(\mathbf{x}_{12}^2)$.

We now select a regularization scheme and proceed with the computation of the integral in (3.7). We choose to remove two half-balls centered in \mathbf{x}_1 and \mathbf{x}_2 , as shown in figure 6. The regularized integral reads

$$I_{ij}^{\hat{\Phi}}(\mathbf{x}_1, \mathbf{x}_2, \epsilon) := \int_{\mathcal{M}_\epsilon} \frac{dzd^d\mathbf{x}}{z^{d+1}} \langle \hat{\Phi}(z, \mathbf{x}) \mathcal{O}_i(\mathbf{x}_1) \mathcal{O}_j(\mathbf{x}_2) \rangle_\lambda \quad (3.9)$$

where \mathcal{M}_ϵ is defined by the restriction $z^2 + |\mathbf{x} - \mathbf{x}_k|^2 \geq \epsilon^2$ for $k = 1, 2$. The three point function inside the integral can be expressed in terms of the bulk-boundary-boundary block in equation (2.45). The integral then reduces to

$$I_{ij}^{\hat{\Phi}}(\mathbf{x}_1, \mathbf{x}_2, \epsilon) = \sum_l b_l^{\hat{\Phi}} C_{ijl} I_{\text{Bbb}}^{\Delta_l, \Delta_i, \Delta_j}(\mathbf{x}_1, \mathbf{x}_2, \epsilon), \quad (3.10)$$

where $I_{\text{Bbb}}^{\Delta_l, \Delta_i, \Delta_j}$ denotes the integrated conformal blocks over \mathcal{M}_ϵ , which reads

$$I_{\text{Bbb}}^{\Delta_l, \Delta_i, \Delta_j} := \int_{\mathcal{M}_\epsilon} \frac{dzd^d\mathbf{x}}{z^{d+1}} \frac{1}{|\mathbf{x}_{12}|^{\Delta_i + \Delta_j}} \left(\frac{|\mathbf{x} - \mathbf{x}_1|^2 + z^2}{|\mathbf{x} - \mathbf{x}_2|^2 + z^2} \right)^{\frac{\Delta_j - \Delta_i}{2}} G_{\text{Bbb}}^{\Delta_l, \Delta_i, \Delta_j}(\chi). \quad (3.11)$$

We note that in (3.10) we swapped the integral over the bulk point and the infinite sum in the block decomposition. Strictly speaking, this operation is mathematically justified only within the region of convergence of the block decomposition. However, as explained in section 2.4, standard conformal blocks diverge at $\chi = 1$, which breaks the convergence of the series in certain regimes. Consequently, performing the integration term-by-term generally yields a divergent asymptotic series. We may, nevertheless, proceed with this formal swapping procedure under the caveat that the resulting series must be properly resummed. We achieve this by employing local blocks, which converge everywhere in AdS and therefore give rise to a convergent series, see the end of this section for the result.

We now return to our main calculation. As explained in appendix B.1, equation (3.11) takes the form

$$I_{\text{Bbb}}^{\Delta_l, \Delta_i, \Delta_j}(\mathbf{x}_1, \mathbf{x}_2, \epsilon) = \frac{1}{|\mathbf{x}_{12}|^{\Delta_i + \Delta_j}} \sum_{p=0}^{\infty} \frac{a_{2p}(\Delta_{ij}, \Delta_l)}{\Delta_{ij} - 2p} \left(\frac{\epsilon}{|\mathbf{x}_{12}|} \right)^{2p - \Delta_{ij}} + (\Delta_i \leftrightarrow \Delta_j). \quad (3.12)$$

The explicit form of the coefficients $a_{2p}(\Delta_{ij}, \Delta_l)$ is not needed, except for the $p = 0$ term, which is easier to compute and reads

$$a_0(\Delta_{ij}, \Delta_l) = \frac{\pi^{\frac{d}{2}} \Gamma\left(\frac{\Delta_l - d}{2}\right)}{2\Gamma\left(\frac{\Delta_l}{2}\right)} {}_3F_2\left(\frac{\Delta_{lj}}{2}, \frac{\Delta_{lj}}{2}, \frac{\Delta_l - d}{2}; \Delta_l + 1 - \frac{d}{2}, \frac{\Delta_l}{2}; 1\right), \quad (3.13)$$

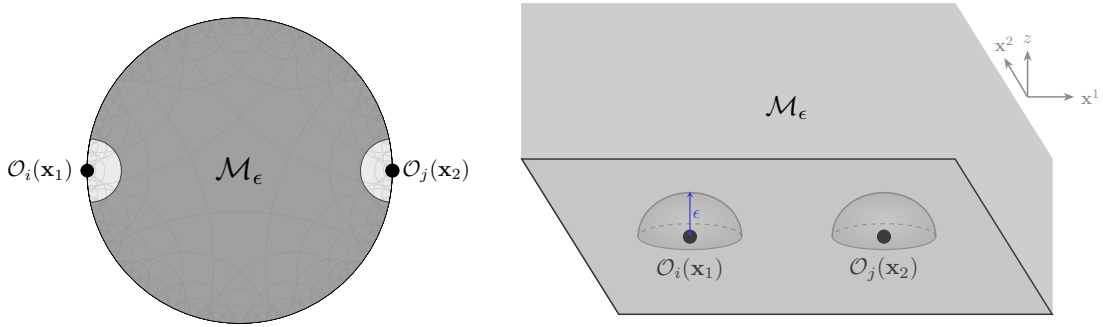


Figure 6. Domain of integration \mathcal{M}_ϵ in (3.9) in ball and half-plane coordinates. We remove the half-balls centered in the positions $\mathbf{x}_{1,2}$ of the boundary operators to regulate the IR divergences arising when the bulk point hits these points.

see again appendix B.1 for the derivation. Let us now replace the result for $I_{\text{Bbb}}^{\Delta_l, \Delta_i, \Delta_j}$ in (3.10) and then in (3.7), and compare it with (3.5). We begin by considering the case $\Delta_i \neq \Delta_j$. We see that matching term by term in \mathbf{x}_{12} we find the explicit expression for the counterterms in this regularization scheme, which reads

$$\delta \mathcal{Z}_{ij;p} = -\frac{\delta \lambda \epsilon^{2p-\Delta_{ij}}}{2^{2p}(\Delta_j)_p(\Delta_j - \frac{d-2}{2})_p} \sum_l b_l^{\hat{\Phi}} \frac{C_{jil} a_{2p}(\Delta_{ij}, \Delta_l)}{\Delta_{ij} - 2p} \quad \text{for } i \neq j \quad (3.14)$$

Now consider the case $\Delta_i = \Delta_j$, which contains the universal logarithmic divergence. Isolating the $p = 0$ term, as higher-order terms vanish in the limit $\epsilon \rightarrow 0$, and taking the limit $\Delta_i \rightarrow \Delta_j$ the integrated block becomes

$$I_{\text{Bbb}}^{\Delta_l, \Delta_i, \Delta_i}(\mathbf{x}_1, \mathbf{x}_2, \epsilon) = \frac{a_0(0, \Delta_l)}{|\mathbf{x}_{12}|^{2\Delta_i}} \log\left(\frac{\mathbf{x}_{12}^2}{\epsilon^2}\right), \quad (3.15)$$

where we used that

$$\left. \frac{da_0(\Delta_{ij}, \Delta_l)}{d\Delta_{ij}} \right|_{\Delta_{ij}=0} = 0. \quad (3.16)$$

Inserting this into the bare two-point function in (3.7) and comparing again with (3.5), we obtain the following matching condition

$$-\delta \lambda \sum_l b_l^{\hat{\Phi}} C_{iil} I_{\text{Bbb}}^{\Delta_l, \Delta_i, \Delta_i}(\mathbf{x}_1, \mathbf{x}_2, \epsilon) = \frac{1}{(\mathbf{x}_{12}^2)^{\Delta_i}} (2\delta \mathcal{Z}_{ii;0} - \delta \Delta_i \log(\mathbf{x}_{12}^2)) \quad (3.17)$$

This equation is satisfied by imposing

$$\delta \mathcal{Z}_{ii;0} = \delta \lambda \sum_l b_l^{\hat{\Phi}} C_{iil} a_0(0, \Delta_l) \log \epsilon, \quad (3.18)$$

$$\delta \Delta_i = \delta \lambda \sum_l b_l^{\hat{\Phi}} C_{iil} a_0(0, \Delta_l). \quad (3.19)$$

The second relation gives the main result of this section, which reads

$$\frac{d\Delta_i}{d\lambda} = \sum_l b_l^{\hat{\Phi}} C_{iil} \mathcal{I}(\Delta_l), \quad (3.20)$$

where

$$\mathcal{I}(\Delta_l) \equiv a_0(0, \Delta_l) = -\frac{2\pi^{d/2}\Gamma(-\frac{d}{2} + \Delta_l + 1)}{\Gamma(\frac{\Delta_l}{2})\Gamma(\frac{\Delta_l+2}{2})(d - \Delta_l)}. \quad (3.21)$$

AdS₃ In AdS₃, the analysis generalizes easily to the case of spinning operators. Following the same logic as the scalar case, we can compute the flow equation for the scaling dimension of operators with generic spin, which reads

$$\frac{d\Delta_i}{d\lambda} = \frac{\int \frac{dzd\bar{z}}{2z^3} \langle \mathcal{O}_i(\mathbf{z}_1, \bar{\mathbf{z}}_1) \mathcal{O}_i(\mathbf{z}_2, \bar{\mathbf{z}}_2) \hat{\Phi}(z, \bar{z}) \rangle_{\lambda} \Big|_{\log}}{\langle \mathcal{O}_i(\mathbf{z}_1, \bar{\mathbf{z}}_1) \mathcal{O}_i(\mathbf{z}_2, \bar{\mathbf{z}}_2) \rangle_{\lambda}}, \quad (3.22)$$

where now the subscript log refers to terms proportional to $\log|\mathbf{z}_{12}|^2$. Looking at the two point function in (2.25) and at the bulk-bulk-boundary block in (2.47), we see that the overall spin structure simplifies and we get

$$\frac{d\Delta_i}{d\lambda} = \sum_l b_l^{\hat{\Phi}} C_{ijl} \int_{\text{AdS}} dX G_{\text{Bbb}}^{\Delta_l, \Delta_i, \Delta_i}(\chi) \Big|_{\log}, \quad (3.23)$$

where the integral over AdS is again generically divergent and needs to be regulated with some cutoff ϵ . Adopting the same regularization scheme that we used for the scalar case, we identify the integral in (3.23) with $I_{\text{Bbb}}^{\Delta_l, \Delta_i, \Delta_i}$ in (3.11), when the limit $\Delta_i \rightarrow \Delta_j$ is taken. Using the results of the previous section, the flow equation for the scaling dimension then reads

$$\frac{d\Delta_i}{d\lambda} = \sum_l b_l^{\hat{\Phi}} C_{iil} \mathcal{I}(\Delta_l) \quad (3.24)$$

with $\mathcal{I}(\Delta_l)$ the same as in (3.21) with $d = 2$.

AdS₄ In AdS₄, the case of spinning operators is treated by generalizing equation (3.8) into

$$\frac{d\Delta_i}{d\lambda} = \frac{\int_X \langle \mathcal{O}_i^{(J)}(P_1, Z_1) \mathcal{O}_i^{(J)}(P_2, Z_2) \Phi(X) \rangle \Big|_{\log}}{\langle \mathcal{O}_i^{(J)}(P_1, Z_1) \mathcal{O}_i^{(J)}(P_2, Z_2) \rangle_{\lambda}}, \quad (3.25)$$

where for convenience we used embedding coordinates. The denominator is given by the two-point function in equation (2.26), while the numerator can be expressed in terms of the bulk-boundary-boundary block in equation (2.48). The latter then becomes

$$\int_X \frac{(H_{1,2})^J}{P_{12}^{\Delta_i+J}} \sum_l b_l^{\hat{\Phi}} \sum_{n=0}^J C_{iil}^{(n)} \mathcal{H}_n(v) G_{\text{Bbb}}^{\Delta_l, n}(\chi) \Big|_{\log}. \quad (3.26)$$

It seems that, in principle, we get contributions from each tensor structure $\mathcal{H}_n(v)$. However, crucially, the only relevant contribution comes from the $n = 0$ term, as all other structures vanish when the integral over X is computed. A simple way to see this is by going to the

special configuration in which we place one boundary operator at the origin in Poincaré coordinates and the other at infinity, while the bulk point remains generic. This corresponds to

$$\begin{aligned} P_1 &= \left(\frac{1}{2}, \mathbf{0}, \frac{1}{2} \right), & P_2 &= \left(\frac{1}{2}, \mathbf{0}, -\frac{1}{2} \right), & Z_1 &= (0, \mathbf{z}_1, 0), & Z_2 &= (0, \mathbf{z}_2, 0) \\ X &= \left(\frac{2+z^2}{2z}, \frac{\mathbf{x}}{z}, -\frac{1}{2z} \right) \end{aligned} \quad (3.27)$$

With this choice of external points, equation (3.26) becomes

$$\int \frac{dz d^3 \mathbf{x}}{z^4} (\mathbf{z}_1 \cdot \mathbf{z}_2)^J \sum_l b_l^{\hat{\Phi}} \sum_{n=0}^J C_{iil}^{(n)} \mathcal{H}_n \left(\frac{(\mathbf{z}_1 \cdot \mathbf{x})(\mathbf{z}_2 \cdot \mathbf{x})}{\mathbf{x}^2 (\mathbf{z}_1 \cdot \mathbf{z}_2)} \right) G_{\text{Bbb}}^{\Delta_l, n} \left(\frac{z^2}{\mathbf{x}^2 + z^2} \right) \Big|_{\log}. \quad (3.28)$$

In this configuration, all the terms in the expansion have the property of being traceless with respect to the full cross-trace, except for the $n = 0$ term:

$$(D_{\mathbf{z}_1} \cdot D_{\mathbf{z}_2})^J \left((\mathbf{z}_1 \cdot \mathbf{z}_2)^J \mathcal{H}_n \left(\frac{(\mathbf{z}_1 \cdot \mathbf{x})(\mathbf{z}_2 \cdot \mathbf{x})}{\mathbf{x}^2 (\mathbf{z}_1 \cdot \mathbf{z}_2)} \right) \right) = 0, \quad n \neq 0. \quad (3.29)$$

This implies that, once indices are opened, each of these terms is proportional to one or more terms in the form

$$\left(\delta^{a_1 a_2} - d \frac{\mathbf{x}^{a_1} \mathbf{x}^{a_2}}{\mathbf{x}^2} \right), \quad (3.30)$$

which give vanishing contribution when integrated over \mathbf{x} by Lorentz invariance. Then, we deduce that the only non-vanishing contribution after integration comes from the $n = 0$ term. This property clearly needs to be true in any configuration.¹¹ equation (3.26) then reduces to

$$\frac{(H_{1,2})^J}{P_{12}^{\Delta_i + J}} \sum_l b_l^{\hat{\Phi}} C_{iil}^{(0)} \int_X G_{\text{Bbb}}^{\Delta_l, \Delta_i, \Delta_i}(\chi) \Big|_{\log}, \quad (3.31)$$

where we used

$$\mathcal{H}_0(v) = 1, \quad G_{\text{Bbb}}^{\Delta_l, 0}(\chi) = G_{\text{Bbb}}^{\Delta_l, \Delta_i, \Delta_i}(\chi), \quad (3.32)$$

where $G_{\text{Bbb}}^{\Delta_l, \Delta_i, \Delta_i}(\chi)$ is the scalar bulk-boundary-boundary block. The tensor structure then simplifies with that of the two-point function in the denominator, and we recover again the integral in $I_{\text{Bbb}}^{\Delta_l, \Delta_i, \Delta_i}$. This implies

$$\frac{d\Delta_i}{d\lambda} = \sum_l b_l^{\hat{\Phi}} C_{iil}^{(0)} \mathcal{I}(\Delta_l), \quad (3.33)$$

with $\mathcal{I}(\Delta)$ given in equation (3.21).

¹¹We explicitly checked that this is true in a generic frame by performing the integral in embedding coordinates in the cases of $J = 1$, $J = 2$ and $J = 3$.

Local blocks As anticipated, to avoid the divergence of the series in the right-hand side of the flow equation, we can use local instead of standard blocks. In practice, this consists in replacing the standard block in (3.11) with the expression of the local block reported in (2.69). With an analogous computation to that presented in appendix B.1, we get that in this setup the variation of the scaling dimension can be expressed as in (3.20), but with $\mathcal{I}(\Delta)$ now replaced with

$$\mathcal{I}^\alpha(\Delta_l) = \frac{\pi^{d/2} \Delta_l \Gamma(\alpha) \Gamma(\alpha - \frac{d}{2}) \Gamma(1 - \frac{d}{2} + \Delta_l)}{(\Delta_l - d) \Gamma(\alpha - \frac{\Delta_l}{2}) \Gamma(\alpha - \frac{d}{2} + \frac{\Delta_l}{2}) \Gamma(1 + \frac{\Delta_l}{2})^2}. \quad (3.34)$$

This is true both for the scalar and the spinning cases.

3.2 Flow of BOE coefficients

Let us now examine the bulk-boundary two-point function

$$\langle \mathcal{O}_i(\mathbf{x}_1) \hat{\Phi}(\mathbf{x}_2, z_2) \rangle_\lambda = b_i^{\hat{\Phi}}(\lambda) \left(\frac{z_2}{\mathbf{x}_{12}^2 + z_2^2} \right)^{\Delta_i(\lambda)}, \quad (3.35)$$

to extract the flow equation for the BOE coefficients $b_i^{\hat{\Phi}}$. We only restrict to the case in which the bulk operator is the deforming operator $\hat{\Phi}$ because this is sufficient to obtain a closed system of differential equations describing the RG flow. Now, following the logic of the previous section, we introduce an infinitesimal shift $\delta\lambda$ to the bulk coupling. Under this shift, both the BOE coefficient and the dimension of the boundary operator get shifted. Moreover, while both bulk and boundary operators generically renormalize, we focus here on the scenario where only the boundary operators do so. Below, we outline the conditions required for this realization, postponing the analysis of the general case to section 7.1.2. The shift then gives

$$\begin{aligned} \langle \mathcal{O}_i^{(\text{bare})}(\mathbf{x}_1) \hat{\Phi}(z_2, \mathbf{x}_2) \rangle_{\lambda+\delta\lambda} &= \sum_j \sum_{n=0}^{\infty} \mathcal{Z}_{ij;n} \square_{\mathbf{x}_1}^n \langle \mathcal{O}_j^{(\text{ren})}(\mathbf{x}_1) \hat{\Phi}(z_2, \mathbf{x}_2) \rangle_{\lambda+\delta\lambda} \\ &= \left(\frac{z_2}{\mathbf{x}_{12}^2 + z_2^2} \right)^{\Delta_i(\lambda)} \left[b_i^{\hat{\Phi}} + b_i^{\hat{\Phi}} \delta\Delta_i \log \left(\frac{z_2}{\mathbf{x}_{12}^2 + z_2^2} \right) + \delta b_i^{\hat{\Phi}} \right] \\ &\quad + \sum_j \sum_{n=0}^{\infty} b_j^{\hat{\Phi}} \delta \mathcal{Z}_{ij;n} \square_{\mathbf{x}_1}^n \left(\frac{z_2}{\mathbf{x}_{12}^2 + z_2^2} \right)^{\Delta_j(\lambda)}. \end{aligned} \quad (3.36)$$

On the other side, we can express the change in the bulk-boundary two-point function in perturbation theory as

$$\langle \mathcal{O}_i^{(\text{bare})}(\mathbf{x}_1) \hat{\Phi}(z_2, \mathbf{x}_2) \rangle_{\lambda+\delta\lambda} = \langle \mathcal{O}_i(\mathbf{x}_1) \hat{\Phi}(z_2, \mathbf{x}_2) \rangle_\lambda - \delta\lambda \int \frac{dz d^d \mathbf{x}}{z^{d+1}} \langle \mathcal{O}_i(\mathbf{x}_1) \hat{\Phi}(z_2, \mathbf{x}_2) \hat{\Phi}(z, \mathbf{x}) \rangle_\lambda + \dots, \quad (3.37)$$

The last integral generically diverges as the integrated bulk point approaches the boundary point \mathbf{x}_1 . Similarly to what we did in the previous section, we then regularize the integral

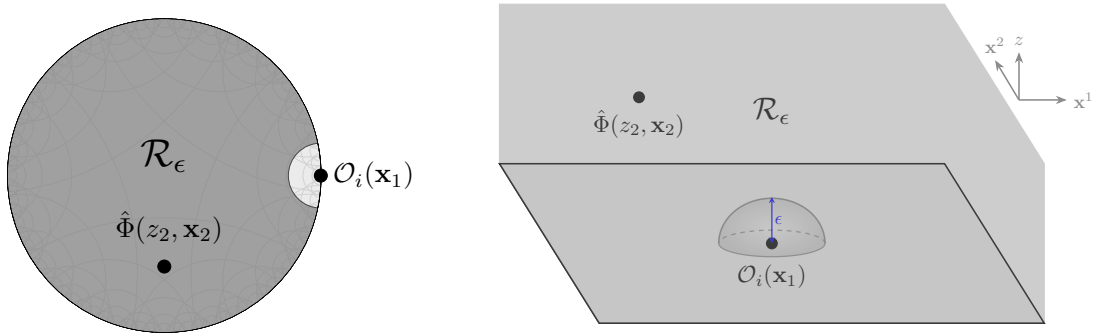


Figure 7. The domain of integration \mathcal{R}_ϵ in (3.38) in ball and half-plane coordinates. We remove the half-ball centered at the position \mathbf{x}_1 of the boundary operator to regulate the IR divergence arising when the integrated bulk field hits this point. There is no UV divergence when the integration point hits the other bulk insertion when assumption (3.41) is satisfied. We discuss how to move past this assumption in section 7

by removing the half-ball around \mathbf{x}_1 , which gives

$$I_i^{\hat{\Phi}\hat{\Phi}}(\mathbf{x}_1, \mathbf{x}_2, z_2, \epsilon) := \int_{\mathcal{R}_\epsilon} \frac{dz d^d \mathbf{x}}{z^{d+1}} \langle \mathcal{O}_i(\mathbf{x}_1) \hat{\Phi}(z_2, \mathbf{x}_2) \hat{\Phi}(z, \mathbf{x}) \rangle_\lambda. \quad (3.38)$$

where \mathcal{R}_ϵ is the region defined by $(\mathbf{x} - \mathbf{x}_1)^2 + z^2 > \epsilon^2$, represented in figure 7.

As anticipated, this is not the only divergence of this integral. Indeed, the integral might also diverge when the integrated point approaches the other bulk point (z_2, \mathbf{x}_2) . This limit is controlled by the UV bulk OPE:

$$\hat{\Phi}(z, \mathbf{x}) \hat{\Phi}(z_2, \mathbf{x}_2) \approx \sum_{\hat{\mathcal{O}}} C_{\hat{\mathcal{O}}\hat{\Phi}\hat{\Phi}}^{\text{UV}} \sum_{n=0}^{\infty} c_n \left(\frac{z z_2}{(z - z_2)^2 + (\mathbf{x} - \mathbf{x}_2)^2} \right)^{\Delta_{\hat{\Phi}}^{\text{UV}} - \frac{\Delta_{\hat{\mathcal{O}}}^{\text{UV}}}{2} - n} \hat{\mathcal{O}}(z_2, \mathbf{x}_2), \quad (3.39)$$

where $\Delta_{\hat{\mathcal{O}}}^{\text{UV}}$ and $C_{\hat{\mathcal{O}}\hat{\Phi}\hat{\Phi}}^{\text{UV}}$ are the CFT data of the bulk UV theory, and n labels curvature corrections to the flat space OPE. The sum over $\hat{\mathcal{O}}$ is taken to run over both primaries and descendants, but we focus on scalars for simplicity. The contribution of spinning operators in the bulk OPE would be killed by choosing a rotationally invariant regulator around (z_2, \mathbf{x}_2) . Notice that the contribution of the identity is zero because $\langle \mathcal{O}_i \rangle = 0$.

Now, using this OPE in (3.37), let us examine the region of integration near (z_2, \mathbf{x}_2) . For that purpose, we change integration variables to $r = \sqrt{(z - z_2)^2 + (\mathbf{x} - \mathbf{x}_2)^2}$ and angular variables which will not be important. The integral in the region close to (z_2, \mathbf{x}_2) is dominated by the contribution of the bulk operator with the minimal scaling dimension $\Delta_{\hat{\mathcal{O}}}^{\text{UV}}$ and in particular by the $n = 0$ term

$$\sim \int_0^\epsilon r^{d-2\Delta_{\hat{\Phi}}^{\text{UV}} + \min(\Delta_{\hat{\mathcal{O}}}^{\text{UV}})}. \quad (3.40)$$

We can thus state that this integral does not suffer from bulk UV divergences if

$$\Delta_{\hat{\Phi}}^{\text{UV}} < \frac{1}{2} \left(d + 1 + \min_{\hat{\mathcal{O}} \in \hat{\Phi} \times \hat{\Phi}} \Delta_{\hat{\mathcal{O}}}^{\text{UV}} \right). \quad (3.41)$$

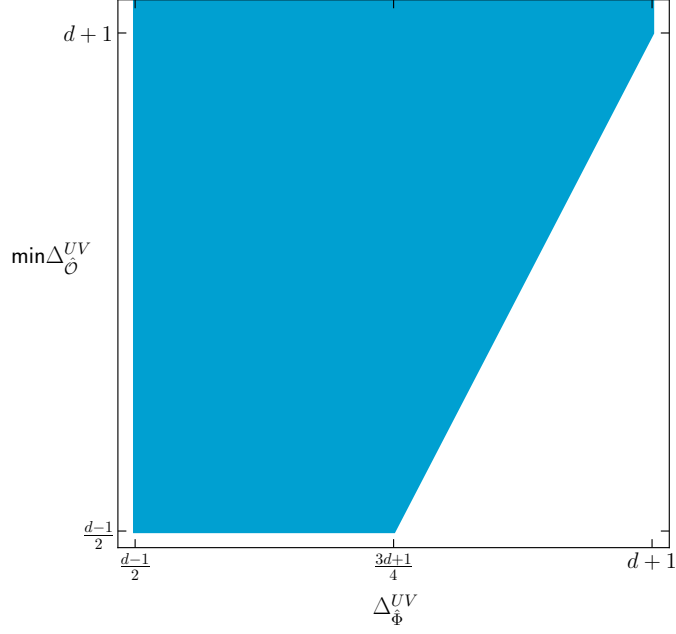


Figure 8. When the lightest bulk relevant operator of the theory appearing in the bulk OPE of the deforming operator $\hat{\Phi} \times \hat{\Phi}$ has UV scaling dimension $\Delta_{\hat{\mathcal{O}}}^{\text{UV}}$ that lies in the blue shape, there are no UV divergences in the derivation of the BOE flow equation. The lower bound $\frac{d-1}{2}$ is the UV unitarity bound. In this section, we assume our theory lies in the blue shape. We discuss how to drop this assumption in section 7.1.2.

We note that if all bulk operators in the UV other than $\hat{\Phi}$ are irrelevant, this inequality is satisfied. If there are some relevant operators other than $\hat{\Phi}$, this is a nontrivial constraint. In figure 8 we plot the values of $\Delta_{\hat{\mathcal{O}}}^{\text{UV}}$ and $\min(\Delta_{\hat{\mathcal{O}}}^{\text{UV}})$ for which this integral is UV finite. In the rest of this section, we will assume our QFT lives in that region. We will discuss extensions of this assumption in section 7.1.2.

Let us now go back to the integral in (3.38). We begin by re-expressing the integrand in terms of the bulk-bulk-boundary block introduced in (2.54). We then obtain

$$I_i^{\hat{\Phi}\hat{\Phi}}(\mathbf{x}_1, \mathbf{x}_2, z_2, \epsilon) = \left(\frac{z_2}{\mathbf{x}_{12}^2 + z_2^2} \right)^{\Delta_i} \int_{\mathcal{R}_\epsilon} \frac{dz d^d \mathbf{x}}{z^{d+1}} \sum_{j,l} b_l^{\hat{\Phi}} b_j^{\hat{\Phi}} C_{lij} G_{\text{BBb}}^{\Delta_l, \Delta_j, \Delta_i}(\xi, \rho). \quad (3.42)$$

Assuming that the sum and the integral can be exchanged, with a similar caveat to that presented below equation (3.11), we get

$$I_i^{\hat{\Phi}\hat{\Phi}}(\mathbf{x}_1, \mathbf{x}_2, z_2, \epsilon) = \left(\frac{z_2}{\mathbf{x}_{12}^2 + z_2^2} \right)^{\Delta_i} \sum_{j,l} b_l^{\hat{\Phi}} b_j^{\hat{\Phi}} C_{lij} I_{\text{BBb}}^{\Delta_l, \Delta_j, \Delta_i}(\mathbf{x}_1, \mathbf{x}_2, z_2, \epsilon), \quad (3.43)$$

where we have introduced the bulk-bulk-boundary integrated block

$$I_{\text{BBb}}^{\Delta_l, \Delta_j, \Delta_i}(\mathbf{x}_1, \mathbf{x}_2, z_2, \epsilon) = \int_{\mathcal{R}_\epsilon} \frac{dz d^d \mathbf{x}}{z^{d+1}} G_{\text{BBb}}^{\Delta_l, \Delta_j, \Delta_i}(\xi, \rho). \quad (3.44)$$

The above integral is finite for $\Delta_j > \Delta_i$, so we can compute it explicitly in this regime and then analytically continue the result to other values of Δ_i, Δ_j . We refer to appendix B.2 for the details, and report here the final result, which reads

$$\begin{aligned}
I_i^{\hat{\Phi}\hat{\Phi}}(\mathbf{x}_1, \mathbf{x}_2, z_2, \epsilon) = & - \left(\frac{z_2}{\mathbf{x}_{12}^2 + z_2^2} \right)^{\Delta_i} \sum_{j,l} b_l^{\hat{\Phi}} b_j^{\hat{\Phi}} C_{lij} [\mathcal{J}_{\Delta_i}(\Delta_l, \Delta_j)]_{\text{reg}} \\
& - b_i^{\hat{\Phi}} \left(\frac{z_2}{\mathbf{x}_{12}^2 + z_2^2} \right)^{\Delta_i} \sum_l b_l^{\hat{\Phi}} C_{iil} \mathcal{I}(\Delta_l) \log \left(\frac{z_2 \epsilon}{\mathbf{x}_{12}^2 + z_2^2} \right) \\
& - \sum_{j \neq i} \sum_{n=0}^{\infty} b_j^{\hat{\Phi}} \frac{\delta \mathcal{Z}_{ij;n}}{\delta \lambda} \square_{\mathbf{x}_1}^n \left(\frac{z_2}{\mathbf{x}_{12}^2 + z_2^2} \right)^{\Delta_j(\lambda)}.
\end{aligned} \tag{3.45}$$

where $[\mathcal{J}_{\Delta_i}(\Delta_l, \Delta_j)]_{\text{reg}}$ denotes the quantity

$$\mathcal{J}_{\Delta_i}(\Delta_l, \Delta_j) = - \frac{\pi^{d/2} \Gamma\left(\frac{\Delta_{ji}}{2}\right) \Gamma\left(\Delta_l - \frac{d-2}{2}\right) \Gamma\left(\Delta_j - \frac{d-2}{2}\right) \Gamma\left(\frac{\Delta_l-d}{2}\right)}{\Delta_l \Gamma\left(\frac{\Delta_l}{2}\right) \Gamma\left(\frac{\Delta_{lj}}{2}\right) \Gamma\left(\frac{\Delta_l+\Delta_j-d+2}{2}\right) \Gamma\left(\frac{\Delta_{lj}-d+2}{2}\right)}, \tag{3.46}$$

with the pole at $\Delta_j = \Delta_i$ subtracted:

$$[\mathcal{J}_{\Delta_i}(\Delta_l, \Delta_j)]_{\text{reg}} := \oint_{\Delta_j} \frac{d\Delta}{2\pi i} \frac{\mathcal{J}_{\Delta_i}(\Delta_l, \Delta)}{\Delta - \Delta_j}. \tag{3.47}$$

From here on, we drop the subscript ‘‘reg’’ and always understand the quantity $\mathcal{J}_{\Delta_i}(\Delta_l, \Delta_j)$ to be regularized in this manner. Replacing everything in (3.37) and comparing with (3.36), we find that the counterterm contributions cancel each other out, while the variation of the scaling dimension is canceled by the sum over l in the second row of (3.45), by means of the first flow equation in (3.20). The final result is a differential equation for the BOE coefficients, which reads

$$\frac{db_i^{\hat{\Phi}}}{d\lambda} = \sum_{l,j} b_l^{\hat{\Phi}} b_j^{\hat{\Phi}} C_{ijl} \mathcal{J}_{\Delta_i}(\Delta_l, \Delta_j). \tag{3.48}$$

The equation involves only scalars, because $\hat{\Phi}$ is a bulk scalar.

Note that the above equation holds for all boundary operators, even for the identity $\mathcal{O}_i = \mathbb{1}$, for which the equation provides the evolution of the vacuum expectation value (vev) of $\hat{\Phi}$. In practice, in the derivation of both flow equations we implicitly subtracted the vev of $\hat{\Phi}$ by never considering the identity $\mathbb{1}$ in the sums over boundary operators in the BOE of $\hat{\Phi}$. Had we not done that, we would have obtained contributions from integrals of the form

$$\int_{\text{AdS}} dX \langle \mathbb{1}(X)(\dots) \rangle = \text{Vol}(\text{AdS}) \langle (\dots) \rangle = \infty. \tag{3.49}$$

We thus always fix

$$b_{\mathbb{1}}^{\hat{\Phi}} \equiv 0, \tag{3.50}$$

for all values of the bulk coupling.

Local blocks As for the first flow equation, we can replace standard blocks with local blocks to obtain a generalized version of the equation in (3.48) with better convergence properties. The result is the same, with $\mathcal{J}_{\Delta_i}(\Delta_l, \Delta_j)$ replaced with

$$\begin{aligned} \mathcal{J}_{\Delta_i}^{(\alpha)}(\Delta_l, \Delta_j) = & -\frac{2\pi^{d/2}\Gamma(\alpha - \frac{d}{2})\Gamma(\alpha + \frac{\Delta_{ij}}{2})\Gamma(1 - \frac{d}{2} + \Delta_j)}{\Delta_{ji}(\Delta_l - d)\Gamma(\frac{2-d+\Delta_j+\Delta_i}{2})\Gamma(\alpha - \frac{\Delta_l}{2})\Gamma(\frac{\Delta_{lj}}{2})} \\ & \times \frac{\Gamma(1 - \frac{d}{2} + \frac{\Delta_l}{2})}{\Gamma(\alpha - \frac{d}{2} + \frac{\Delta_{ij}}{2})} {}_3F_2\left(\frac{\Delta_l-d}{2}, \alpha + \frac{\Delta_l-d}{2}, \frac{\Delta_{ilj}}{2}; 1\right), \end{aligned} \quad (3.51)$$

which is meant to be regularized as explained in (3.47).

3.3 Closing the system with crossing

In order to have a closed set of equations, [1] also derived a flow equation for $\frac{dC_{ijk}}{d\lambda}$ in AdS₂ by studying how the three-point function of boundary operators varies under a change in coupling of the bulk relevant deformation. The result depended on a kinematic function \mathcal{K} which is the regulated integral of a bulk-boundary-boundary-boundary conformal block, and which is only known through a complicated integral representation. Here, we do not follow that route, due to the increased difficulty in higher dimensions and the inefficacy of the numerical evaluation of the final result, even in 2D. Nevertheless, we study some properties of that equation in higher dimensions in appendix C.

Instead, we propose using crossing. The crossing equation, at the basis of the modern conformal bootstrap [46], is obtained by decomposing four-point functions of conformal primaries by taking the OPE with two different pairings and equating the result. Let us discuss the AdS₃ and AdS₄ cases separately

AdS₃ In AdS₃, as discussed in the preliminaries, there is only one OPE coefficient for a triplet of boundary operators. In the flow equation for the scaling dimensions, the OPE coefficients C_{lji} appear, with \mathcal{O}_l being a scalar operator and \mathcal{O}_i can be a scalar or a spinning operator. The flow equation for the BOE coefficients (3.48) instead features the OPE coefficients C_{lij} , where all three operators are scalars. Since the OPE of two scalars contains spinning operators, the equations do not close if we only consider crossing with external scalars. In fact, we need to know the scaling dimension of the exchanged spinning operators, which would be evolved by the first flow equation (3.8). This then requires knowing the OPE coefficients with two spinning operators and a scalar. Hence, the minimal way to close the system of equations is to consider crossing for the four-point function $\langle \mathcal{O}_i(0,0)\mathcal{O}_i(\eta,\bar{\eta})\mathcal{O}_j(1,1)\mathcal{O}_j(\infty,\infty) \rangle$ in the case where \mathcal{O}_i and \mathcal{O}_j are both scalars, and the case where one of them has spin. Following the discussion in section 2.3.4, taking into account all prefactors, the associated crossing equation becomes

$$\sum_l \left(C_{lij}^2 \mathcal{F}_{i,j,l}^t(\eta, \bar{\eta}) - C_{iil} C_{ljj} \mathcal{F}_{i,j,l}^s(\eta, \bar{\eta}) \right) = \mathcal{F}_{i,j,1}^s(\eta, \bar{\eta}) \quad (3.52)$$

where

$$\begin{aligned}\mathcal{F}_{i,j,l}^s(\eta, \bar{\eta}) &\equiv G_{h_i, \bar{h}_i}^{iijj}(\eta, \bar{\eta}) \\ \mathcal{F}_{i,j,l}^t(\eta, \bar{\eta}) &\equiv \frac{\eta^{2h_i} \bar{\eta}^{2\bar{h}_i}}{(1-\eta)^{h_i+h_j} (1-\bar{\eta})^{\bar{h}_i+\bar{h}_j}} G_{h_i, \bar{h}_i}^{jijj}(1-\eta, 1-\bar{\eta})\end{aligned}\quad (3.53)$$

and the conformal blocks $G_{h_m, \bar{h}_m}^{lijk}$ are reported explicitly in (2.63).

AdS₄ In AdS₄, we have more complications. Triplets of boundary operators have many independent OPE coefficients. The first equation involves $C_{l_{ii}}^{(0)}$, where \mathcal{O}_i can have spin and \mathcal{O}_l is a scalar. The BOE flow equation involves only scalars. Analogously with what we discussed for AdS₃, the minimal way to close the flow equations is to consider crossing for four-point functions of the kind $\langle \mathcal{O}_i \mathcal{O}_i \mathcal{O}_j \mathcal{O}_j \rangle$ in cases where \mathcal{O}_i and \mathcal{O}_j are both scalars, and cases where one of them has spin. Here we write the equations for the case where \mathcal{O}_j has spin. Crossing then reads

$$\sum_l \left(\sum_{a,b} C_{l_{ij}}^{(a)} C_{l_{ij}}^{(b)} \mathcal{F}_{i,j,l;I}^{t(a,b)}(v, u) - C_{l_{ii}} \sum_c C_{l_{jj}}^{(c)} \mathcal{F}_{i,j,l;I}^{s(c)}(u, v) \right) = \mathcal{F}_{i,j,\mathbb{1};I}^{s(c)}(u, v), \quad (3.54)$$

where the index I labels 4-point tensor structures, while the latin indices a, b, c label 3-point tensor structures. The blocks \mathcal{F} are not known in closed form, but they can be computed through recursion relations [42–45].

3.4 Convergence of sums in the flow equations

Any practical application of the flow equations (1.3) will have to deal with the issue that the sums over boundary operators must be truncated. The convergence of these sums is thus an important aspect that needs to be studied. Here we will consider the convergence of these sums when the coefficients \mathcal{I} and \mathcal{J} are standard and local conformal blocks. In the free theory checks described in section 4, we will show that suitably defined Padé approximants of the partial sums over standard blocks converge fastest. We will explain this fact in section 5, where we also discuss possible generalizations of this property to interacting theories.

For our discussion, it will be useful to consider the universal large Δ_l behavior of the QFT data, which we derive in appendix D using Tauberian theorems:

$$\left| b_l^{\hat{\Phi}} \right| \Delta_l \xrightarrow{\Delta_l \rightarrow \infty} \Delta_l^{\Delta_{\hat{\Phi}}^{\text{UV}} - \frac{d+2}{4}}, \quad |C_{lij}| \Delta_l \xrightarrow{\Delta_l \rightarrow \infty} 2^{-\Delta_l} \Delta_l^{\Delta_i + \Delta_j - \frac{3d}{4}}. \quad (3.55)$$

where in all estimates we omit numerical pre-factors.

3.4.1 Flow of scaling dimensions

The flow equation describing the evolution of the scaling dimensions reads

$$\frac{d\Delta_i}{d\lambda} = \sum_l b_l^{\hat{\Phi}} C_{l_{ii}} \mathcal{I}(\Delta_l). \quad (3.56)$$

Studying the explicit expression of \mathcal{I} (3.21), using (3.55) we can estimate the absolute convergence of the sum, giving us a sufficient condition for convergence. Treating the sum as an integral over a smooth density, we find

$$\sum_l^{l_{\max}} \left| b_l^{\hat{\Phi}} C_{lii} \mathcal{I}(\Delta_l) \right| \stackrel{\Delta_{l_{\max}} \rightarrow \infty}{\sim} \int^{\Delta_{l_{\max}}} d\Delta_l \Delta_l^{2\Delta_i + \Delta_{\hat{\Phi}}^{\text{UV}} - \frac{3d}{2} - 1} \sim \Delta_{l_{\max}}^{2\Delta_i + \Delta_{\hat{\Phi}}^{\text{UV}} - \frac{3d}{2}}, \quad (3.57)$$

which implies the sum involved in the flow equation of $\frac{d\Delta_i}{d\lambda}$ converges absolutely only if

$$2\Delta_i + \Delta_{\hat{\Phi}}^{\text{UV}} < \frac{3d}{2}, \quad (3.58)$$

a condition which is violated by most boundary operators \mathcal{O}_i .

One way to render these sums absolutely convergent is to use local blocks, leading to a modification of \mathcal{I} into expression (3.34). The summands then behave as

$$\sum_l^{l_{\max}} \left| b_l^{\hat{\Phi}} C_{lii} \mathcal{I}^\alpha(\Delta_l) \right| \stackrel{\Delta_{l_{\max}} \rightarrow \infty}{\sim} \Delta_{l_{\max}}^{2\Delta_i + \Delta_{\hat{\Phi}}^{\text{UV}} - d + 1 - 2\alpha}, \quad (3.59)$$

leading to a power-law convergent sum when we choose $\alpha > \Delta_i + \frac{\Delta_{\hat{\Phi}}^{\text{UV}} - d + 1}{2}$.

We can choose the coefficient α to depend on the truncation $\Delta_{l_{\max}}$. Following appendix F.3.2 from [1], we find the same optimal relation found there

$$\alpha_{\text{optimal}} = \frac{\Delta_{l_{\max}}}{2}. \quad (3.60)$$

3.4.2 Flow of BOE coefficients

The flow equation describing the evolution of the BOE coefficients reads

$$\frac{db_i^{\hat{\Phi}}}{d\lambda} = \sum_l \sum_j b_l^{\hat{\Phi}} b_j^{\hat{\Phi}} C_{lij} \mathcal{J}_{\Delta_i}(\Delta_l, \Delta_j). \quad (3.61)$$

We will treat the two sums as follows: first we fix j and consider the sum over l , then we carry out the sum over j . In practice that means we will always choose a much larger truncation for Δ_l than Δ_j . Using (3.55) and the explicit expression of \mathcal{J} (3.46), the fixed- j large Δ_l asymptotic behavior is the same as in the scaling dimension flow

$$\sum_l^{l_{\max}} \left| b_l^{\hat{\Phi}} b_j^{\hat{\Phi}} C_{lij} \mathcal{J}_{\Delta_i}(\Delta_l, \Delta_j) \right| \stackrel{\Delta_{l_{\max}} \rightarrow \infty}{\sim} \Delta_{l_{\max}}^{\Delta_i + \Delta_j + \Delta_{\hat{\Phi}}^{\text{UV}} - \frac{3d}{2}} \quad (3.62)$$

hence the sum for fixed Δ_j converges absolutely if

$$\Delta_i + \Delta_j + \Delta_{\hat{\Phi}}^{\text{UV}} < \frac{3d}{2}, \quad (3.63)$$

which is generically not satisfied, especially since we have to sum over Δ_j . For fixed Δ_l , the sum over j behaves as

$$\sum_j^{j_{\max}} \left| b_l^{\hat{\Phi}} b_j^{\hat{\Phi}} C_{lij} \mathcal{J}_{\Delta_i}(\Delta_l, \Delta_j) \right| \stackrel{\Delta_{j_{\max}} \rightarrow \infty}{\sim} \Delta_{j_{\max}}^{\Delta_i + \Delta_{\hat{\Phi}}^{\text{UV}} - \frac{d}{2}} \quad (3.64)$$

With local blocks (3.51), the large Δ_l fixed Δ_j regime now gives

$$\sum_l^{l_{\max}} \left| b_l^{\hat{\Phi}} b_j^{\hat{\Phi}} C_{lij} \mathcal{J}_{\Delta_i}^\alpha(\Delta_l, \Delta_j) \right| \stackrel{\Delta_{l_{\max}} \rightarrow \infty}{\sim} \Delta_{l_{\max}}^{\Delta_i + \Delta_j + \Delta_{\hat{\Phi}}^{\text{UV}} - d - 2\alpha}, \quad (3.65)$$

Choosing an α which grows with Δ_j thus ensures absolute convergence of the fixed Δ_j sum. At the same time, the large Δ_j fixed Δ_l behavior is the same as with standard blocks

$$\sum_j^{j_{\max}} \left| b_l^{\hat{\Phi}} b_j^{\hat{\Phi}} C_{lij} \mathcal{J}_{\Delta_i}^\alpha(\Delta_l, \Delta_j) \right| \stackrel{\Delta_{j_{\max}} \rightarrow \infty}{\sim} \Delta_{j_{\max}}^{\Delta_i + \Delta_{\hat{\Phi}}^{\text{UV}} - \frac{d}{2}}. \quad (3.66)$$

We thus do not generically expect the double series in l and j to be absolutely convergent, even when using local blocks. In practice, we observe that choosing a truncation such that $l_{\max} \gg j_{\max}$ leads to convergent sums in our checks in section 4, while the opposite ordering of truncations does not. As we will discuss in section 5, using Padé approximants gives convergent sums even with symmetric truncations.

4 Checks in free theories

The flow equations (1.3) apply to any QFT in AdS realized as a relevant deformation of a UV CFT. In free theories, we can check their validity explicitly at any arbitrary value of the coupling, which will be taken to be the mass of the free field in units of the AdS radius. Here, we quantify the relative errors obtained by comparing the truncated flow equations to the expected analytic results for the derivatives of the CFT data for some value of the mass. We will compare the usage of standard conformal blocks, local blocks, and Padé approximants of both. Surprisingly we find that, despite the fact that the sequence of partial sums of integrated standard blocks does not converge, the sequences of their Padé approximants are the ones that converge fastest. We explain this fact in section 5.

In this section, for any partial sum S_a defined by truncating the flow equations (1.3), we quantify the relative error from the analytic expression of the derivative of a piece of QFT data a as

$$\text{err}_a(l_{\max}) \equiv \left| \frac{\frac{da}{d\lambda} - S_a(l_{\max})}{\frac{da}{d\lambda}} \right|, \quad a = \Delta_i \text{ or } b_i^{\hat{\Phi}}. \quad (4.1)$$

Throughout this section, we will use \mathcal{I} and \mathcal{J} to indicate integrated blocks, whether standard (3.21), (3.46) or local (3.34), (3.51). The plot legends will state whether a certain curve was obtained with standard or local blocks. All plots can be reproduced with the attached Mathematica notebook.

4.1 Flow of scaling dimensions

Here we present checks of the first flow equation; for conciseness we focus on AdS₄

$$\frac{d\Delta_i}{d\lambda} = \sum_l b_l^{\hat{\Phi}} C_{lii} \mathcal{I}(\Delta_l). \quad (4.2)$$

We specifically compare the convergence of the sum over boundary operators when using integrated standard conformal blocks and local blocks. We will indicate the partial sums as

$$S_i(l_{\max}) \equiv \sum_l^{l_{\max}} b_l^{\hat{\phi}} C_{lii} \mathcal{I}(\Delta_l). \quad (4.3)$$

We also compare these to Padé approximants, which we discuss in detail in section 5. Considering that in free theories the spectrum of scalars created by the bulk deformation is integer spaced $\Delta_l = 2\Delta_1 + 2l$, we define the function

$$f_{i,l_{\max}}(x) \equiv \sum_{l=0}^{l_{\max}} b_l^{\hat{\phi}} C_{lii} \mathcal{I}(\Delta_l) x^l \quad (4.4)$$

and consider the sequence of its diagonal Padé approximants (for a definition, see (5.3)) at $x = 1$

$$S_i^{\text{Padé}}(l_{\max}) \equiv \left[\left[\frac{l_{\max}}{2} \right] \right]_{f_{i,l_{\max}}} \quad (1) \quad (4.5)$$

4.1.1 Free scalar

Consider a free massive scalar in AdS_{d+1}

$$S = \frac{1}{2} \int \frac{dz d^d \mathbf{x}}{z^{d+1}} \left[\partial_\mu \hat{\phi} \partial^\mu \hat{\phi} + m^2 \hat{\phi}^2 \right], \quad (4.6)$$

where we absorbed the coupling between the scalar and the AdS curvature in the definition of m^2 . We will consider how the QFT data of this theory varies under an infinitesimal change of the dimensionless coupling

$$\lambda \equiv \frac{1}{2} m^2 R^2 \quad (4.7)$$

around an arbitrary value. This theory in particular includes the boundary primary operator ϕ , appearing in the BOE of the bulk operator $\hat{\phi}$, with scaling dimension

$$\Delta_\phi(\lambda) = \frac{d}{2} \pm \sqrt{\frac{d^2}{4} + 2\lambda}. \quad (4.8)$$

The choice of sign corresponds to the choice of boundary condition for the scalar (Dirichlet: +, Neumann: -), where Neumann exists and is unitary only for $-\frac{d^2}{8} < \lambda < \frac{4-d^2}{8}$ ¹², while Dirichlet exists for all $\lambda > -\frac{d^2}{8}$. We will also consider the boundary spin J primaries $[\phi^2]_{n,J}$ appearing for example in the OPE between two ϕ operators. Their scaling dimensions are

$$\Delta_{[\phi^2]_{n,J}}(\lambda) = 2\Delta_\phi(\lambda) + 2n + J \quad (4.9)$$

The flow equation for the scaling dimensions of ϕ reads

$$\frac{d\Delta_\phi}{d\lambda} = \frac{2}{2\Delta_\phi - d} = \sum_{n=0}^{\infty} b_{[\phi^2]_{n,0}}^{\hat{\phi}^2} C_{\phi\phi[\phi^2]_{n,0}} \mathcal{I}(\Delta_{[\phi^2]_{n,0}}), \quad (4.10)$$

¹²This upper bound assumes $d \geq 2$. For AdS_2 , Neumann exists and is unitary for $-\frac{1}{8} < \lambda < 0$

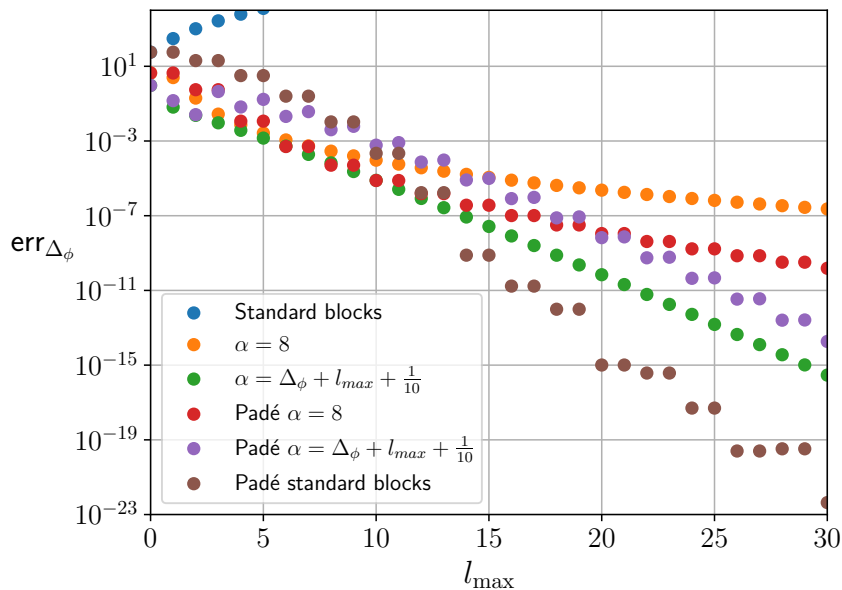


Figure 9. The relative error (4.1) of the partial sums in the scaling dimension flow equation reproducing the derivative of Δ_ϕ in free scalar theory in AdS₄ at the point $\lambda = \frac{1}{2}m^2R^2 = 4$. We compare the partial sum over integrated standard blocks, local blocks with fixed α , local blocks with $\alpha \propto l_{\max}$, and Padé approximants of all previous cases. The Padé approximants of the integrated standard blocks partial sums perform best.

where the coefficients $b_{[\phi^2]_{n,0}}^{\hat{\phi}^2}$ and $C_{\phi\phi[\phi^2]_{n,0}}$ are given explicitly in (E.4) and (E.5).

Notice that only the scalar double trace operators appear, due to the fact that the equation originates from the BOE of a scalar, $\hat{\phi}^2$.

In figure 9 we plot the relative errors of the partial sums for this flow equation in the case of AdS₄. We make the following observations:

- The sequence of partial sums over standard integrated blocks diverges, as expected.
- Padé approximants improve the behavior of the partial sums over local integrated blocks when α is fixed, but worsen it when α scales with l_{\max} .
- The sequence of partial sums which converges fastest is the one of Padé approximants of standard integrated blocks. Even though this is counterintuitive, we explain this fact in section 5.

In the free scalar theory we checked also $\frac{d\Delta_{[\phi^2]_{n,0}}}{d\lambda}$ for some values of n and $\frac{d\Delta_{\phi^3}}{d\lambda}$, and obtained the same qualitative behavior with comparable precision. The OPE coefficients relevant for these cases are reported in appendix E.

4.1.2 Free traceless symmetric tensor

Let us consider the flow of the scaling dimension of a boundary operator with spin. To exemplify this, we study the theory of a free traceless symmetric tensor in AdS₄

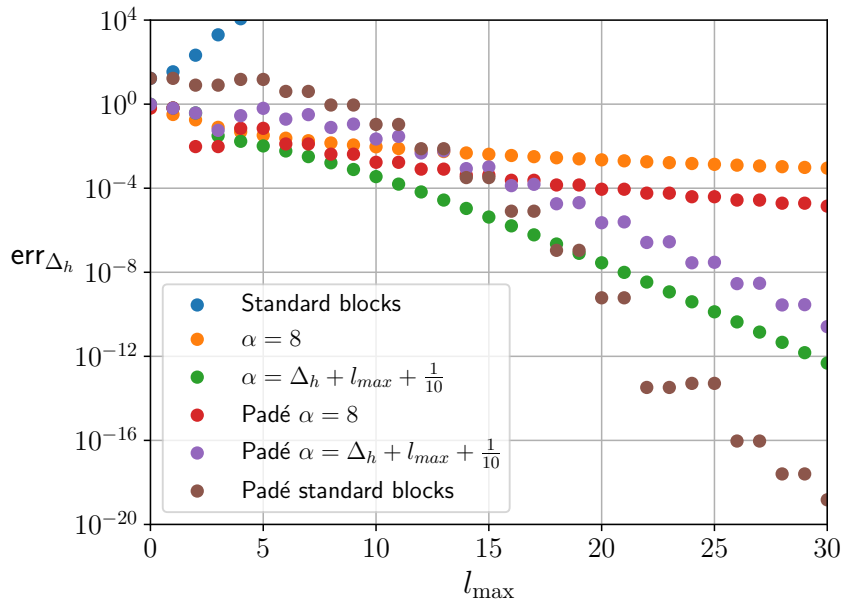


Figure 10. The relative error (4.1) of the partial sums in the scaling dimension flow equation reproducing the derivative of Δ_h in the theory of a free massive traceless symmetric tensor in AdS_4 at the point $\lambda = \frac{1}{2}m^2R^2 = 4$. We compare the partial sum over integrated standard blocks, local blocks with fixed α , local blocks with $\alpha \propto l_{\max}$, and Padé approximants of all previous cases. The Padé approximants of the integrated standard blocks partial sums perform best.

$$S = \frac{1}{2} \int \frac{dz d^3\mathbf{x}}{z^4} \left[\nabla_\mu \hat{h}^{\nu\alpha} \nabla^\mu \hat{h}_{\nu\alpha} - 2 \nabla^\mu \hat{h}^{\nu\alpha} \nabla_\alpha \hat{h}_{\mu\nu} + (m^2 + 6) \hat{h}_{\mu\nu} \hat{h}^{\mu\nu} \right], \quad (4.11)$$

where we chose the definition of m^2 such that in the limit $m^2 \rightarrow 0$ we get the action of the AdS linearized graviton (although one should restore terms proportional to $\hat{h}_\mu{}^\mu$ for gauge invariance).

Once again we will consider the derivatives of the QFT data as we vary the dimensionless mass $\lambda \equiv \frac{1}{2}m^2R^2$. In particular, we will focus on the spin 2 boundary operator h_{ab} appearing in the BOE of $\hat{h}_{\mu\nu}$, with scaling dimension

$$\Delta_h(\lambda) = \frac{3}{2} \pm \sqrt{\frac{9}{4} + 2\lambda} \quad (4.12)$$

where once again the sign corresponds to the choice of Dirichlet vs Neumann boundary conditions. We will focus on Dirichlet. We will need to consider also the boundary scalar primaries $[h^2]_{n,0}$ associated to the BOE of $\hat{h}_{\mu\nu} \hat{h}^{\mu\nu}$ with scaling dimensions

$$\Delta_{[h^2]_{n,0}} = 2\Delta_h(\lambda) + 2n. \quad (4.13)$$

The flow equation for the scaling dimensions of h_{ab} reads

$$\frac{d\Delta_h}{d\lambda} = \frac{2}{2\Delta_h - 3} = \sum_{n=0}^{\infty} b_{[h^2]_{n,0}}^{\hat{h}^2} C_{hh[h^2]_{n,0}}^{(0)} \mathcal{I}(\Delta_{[h^2]_{n,0}}), \quad (4.14)$$

where the product of the coefficients $b_{[h^2]_{n,0}}^{\hat{h}^2} C_{hh[h^2]_{n,0}}^{(0)}$ is given explicitly in (E.16).

Analyzing the sequence of partial sums, we find analogous behaviors as in the scalar case. We plot them in figure 10.

4.2 Flow of BOE coefficients

Now let us consider the second flow equation

$$\frac{db_i^{\hat{\phi}}}{d\lambda} = \sum_l \sum_j b_l^{\hat{\phi}} b_j^{\hat{\phi}} C_{ilj} \mathcal{J}_{\Delta_i}(\Delta_l, \Delta_j) \quad (4.15)$$

Since the deformation is taken to be a bulk scalar, only boundary scalar operators are involved in this equation. When only one of the sums is involved, like in the case where we evolve for example $b_{\phi}^{\hat{\phi}}$, the partial sums and their Padé approximants are defined as in the previous section. When two sums are involved, we need to carry out the sum over l first, and then the sum over j .

$$S_i(j_{\max}) \equiv \sum_j^{j_{\max}} \sum_l^{j+j_{\max}} b_l^{\hat{\phi}} b_j^{\hat{\phi}} C_{ilj} \mathcal{J}_{\Delta_i}(\Delta_l, \Delta_j) \quad (4.16)$$

The sequence of Padé approximants of the partial sums with standard blocks, instead, does not require this procedure, and so can be designed to include a smaller set of operators. Once again, since we are considering free theories we have $\Delta_l = 2\Delta_1 + 2l$ and similarly for Δ_j . Since there are two sums, we will proceed as follows: we define the functions

$$f_{i,j,l_{\max}}(x) \equiv \sum_{l=0}^{l_{\max}} b_l^{\hat{\phi}} b_j^{\hat{\phi}} C_{ilj} \mathcal{J}_{\Delta_i}(\Delta_l, \Delta_j) x^l, \quad (4.17)$$

and take their diagonal Padé approximants at $x = 1$, defined in (5.3)

$$S_{i,j}^{\text{Padé}}(l_{\max}) = \left[\left[\frac{l_{\max}}{2} \right] \right]_{f_{i,j,l_{\max}}} (1). \quad (4.18)$$

Then, we do the same again for the sum over j . We construct a function $g_{i,l_{\max}}(y)$ and construct its Padé approximants around $\epsilon = 0$, then evaluated at $y = 1$

$$g_{i,l_{\max}}(y) \equiv \sum_j^{l_{\max}} S_{i,j}^{\text{Padé}}(l_{\max}) y^j, \quad S_i^{\text{Padé}}(l_{\max}) = \left[\left[\frac{l_{\max}}{2} \right] \right]_{g_{i,l_{\max}}} (1). \quad (4.19)$$

These are the partial sums of which we plot the error for example in figure 12.

4.2.1 Free scalar

In the theory of a free scalar in AdS_{d+1} , with action (4.6), we can consider the evolution of the BOE coefficients of the bulk primaries $\hat{\phi}$ and $\hat{\phi}^2$. Since the BOE of $\hat{\phi}$ involves a single boundary primary operator, the associated flow equation only involves one sum

$$\frac{db_{\phi}^{\hat{\phi}}}{d\lambda} = b_{\phi}^{\hat{\phi}} \sum_{l=0}^{\infty} b_{[\phi^2]_{l,0}}^{\hat{\phi}^2} C_{\phi\phi[\phi^2]_{l,0}} \mathcal{J}_{\Delta_{\phi}}(\Delta_{[\phi^2]_{l,0}}, \Delta_{\phi}) \quad (4.20)$$

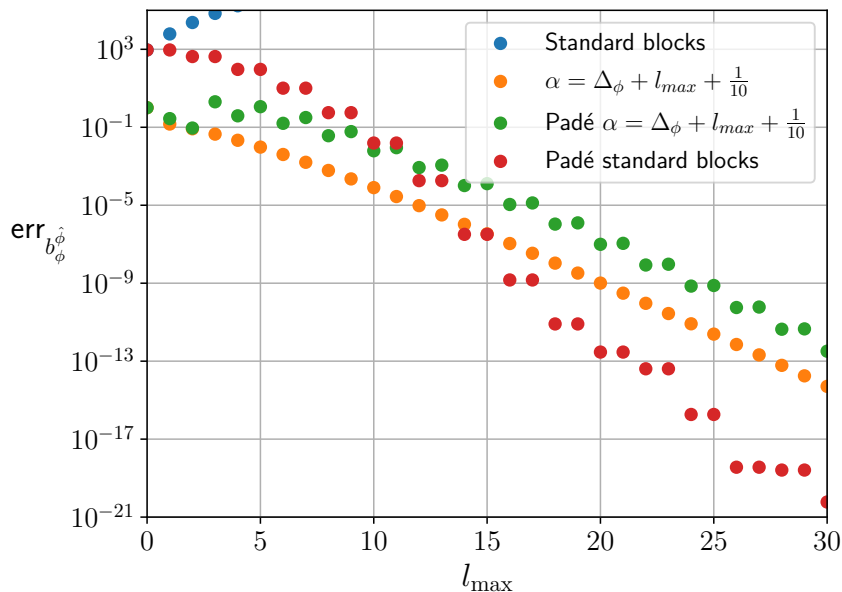


Figure 11. The relative error (4.1) of the partial sums in the BOE coefficient flow equation reproducing the derivative of $b_{\hat{\phi}}$ in the theory of a free massive scalar in AdS_4 at the point $\lambda = \frac{1}{2}m^2R^2 = 4$. We compare the partial sum over integrated standard blocks, local blocks with $\alpha \propto l_{\max}$, and Padé approximants of all previous cases. The Padé approximants of the integrated standard blocks partial sums perform best.

We plot the relative errors (defined in (4.1)) of the partial sums in figure 11. In this case standard blocks, local blocks and Padé approximants all behave similarly to the flow equation of the scaling dimensions.

A more emblematic example is that of the flow of $b_{\phi^2}^{\hat{\phi}}$. In this case, two sums are involved

$$\frac{db_{\phi^2}^{\hat{\phi}}}{d\lambda} = \sum_{l=0}^{\infty} \sum_{j=0}^{\infty} b_{[\phi^2]_{l,0}}^{\hat{\phi}} b_{[\phi^2]_{j,0}}^{\hat{\phi}} C_{\phi^2[\phi^2]_{l,0}[\phi^2]_{j,0}} \mathcal{J}_{\Delta_{\phi^2}}(\Delta_{[\phi^2]_{l,0}}, \Delta_{[\phi^2]_{j,0}}). \quad (4.21)$$

with the BOE and OPE coefficients given in (E.4) and (E.7) respectively. This case is where the Padé approximants bring the biggest improvement over local blocks. In figure 12 we show the error, defined in (4.1), of the partial sums truncated as described in (4.16) and of the Padé approximants (4.19). We explain the reason why Padé approximants work this well in these examples in section 5.

4.3 OPE coefficients from crossing

To fix the OPE coefficients at a given step in a numerical application of the flow equations, we advocate for the use of the crossing equation. Concretely, one can devise a numerical algorithm where the scaling dimensions of the boundary operators are evolved in an infinitesimal step from the first flow equation, and then crossing is solved with the updated spectrum. Here we exemplify that, when the spectrum is known, crossing can be reliably and cheaply solved with various numerical methods in this setting with good precision. Of

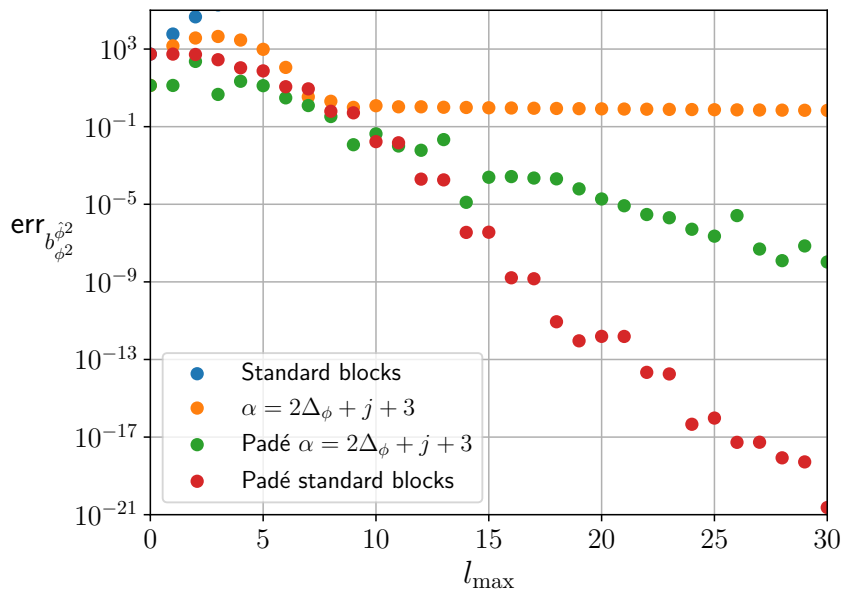


Figure 12. The relative error (4.1) of the partial sums in the BOE coefficient flow equation reproducing the derivative of $b_{\phi^2}^{j^2}$ in the theory of a free massive scalar in AdS_4 at the point $\lambda = \frac{1}{2}m^2R^2 = 4$. We compare the partial sum over integrated standard blocks, local blocks with $\alpha \propto j$, and their Padé approximants. Despite appearances, the orange dots are slowly decaying. It is evident that Padé approximants introduce a significant improvement over local blocks. Padé approximants of standard blocks perform best here too.

course, signs cannot be determined this way. One can argue that the signs are fixed by the previous step in the iterative solution of the ODEs, or that they can be checked, for example, using the linear sum rules (7.13). For now, we focus on determining the absolute values of the coefficients, and study cases with two identical operators. We postpone the development of more sophisticated numerical methods for non-identical operators and operators with spin to future works.

AdS₂ In the 2D case, using the expression of the blocks in 2.3.4, focusing on the case $\mathcal{O}_i = \mathcal{O}_j$, the crossing equation takes the form

$$\sum_m C_{im}^2 (G_{\Delta_m}^{iiii}(\zeta) - G_{\Delta_m}^{iiii}(1 - \zeta)) = G_0^{iiii}(1 - \zeta) - G_0^{iiii}(\zeta) \quad (4.22)$$

where we've separated the contribution of the identity by hand to highlight that we fixed $C_{i\mathbb{1}} = 1$ in line with our normalization for boundary two-point functions.

To solve for the OPE coefficients, we set up the following optimization problem. We choose a finite set of points ζ_n , we find it convenient to take them $\zeta_n \in (\frac{1}{4}, \frac{1}{2})$. Then, we build a matrix M and a vector b by choosing also a finite set of operators \mathcal{O}_m to sum over

$$M_{mn} \equiv G_{\Delta_m}^{iiii}(\zeta_n) - G_{\Delta_m}^{iiii}(1 - \zeta_n), \quad b_n \equiv G_0^{iiii}(1 - \zeta_n) - G_0^{iiii}(\zeta_n). \quad (4.23)$$

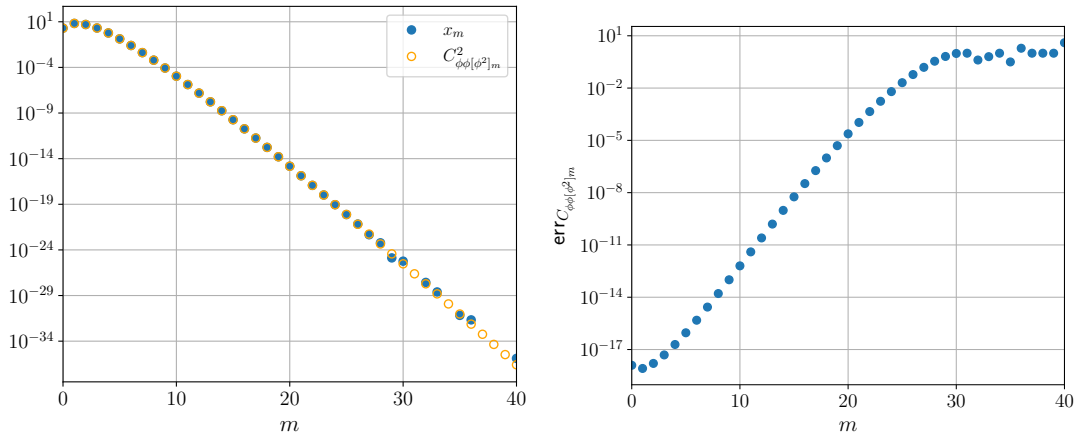


Figure 13. We show the numerical estimate x_m of the OPE coefficients $C_{\phi\phi[\phi^2]_m}$ in free scalar theory in AdS₂ obtained by solving the linear optimization problem (4.24) with $m_{\max} = 40$ states and $\Delta_\phi = \frac{27}{11}$ compared to the analytic value. On the left we compare the absolute values, on the right we show the relative error (4.25). We used Mathematica’s `LinearOptimization` function. The coefficients determined with most accuracy are those of the lightest operators. The missing blue dots on the left are $x_m = 0$ within the numerical accuracy we used.

Finally, we ask a linear optimizer (`LinearOptimization` on Mathematica) to find the vector x_m which minimizes the residuals, parametrized by a positive number δ

$$|(M \cdot x)_n - b_n| \leq \delta, \quad \forall n. \quad (4.24)$$

We then identify the solution x_m with the vector of approximate squared OPE coefficients C_{im}^2 .

In figure 13 we show the error with which we determine x_m in the free scalar theory, defined as

$$\text{err}_{C_{\phi\phi[\phi^2]_m}} = \left| \frac{x_m - C_{\phi\phi[\phi^2]_m}^2}{C_{\phi\phi[\phi^2]_m}^2} \right| \quad (4.25)$$

where x_m is the numerical vector determined by the optimizer. We truncated the double trace operators at $m_{\max} = 40$ and chose $\Delta_\phi = \frac{27}{11}$. The lightest OPE coefficients are determined with the greatest relative accuracy.

AdS₃ In the 3D case, following the discussion in section 2.3.4, the crossing equation for identical external operators reads

$$\sum_m C_{im}^2 \left(\tilde{G}_{\Delta_m, J_m}^{\Delta_i}(\eta, \bar{\eta}) - \tilde{G}_{\Delta_m, J_m}^{\Delta_i}(1 - \eta, 1 - \bar{\eta}) \right) = \tilde{G}_{0,0}^{\Delta_i}(\eta, \bar{\eta}) - \tilde{G}_{0,0}^{\Delta_i}(1 - \eta, 1 - \bar{\eta}) \quad (4.26)$$

where we are using that, when external operators are scalars, the OPE coefficients of operators related by parity can be collected, since $C_{i\bar{m}} = C_{im}$ in that case, and the blocks

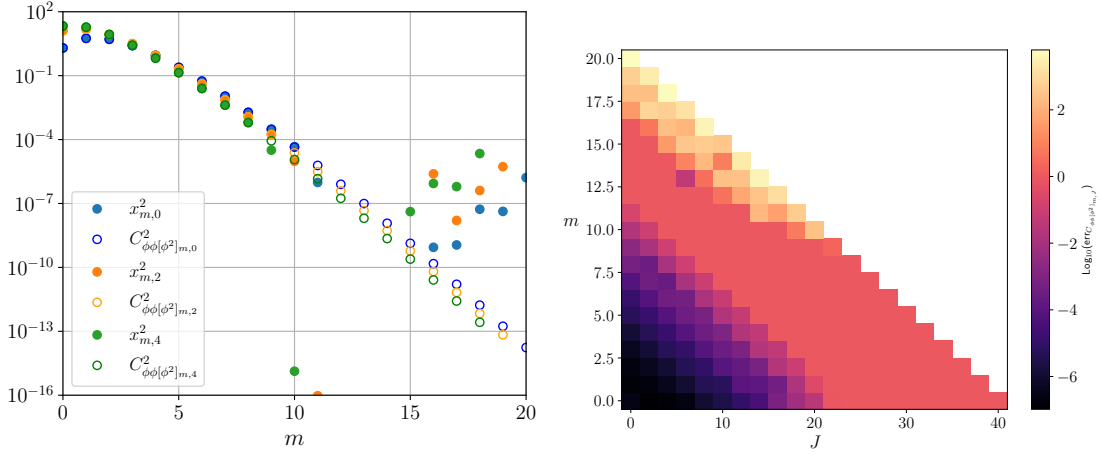


Figure 14. Numerical estimate of the OPE coefficients $C_{\phi|\phi^2|m,J}$ using Mathematica’s FindMinimum on the function (4.29) in free scalar theory in AdS₃ with $\Delta_\phi = \frac{37}{11}$. On the left, we compare the numerical values with the analytic ones in the cases $J = 0, 2, 4$. On the right, the relative errors (4.25). The lightest states are determined with the highest relative precision. The missing blue dots on the left are zero up to numerical precision.

simplify as follows¹³

$$\begin{aligned} \tilde{G}_{\Delta_m, J_m}^{\Delta_i}(\eta, \bar{\eta}) &= \frac{1}{1 + \delta_{0, J_m}} \frac{1}{(\eta \bar{\eta})^{\frac{2\Delta_i - \Delta_m + J_m}{2}}} \\ &\times \left[\eta^{J_m} {}_2F_1\left(\frac{\Delta_m - J_m}{2}, \frac{\Delta_m - J_m}{2}; \bar{\eta}\right) {}_2F_1\left(\frac{\Delta_m + J_m}{2}, \frac{\Delta_m + J_m}{2}; \eta\right) + (\eta \leftrightarrow \bar{\eta}) \right]. \end{aligned} \quad (4.27)$$

Now we need to choose a numerical method to solve for the OPE coefficients. It turns out that the linear optimizer we used in AdS₂ is much slower here due to spin causing a proliferation of states when choosing a certain cutoff in Δ_m . A faster method is to construct an auxiliary quadratic function which we ask Mathematica’s FindMinimum to minimize.

The steps are the following. We choose a finite set of pairs of points $\{(\eta, \bar{\eta})_n\}$ over which we scan and a truncation $\Delta_{m_{\max}}$. Then, we build the matrix and vector

$$\begin{aligned} M_{mn} &\equiv \tilde{G}_{\Delta_m, J_m}^{\Delta_i}(\eta_n, \bar{\eta}_n) - \tilde{G}_{\Delta_m, J_m}^{\Delta_i}(1 - \eta_n, 1 - \bar{\eta}_n), \\ b_n &\equiv \tilde{G}_{0,0}^{\Delta_i}(\eta_n, \bar{\eta}_n) - \tilde{G}_{0,0}^{\Delta_i}(1 - \eta_n, 1 - \bar{\eta}_n) \end{aligned} \quad (4.28)$$

and construct the function

$$f(x) = \sum_n ((M \cdot x^2)_n - b_n)^2 \quad (4.29)$$

where here $x^2 \equiv (x_0^2, x_1^2, \dots, x_{m_{\max}}^2)$. Finally, we feed the function to Mathematica’s FindMinimum and ask it to find the x^2 which minimizes (4.29) through a Levenberg-Marquardt algorithm. The resulting values will be identified with approximate OPE coefficients squared $x_m^2 \equiv C_{im}^2$.

¹³The Kronecker delta δ_{0, J_m} is there to avoid double counting of scalar operators which have $h_m = \bar{h}_m$.

In practice, we check this method in free scalar theory. We choose $\Delta_\phi = \frac{37}{11}$, and truncate the double trace operators at $\Delta_{\max} = 2\Delta_\phi + 40$. Since the dimensions of the double trace operators are $\Delta_{[\phi^2]_{m,J}} = 2\Delta_\phi + 2m + J$, we have to implement the truncation by summing over m up to 20 and over J up to $40 - 2m$, so that we have 231 unknowns. We have to choose at least 231 pairs of points $\{(\eta, \bar{\eta})_n\}$, we pick 256. Finally, this sort of algorithm requires an initial guess of x from which the minimization procedure starts. To simulate the ignorance we would have of the OPE coefficients from a previous step in an iterative solution of the flow equations, we generate the initial condition by using the actual analytic expression of $C_{\phi\phi[\phi^2]_{m,J}}$ and multiplying each element by a 10% random noise. We show the errors, defined as in (4.25), of an application of this algorithm in figure 14. More details and the whole code to reproduce this plot are in the ancillary Mathematica notebook.

Let us make a final comment. Of course, these are rudimentary methods to determine OPE coefficients from crossing. More sophisticated methods achieving higher precision can be used when one will attempt a numerical application of the flow equations to an interacting theory. Our point is simply to demonstrate the kind of numerical accuracy one can achieve with fast evaluations on a standard laptop.

5 The (un)reasonable effectiveness of Padé

As we showed in section 3.4, the sums appearing in the flow equations (1.3) are divergent when using standard blocks and power-law convergent when using local blocks. However, in the flow equation for the BOE coefficients, the rate of convergence is particularly unsatisfactory (see for example the error when using local blocks in figure 12). Here we explain why our alternative approach, based on Padé approximants, leads to a drastic improvement in the convergence of the sums in the free theory checks in section 4. We then discuss a proposal on how to extend the applicability of these improvements to interacting theories.

Let us start with a lightning introduction to Padé approximants. See [47] for a textbook on the subject.

5.1 Quick intro to Padé approximants

Given a function of a single real variable $f(x)$, and two integers $m \geq 0$ and $n \geq 1$, the $\left[\frac{m}{n}\right]$ Padé approximant of $f(x)$ is defined as

$$\left[\frac{m}{n}\right]_f(x) \equiv \frac{\sum_{i=0}^m a_i x^i}{1 + \sum_{j=1}^n b_j x^j}, \quad (5.1)$$

where the coefficients a_i and b_j are uniquely fixed by requiring that all derivatives at a certain point (here taken to be $x = 0$) match

$$\frac{d^k}{dx^k} \left[\frac{m}{n}\right]_f(x) \Big|_{x=0} = \frac{d^k}{dx^k} f(x) \Big|_{x=0}, \quad k = 0, \dots, m+n \quad (5.2)$$

This ensures that the Taylor series of the function and its Padé approximant agree up to order $m + n$. We will in particular use diagonal Padé approximants, where $m = n$, and we will indicate them as

$$[m]_f(x) \equiv \left[\frac{m}{m} \right]_f(x). \quad (5.3)$$

The power of Padé approximants lies in the fact that, by allowing a more general ansatz than just simple powers, they can extend the domain of convergence of a series. Consider the series representation of the logarithm

$$f(x) \equiv \log(1+x) = \sum_{n=1}^{\infty} \frac{(-1)^{n-1}}{n!} x^n. \quad (5.4)$$

This series has radius of convergence $|x| < 1$, due to the singularity at $x = -1$. Attempting to use the truncated Taylor series to reproduce $\log(2)$ is highly inefficient¹⁴. On the other hand, the sequence of Padé approximants converges perfectly well. The error obtained by using the 4-th order Padé approximant is

$$\left| \frac{[4]_f(1) - \log(2)}{\log(2)} \right| \sim 10^{-6} \quad (5.5)$$

We will see that, at least in free theory, the way in which Padé improves the convergence of our sums is quite analogous to this example.

5.2 Padé for exponential convergence in free theory

5.2.1 Flow of scaling dimensions

In free theories in AdS, the scaling dimensions of scalar boundary operators take the form

$$\Delta_{q,n} = q\Delta_1 + 2n, \quad q, n \in \mathbb{N} \quad (5.6)$$

where Δ_1 is the lightest operator above the identity and generically there are multiple degenerate operators with the same $\Delta_{q,n}$. Since the values of q appearing in the flow equations depend on which bulk deformation we are considering, in free theories we only have to deal with $q = 2$. We are thus left with sums over n , which as we discussed are divergent when using standard blocks. We thus introduce the following function $f(x)$ constructed from the summands in the scaling dimension flow equation (3.20) with standard integrated blocks

$$f_i(x) \equiv \sum_{n=0}^{\infty} x^n b_{[\phi^2]_{n,0}}^{\hat{\phi}^2} C_{[\phi^2]_{n,0}ii} \mathcal{I}(2\Delta_\phi + 2n). \quad (5.7)$$

We are interested in the analytic structure of $f_i(x)$, which is governed by the asymptotic behavior of this sum. In section 4 we studied the specific cases of the flow equations evolving Δ_ϕ , Δ_{ϕ^2} and Δ_{ϕ^3} in free scalar theory. In all of them, the OPE coefficients $C_{ii[\phi^2]_n}$ exhibit alternating signs. In appendix E, we found that $C_{\phi^m\phi^m[\phi^2]_n} = mC_{\phi\phi[\phi^2]_n}$, hence for every i in f_i this property will be verified.

¹⁴The Taylor series still converges conditionally at $x = 1$, but slowly (the error goes to zero as n_{\max}^{-1}).

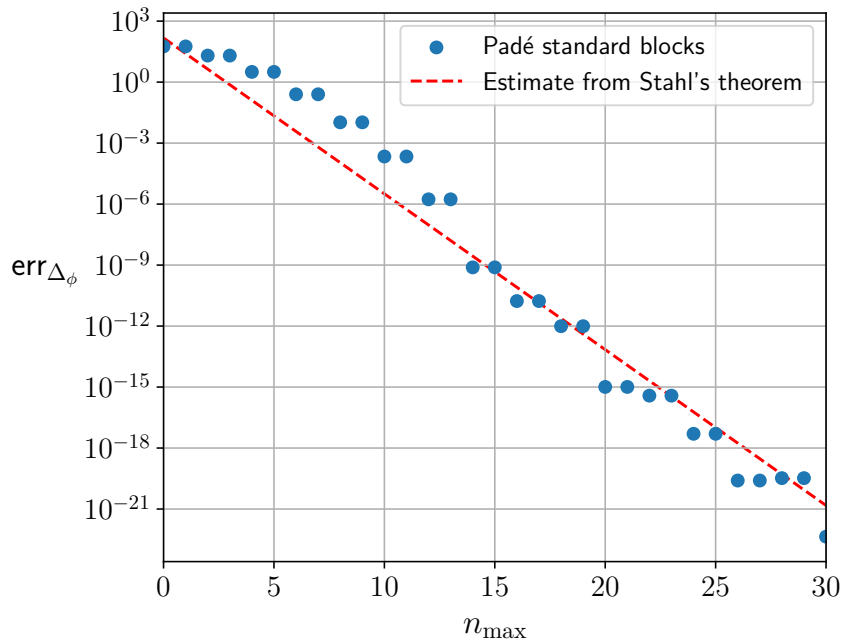


Figure 15. Comparison of the error (defined in (4.1)) of the Padé approximants of the partial sums in the flow equation (4.10) and the estimate from Stahl’s theorem (5.12).

Using the explicit forms of the OPE and BOE coefficients from appendix E, the asymptotic form of this sum is

$$\sum_n^{n_{\max}} b_{[\phi^2]_n}^{\hat{\phi}^2} C_{ii[\phi^2]_n} \mathcal{I}(\Delta_{[\phi^2]_n}) x^n \stackrel{n_{\max} \rightarrow \infty}{\sim} \sum_n^{n_{\max}} (-1)^n (2n)^a x^n \stackrel{n_{\max} \rightarrow \infty}{\sim} 2^a \text{Li}_{-a}(-x), \quad (5.8)$$

where

$$a = 2\Delta_\phi - \frac{d+2}{2}. \quad (5.9)$$

Our function $f_i(x)$ thus shares the analytic structure of the polylogarithm $\text{Li}_{-a}(-x)$: it possesses a branch cut along the negative real axis for $x \in (-\infty, -1]$, but it is entirely analytic at the physical evaluation point $x = 1$.

While the series expansion diverges at $x = 1$, due to a being generically positive, the underlying function $f_i(1)$ is finite. We are exactly in a situation analogous to the toy example (5.4), where an originally divergent sum is analytically continued by Padé approximants. Furthermore, because $f_i(x)$ is analytic in the cut plane, the theory of Padé approximants (specifically theorems by Stahl [48, 49]) guarantees that the error of the diagonal $[n]$ approximants evaluated at $x = 1$ will decay exponentially with the truncation order.

More precisely, Stahl’s theorems imply that for a function $f(x)$ with a branch cut at $(-\infty, -1]$, the error of the Padé approximant is related to the transformation that maps the cut plane to the unit disk

$$w : \mathbb{C} \setminus (-\infty, -1] \rightarrow \mathbb{D}, \quad w(x) = \frac{\sqrt{1+x} - 1}{\sqrt{1+x} + 1}. \quad (5.10)$$

Concretely, the asymptotic error of the diagonal Padé approximant is strictly bounded as follows [48, 49]

$$\limsup_{N_{\max} \rightarrow \infty} |f(x) - [N_{\max}]_f(x)|^{\frac{1}{2N_{\max}}} = |w(x)| \quad (5.11)$$

In our case, this tells us that the error should at most asymptotically scale as

$$\text{err}_{\Delta_\phi} \sim |w(1)|^{l_{\max}} = (3 - 2\sqrt{2})^{l_{\max}} \sim e^{-1.765l_{\max}}. \quad (5.12)$$

We compare this expectation with numerics in figure 15, and find that they approximately saturate this estimate. Notice that the convergence rate does not depend on a .

We can ask ourselves whether Padé approximants also improve the convergence of this sum when using local blocks. In that case, the explicit expression of $\mathcal{I}^\alpha(\Delta_{[\phi^2]_n})$ happens to compensate the alternation of signs in $C_{ii[\phi^2]_n}$, thus leading to

$$\sum_n^{n_{\max}} b_{[\phi^2]_n}^{\hat{\phi}^2} C_{ii[\phi^2]_n} \mathcal{I}^\alpha(\Delta_{[\phi^2]_n}) x^n \stackrel{n_{\max} \rightarrow \infty}{\sim} \sum_n^{n_{\max}} (2n)^a x^n \stackrel{n_{\max} \rightarrow \infty}{\sim} 2^a \text{Li}_{-a}(x), \quad (5.13)$$

where now

$$a = 2(\Delta_\phi - \alpha). \quad (5.14)$$

Our function has a convergent series representation at $x = 1$ for α large enough, but it also has a non-analyticity there. Because the branch cut now originates at $x = 1$, the map to the unit disk becomes $w(x) = \frac{\sqrt{1-x}-1}{\sqrt{1-x}+1}$ and Stahl's theorem provides no guarantee of exponential convergence:

$$\limsup_{N_{\max} \rightarrow \infty} |f(1) - [N_{\max}]_f(1)| = 1, \quad (5.15)$$

explaining why we observed no improvement when using Padé approximants on local blocks, for example in figure 9.

5.2.2 Flow of BOE coefficients

Now consider the sums involved in the flow equation of the BOE coefficients (1.3). The formula involves a double series, and the theory of Padé approximants of two variables is not fully developed. Instead, we will take the approach of using Padé sequentially. We will introduce two auxiliary variables x and y

$$\begin{aligned} f_i(x, y) &\equiv \sum_{m=0}^{\infty} b_{[\phi^2]_{m,0}}^{\hat{\phi}^2} y^m f_{i,m}(x), \\ f_{i,m}(x) &\equiv \sum_{n=0}^{\infty} b_{[\phi^2]_{n,0}}^{\hat{\phi}^2} C_{i, [\phi^2]_n [\phi^2]_m} \mathcal{J}_{\Delta_i}(2\Delta_\phi + 2n, 2\Delta_\phi + 2m) x^n \end{aligned} \quad (5.16)$$

We will first compute the Padé approximant of $f_{i,m}(x)$ around $x = 0$. Then, after taking $x \rightarrow 1$, we do the Padé approximant of $f_i(1, y)$ around $y = 0$ and finally take $y \rightarrow 1$.

Let us focus on the case $\mathcal{O}_i = \phi^2$, which we studied in section 4. While we already know the universal asymptotic behaviors of these sums individually, (3.62) and (3.64), ensuring

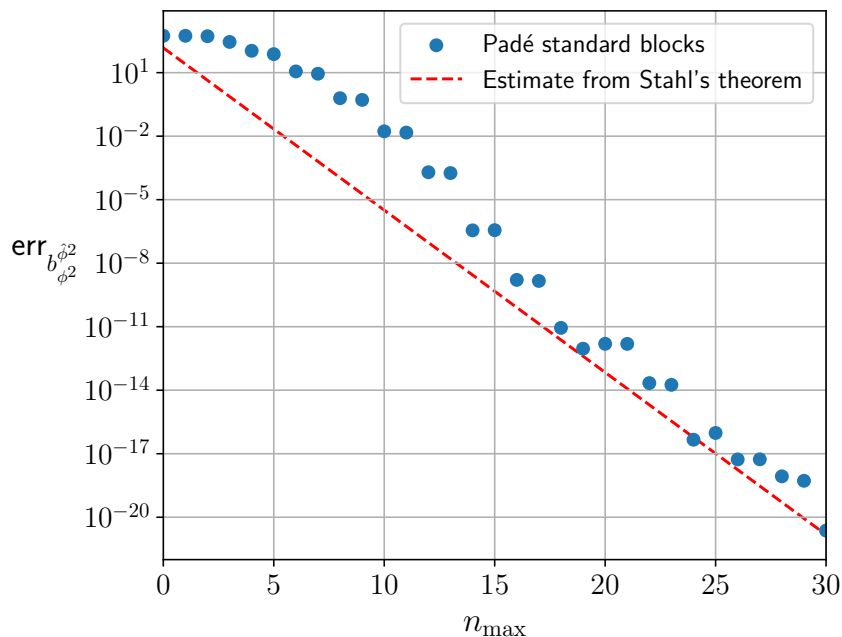


Figure 16. Comparison of the error (defined in (4.1)) of the Padé approximants of the partial sums in the flow equation (4.21) and the estimate from Stahl’s theorem (5.12).

the success of sequential Padé approximants requires understanding the regime of large n and large m with fixed ratio n/m . We can study that regime explicitly in this case, and we find that the summands factorize completely, and that signs alternate

$$b_{[\phi^2]_n}^{\hat{\phi}^2} b_{[\phi^2]_m}^{\hat{\phi}^2} C_{\phi^2[\phi^2]_n[\phi^2]_m} \mathcal{J}_{\Delta_{\phi^2}}(\Delta_{[\phi^2]_n}, \Delta_{[\phi^2]_m}) \xrightarrow{n,m \rightarrow \infty} (-1)^{n+m} m^{\frac{d-4}{2}} n^{2\Delta_{\phi^2} - \frac{d+4}{2}}, \quad (5.17)$$

In this particular case, the nested Padé procedure we outlined thus also essentially factorizes. The power-law behavior in m and n is totally analogous to the one described in the previous section, thus leading to the same exponential decay of the error. We choose equal truncations on n and m and compare the error of the double truncated Padé sum with the estimate from Stahl’s theorem in figure 16.

5.3 Proposal for Padé in interacting theories

In this section we will propose a Padé procedure for interacting theories which are deformations of free theories

$$S(\lambda) = S_{\text{free}} + \lambda \int_{\text{AdS}} \hat{\Phi} \quad (5.18)$$

In such theories, the spectrum at $\lambda = 0$ is organized as in (5.6). For finite λ , degeneracies are lifted and dimensions are not integer spaced, but each state can be continuously traced back as originating from a certain (q, n) family at $\lambda = 0$. The generalization of (5.7) we propose is thus to group operators by their original free theory family and introduce two

auxiliary variables

$$f_i(x, y) \equiv \sum_{n=0}^{\infty} x^n \sum_{q=1}^{\infty} y^q \sum_{l \in (q, n) \text{ family}} b_l^{\hat{\phi}} C_{li} \mathcal{I}(\Delta_l), \quad (5.19)$$

where “ $l \in (q, n)$ family” means $\Delta_l(\lambda \rightarrow 0) = q\Delta_1 + 2n$. Notice that for finite λ the sum over q does not truncate. For small λ , BOE coefficients that were zero in free theory will be highly suppressed, ensuring the convergence of the sum over q , and signs will keep alternating in n . But at large values of λ , nothing guarantees these facts. If the signs asymptotically alternate in q and n in a pseudo-random manner, theorems by Paley and Zygmund [50, 51] state that the function almost surely¹⁵ will develop natural boundaries at $|x| = 1$ and $|y| = 1$. In that case it would be impossible for Padé to analytically continue the function to $x = 1, y = 1$ ¹⁶.

In a generic CFT, the eigenstate thermalization hypothesis (ETH) [52] would lead us to expect this pseudo-random behavior for the signs of the OPE coefficients. However, we are studying in particular CFTs that live on the boundary of AdS. Bulk locality has been shown to imply nontrivial constraints on CFT data [25, 53, 54]. So we do not exclude the possibility that the summands in (5.19) will present a structured sign modulation for high values of q and n . That would immediately ensure the convergence of the Padé approximants, unless the signs are all positive.

Let us remind the reader that there is an alternative to achieve convergence, which is to use local integrated blocks.

6 Merger-annihilation and level repulsion

The flow equations (1.3) exhibit many interesting properties. In 2D [1] it was shown that they generically imply level repulsion, the phenomenon by which different curves of the QFT data, when approaching each other, effectively repel; and merger-annihilation, where one boundary operator hitting marginality ($\Delta_i = d$) generically implies all the QFT data exhibits a square root-like behavior and becomes complex after a critical value of λ . Here we will generalize these facts to higher dimensions, closely following the arguments in [1].

The equations in this section are valid when the sums converge. That means they are valid when using local blocks $\mathcal{I}^\alpha, \mathcal{J}^\alpha$ or the Padé procedure. We simply indicate \mathcal{I} and \mathcal{J} , omitting the superscripts. We also focus specifically on scalar states, but we expect the generalization to spinning states to be straightforward.

6.1 Merger-annihilation

Throughout the paper, we have assumed all boundary operators are irrelevant, $\Delta_i > d$. Now let us imagine that the lightest operator above the identity, with dimension $\Delta_1(\lambda)$, approaches d from above at some critical λ_c . Here we assume this happens when we

¹⁵Here “almost surely” should be intended in the sense of probability theory.

¹⁶These theorems technically apply to functions of a single variable. We expect the situation can only be worse with two variables.

approach λ_c from above, but identical formulae with adjusted signs can be derived in the scenario where marginality is reached as $\lambda \rightarrow \lambda_c$ from below.

6.1.1 Scaling dimensions near merger-annihilation

We start by observing that the explicit forms of $\mathcal{I}(\Delta)$ (3.21) and $\mathcal{I}^\alpha(\Delta)$ (3.34) have a pole at $\Delta = d$ with residue $\text{Vol}(S^{d-1})$. When $\Delta_1 \rightarrow d$, the whole sum over boundary operators is thus dominated by the lightest term. If we study the derivative of Δ_1 we find

$$\frac{d\Delta_1}{d\lambda} \approx \frac{\text{Vol}(S^{d-1})b_1^{\hat{\Phi}}C_{111}}{\Delta_1 - d} \implies \Delta_1(\lambda) \approx d \pm \sqrt{(\lambda - \lambda_c)\text{Vol}(S^{d-1})b_1^{\hat{\Phi}}C_{111}} \quad (6.1)$$

where the QFT data on the right-hand side is evaluated at $\lambda = \lambda_c$.

The square root behavior is typical of fixed-point annihilation [55–57]. We see that for $\lambda > \lambda_c$ there are two sets of consistent QFT data, merging at $\lambda = \lambda_c$. For $\lambda < \lambda_c$, the data becomes complex, so there is no unitary QFT there.

The rest of the scaling dimensions generically inherits the same square root behavior, even though they're far from marginality. That is because \mathcal{O}_1 appears in the sums in the other flow equations as well, leading to

$$\frac{d\Delta_i}{d\lambda} \approx \frac{\text{Vol}(S^{d-1})b_1^{\hat{\Phi}}C_{1ii}}{\Delta_1 - d} \implies \Delta_i(\lambda) \approx \Delta_i \pm C_{1ii} \sqrt{(\lambda - \lambda_c) \frac{\text{Vol}(S^{d-1})b_1^{\hat{\Phi}}}{C_{111}}}. \quad (6.2)$$

In a theory with a global symmetry we expect merger-annihilation only when a singlet hits marginality. This is consistent with our results, since $b_1^{\hat{\Phi}} = 0$ if \mathcal{O}_1 is not a singlet because $\hat{\Phi}$ only creates singlets.

6.1.2 BOE coefficients near merger-annihilation

The same phenomenon takes place for the BOE coefficients. The coefficients $\mathcal{J}_{\Delta_i}(\Delta_l, \Delta_j)$ (3.46) also have a pole at $\Delta_l = d$. This time, the residue nontrivially depends on Δ_i and Δ_j

$$\begin{aligned} F_{\Delta_i}(\Delta_j) &\equiv \text{Res}_{\Delta_l=d} \mathcal{J}_{\Delta_i}(\Delta_l, \Delta_j) \\ &= \oint_{\Delta_j} \frac{d\Delta}{2\pi i} \frac{1}{\Delta - \Delta_j} \frac{2\pi^{d/2}\Gamma(\Delta - \frac{d-2}{2})}{(\Delta - \Delta_i)\Gamma(\frac{d-\Delta_i+\Delta}{2})\Gamma(\frac{\Delta_i+\Delta+2-d}{2})} \end{aligned} \quad (6.3)$$

where the contour integral here has nothing to do with the residue at $\Delta_l = d$, but rather the regulated form of \mathcal{J} (3.47).

We thus get, in the limit where $\Delta_1 \rightarrow d$,

$$\frac{db_i^{\hat{\Phi}}}{d\lambda} \approx \frac{b_1^{\hat{\Phi}}}{\Delta_1 - d} \sum_j b_j^{\hat{\Phi}} C_{ij1} F_{\Delta_i}(\Delta_j) \quad (6.4)$$

implying

$$b_i^{\hat{\Phi}}(\lambda) \approx b_i^{\hat{\Phi}}(\lambda_c) \pm \sqrt{\frac{(\lambda - \lambda_c)b_1^{\hat{\Phi}}}{\text{Vol}(S^{d-1})C_{111}}} \sum_j b_j^{\hat{\Phi}} C_{ij1} F_{\Delta_i}(\Delta_j), \quad (6.5)$$

where again all the QFT data on the right hand side is evaluated at $\lambda = \lambda_c$.

6.1.3 OPE coefficients near merger-annihilation

We expect the same phenomenon to take place for OPE coefficients. In AdS₂, this was shown explicitly in [1]. We did not derive an ODE that couples the derivative of the OPE coefficients to the rest of the QFT data in higher dimensions, instead we use the crossing equation to fix OPE coefficients independently.

In appendix C, we nevertheless study certain properties of such an ODE. Concretely, we find that for triplets ijk of scalar operators,

$$\frac{dC_{ijk}}{d\lambda} = \sum_l b_l^{\hat{\Phi}} \sum_m C_{lim} C_{mjk} \mathcal{K}_{\Delta_i \Delta_j \Delta_k}(\Delta_l, \Delta_m) + \text{perms.} + \text{spin} \quad (6.6)$$

where “perms.” are the cyclic permutations of the i, j, k indices, and “spin” indicates contributions from exchanged spinning operators, which we will not need to consider here, and \mathcal{K} is an integrated conformal block which we do not compute explicitly.

The main property we need here is that, as we argued in appendix C, the kinematic coefficients \mathcal{K} must have a pole at $\Delta_l = d$. Following the discussion for scaling dimensions and BOE coefficients, this immediately implies

$$C_{ijk}(\lambda) \approx C_{ijk}(\lambda_c) \pm \sqrt{\frac{(\lambda - \lambda_c) b_1^{\hat{\Phi}}}{\text{Vol}(S^{d-1}) C_{111}}} \sum_m C_{lim} C_{mjk} H_{\Delta_i \Delta_j \Delta_k}(\Delta_m) + \text{perms.} \quad (6.7)$$

where we do not know the explicit expression of $H \equiv \text{Res}_{\Delta_l=d} \mathcal{K}$ in $d + 1 > 2$.

6.2 Level repulsion

When a Hamiltonian depends on a continuous parameter λ , its eigenvalues are known to generically experience level repulsion: when two eigenvalues get close they repel each other, and never cross¹⁷ [58]. The scaling dimensions of boundary operators in QFT in AdS are the eigenvalues of the Hamiltonian in cylinder coordinates, and as λ varies, they experience level repulsion too. It requires a few steps to prove this. We follow the arguments in [1], themselves inspired by [13].

Consider two boundary operators \mathcal{O}_1 and \mathcal{O}_2 , which have scaling dimensions Δ_1 and Δ_2 such that $0 < \Delta_{21} \ll |\Delta_{ij}|$ for all other pairs ij (here we use the notation $\Delta_{ij} \equiv \Delta_i - \Delta_j$). We want to show that

$$\frac{d^2 \Delta_{21}}{d\lambda^2} = \frac{c^2}{\Delta_{21}(\lambda_0)^3} + O(\Delta_{21}^{-2}), \quad c \in \mathbb{R}. \quad (6.8)$$

This is enough to argue for level repulsion: as $\Delta_{21} \rightarrow 0$ from above, the singularity on the right hand side of this equation acts as a potential barrier which prevents the difference of scaling dimensions from ever becoming 0 and flipping sign.

We start by taking a derivative of the scaling dimension flow equation for Δ_2

$$\frac{d^2 \Delta_2}{d\lambda^2} = \sum_l \left(b_l^{\hat{\Phi}} \frac{dC_{22l}}{d\lambda} \mathcal{I}(\Delta_l) + \frac{db_l^{\hat{\Phi}}}{d\lambda} C_{22l} \mathcal{I}(\Delta_l) + b_l^{\hat{\Phi}} C_{22l} \frac{d\mathcal{I}(\Delta_l)}{d\lambda} \right). \quad (6.9)$$

¹⁷They can cross if the two energy eigenstates belong to different charge sectors of the theory.

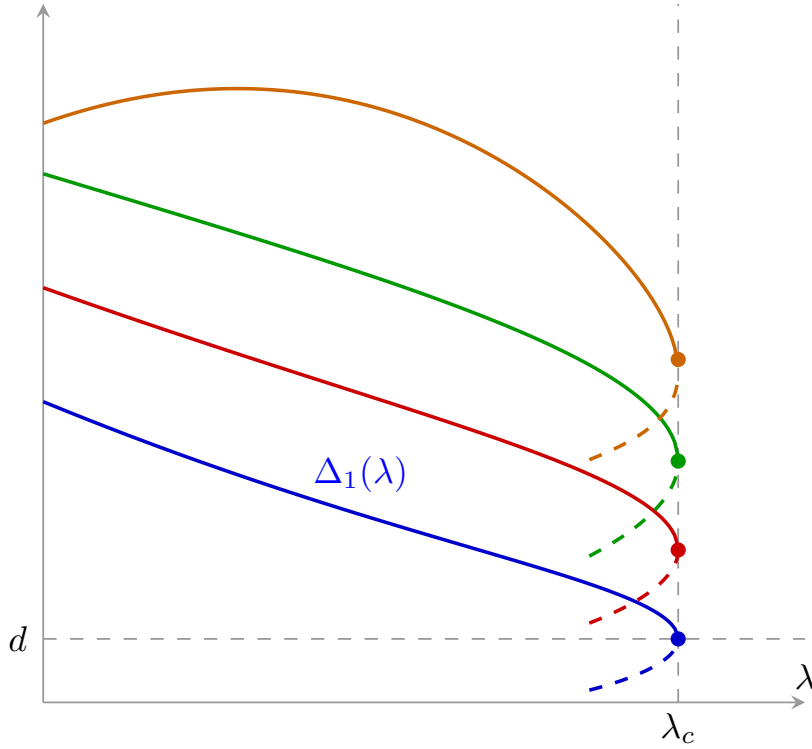


Figure 17. When the scaling dimension Δ_1 of the lightest boundary operator above the identity hits marginality, generically all the QFT data has a square root behavior. The curves can in principle be prolonged along the other branch of the square root, and a new consistent set of QFT data is found. They can also be prolonged for $\lambda > \lambda_c$ leading to complex QFT data, we do not show that in this figure. The curves above $\Delta_1(\lambda)$ can represent any other piece of QFT data: $\Delta_i(\lambda)$, $b_i^{\hat{\phi}}(\lambda)$, $C_{ijk}(\lambda)$.

Let us study each term in the limit $\Delta_1 \rightarrow \Delta_2$.

For the first term, we once again appeal to the fact that an ODE for $\frac{dC_{ijk}}{d\lambda}$ would have the form (6.6). As stated before, we do not have the explicit expression of $\mathcal{K}_{\Delta_i\Delta_j\Delta_k}(\Delta_l, \Delta_m)$ in $d+1 > 2$, but we do not need it for our arguments. The only fact we need is that \mathcal{K} must possess a pole at $\Delta_m = \Delta_i$, with residue proportional to \mathcal{I} . We prove this in appendix C. Near this pole, it must behave as

$$\mathcal{K}_{\Delta_i\Delta_j\Delta_k}(\Delta_l, \Delta_m) \sim -\frac{\mathcal{I}(\Delta_l)}{\Delta_m - \Delta_i} + O(1) \sim \mathcal{K}_{\Delta_i\Delta_k\Delta_j}(\Delta_l, \Delta_m). \quad (6.10)$$

Now, the sum over Δ_m contains both Δ_1 and Δ_2 . The exact pole at $\Delta_m = \Delta_2$ would be removed by renormalization, just like it happens for \mathcal{J} (explained in appendix B.2). The approximate singularity as $\Delta_1 \rightarrow \Delta_2$, though, is physical and dominates $\frac{dC_{22l}}{d\lambda}$. Taking this

into account, we get

$$\begin{aligned} \sum_l b_l^{\hat{\Phi}} \frac{dC_{22l}}{d\lambda} \mathcal{I}(\Delta_l) &= \sum_l b_l^{\hat{\Phi}} \mathcal{I}(\Delta_l) \sum_p \sum_m b_p^{\hat{\Phi}} \left[2C_{p2m} C_{m2l} \mathcal{K}_{\Delta_2 \Delta_2 \Delta_l}(\Delta_p, \Delta_m) \right. \\ &\quad \left. + C_{plm} C_{m22} \mathcal{K}_{\Delta_l \Delta_2 \Delta_2}(\Delta_p, \Delta_m) \right] \\ &\approx \frac{1}{\Delta_{21}} \Omega_{12} \left[2\Omega_{12} + b_2^{\hat{\Phi}} C_{122} \mathcal{I}(\Delta_2) - b_1^{\hat{\Phi}} C_{222} \mathcal{I}(\Delta_1) \right] \end{aligned} \quad (6.11)$$

where we defined the shorthand

$$\Omega_{12} \equiv \sum_l b_l^{\hat{\Phi}} C_{12l} \mathcal{I}(\Delta_l) \quad (6.12)$$

Now let us focus on the second term.

$$\sum_l \frac{db_l^{\hat{\Phi}}}{d\lambda} C_{22l} \mathcal{I}(\Delta_l) = \sum_l C_{22l} \mathcal{I}(\Delta_l) \sum_j \sum_k b_j^{\hat{\Phi}} b_k^{\hat{\Phi}} C_{ljk} \mathcal{J}_{\Delta_l}(\Delta_j, \Delta_k) \quad (6.13)$$

The coefficient $\mathcal{J}_{\Delta_l}(\Delta_j, \Delta_k)$ (3.46) has the following analytic structure near $\Delta_k = \Delta_l$:

$$\mathcal{J}_{\Delta_l}(\Delta_j, \Delta_k) = -\frac{\mathcal{I}(\Delta_j)}{\Delta_k - \Delta_l} + O(1) \quad (6.14)$$

so that in the limit $\Delta_1 \rightarrow \Delta_2$, the sums are dominated by $l = 1, k = 2$ and $l = 2, k = 1$, giving

$$\sum_l \frac{db_l^{\hat{\Phi}}}{d\lambda} C_{22l} \mathcal{I}(\Delta_l) \approx -\frac{\Omega_{12}}{\Delta_{21}} \left(b_2^{\hat{\Phi}} C_{221} \mathcal{I}(\Delta_1) - b_1^{\hat{\Phi}} C_{222} \mathcal{I}(\Delta_2) \right) \quad (6.15)$$

Finally, the third term in (6.9) is not divergent as $\Delta_1 \rightarrow \Delta_2$, hence it is subleading to the first two.

Now, plugging (6.15) and (6.11) into (6.9), and slightly rearranging terms, we get

$$\frac{d^2 \Delta_2}{d\lambda^2} \approx \frac{1}{\Delta_{21}} \left[2\Omega_{12}^2 + \Omega_{12} \left(b_2^{\hat{\Phi}} C_{221} + b_1^{\hat{\Phi}} C_{222} \right) \left(\mathcal{I}(\Delta_2) - \mathcal{I}(\Delta_1) \right) \right] \approx \frac{2\Omega_{12}^2}{\Delta_{21}}. \quad (6.16)$$

Repeating again for $\frac{d^2 \Delta_1}{d\lambda^2}$ and taking the difference, we get

$$\frac{d^2 \Delta_{21}}{d\lambda^2} \approx \frac{4\Omega_{12}^2}{\Delta_{21}}, \quad (6.17)$$

and what remains to be done is to determine the scaling of Ω_{12}^2 as $\Delta_{21} \rightarrow 0$. To do that, consider that

$$\begin{aligned} \frac{d\Omega_{12}}{d\lambda} &= \sum_l \left[\frac{db_l^{\hat{\Phi}}}{d\lambda} C_{12l} \mathcal{I}(\Delta_l) + b_l^{\hat{\Phi}} \frac{dC_{12l}}{d\lambda} \mathcal{I}(\Delta_l) + b_l^{\hat{\Phi}} C_{12l} \frac{d\mathcal{I}(\Delta_l)}{d\lambda} \right] \\ &\approx \frac{\Omega_{12}}{\Delta_{21}} \left[(b_1^{\hat{\Phi}} C_{122} + b_2^{\hat{\Phi}} C_{112}) (\mathcal{I}(\Delta_2) - \mathcal{I}(\Delta_1)) - \frac{d\Delta_{21}}{d\lambda} \right] \\ &\approx -\frac{\Omega_{12}}{\Delta_{21}} \frac{d\Delta_{21}}{d\lambda}, \end{aligned} \quad (6.18)$$

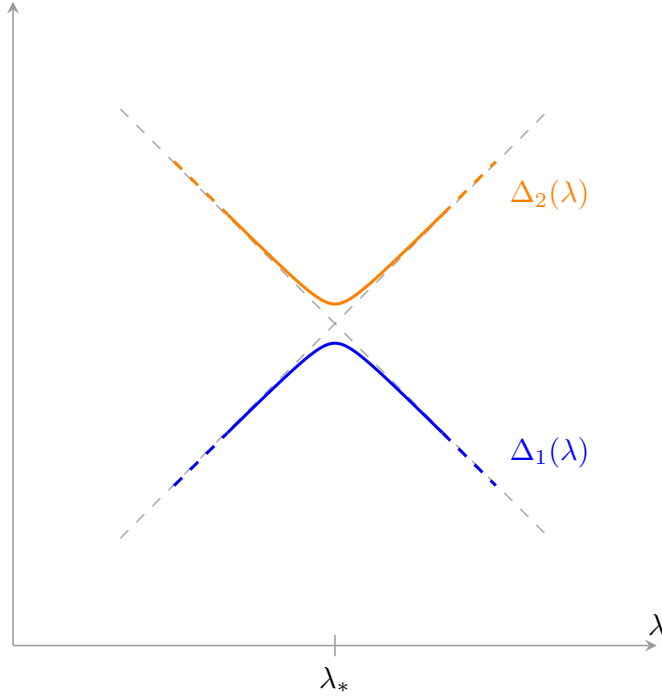


Figure 18. When two scaling dimension get close to each other, they repel. This is the phenomenon of level repulsion, predicted by the flow equations, and for $\lambda \sim \lambda_*$ it is captured by equation (6.20). After the repulsion event, the two curves exchange slopes.

where to go from the first to the second line we repeated the steps in (6.11) but now for C_{12l} instead of C_{22l} , and we used the scaling dimension flow equation to repackage some of the terms as $\frac{d\Delta_{21}}{d\lambda}$.

Formula (6.18) implies that $\Omega_{12} \sim c/\Delta_{21}$. Plugging it into (6.17) we get the differential equation we wanted to prove

$$\frac{d^2\Delta_{21}}{d\lambda^2} \approx \frac{c^2}{\Delta_{21}^3} \quad (6.19)$$

This differential equation can be solved, leading to an approximate solution valid when $0 < \Delta_{21} \ll |\Delta_{ij}|$:

$$\Delta_{21}(\lambda) \approx \pm \sqrt{c_1(\lambda - \lambda_*)^2 + \frac{c^2}{\lambda_*}} \quad (6.20)$$

where c_1 and λ_* are integration constants. This implies that, in the vicinity of $\lambda \approx \lambda_*$, the two curves exchange slopes after experiencing level repulsion.

7 Discussion

Let us discuss some further properties of the flow equations and some open research directions which shall be explored in future work.

7.1 Beyond our assumptions

Let us start by discussing extensions of our framework beyond the original assumptions. In particular, we will discuss the effect of having relevant boundary operators and bulk operators which violate assumption (3.41).

As in the previous section, we use \mathcal{I} and \mathcal{J} to indicate the integrated blocks. In practice one should use their local versions \mathcal{I}^α and \mathcal{J}^α or Padé approximants to make the sums convergent, and any equation we write is intended implicitly with one of the two methods applied.

7.1.1 Relevant boundary operators

Throughout this work we have assumed that all boundary operators have irrelevant scaling dimensions $\Delta_i > d$. In section 6, we studied what happens when the lightest operator hits marginality, $\Delta_i \rightarrow d$. More generally, one can ask whether the flow equations are valid when there are multiple relevant operators. The discussion is totally analogous with the 2D case [1]:

Consider the integrals of correlation functions which we computed in section 3 to derive the flow equations. The presence of relevant boundary operators would introduce power-law IR divergences. Introducing a cutoff δ near the boundary of AdS in Poincaré coordinates, we would have

$$\int_{z>\delta} \frac{dz d^d \mathbf{x}}{z^{d+1}} \langle \hat{\Phi}(z, \mathbf{x}) \cdots \rangle = \sum_{\Delta_l < d} \frac{\delta^{\Delta_l - d}}{d - \Delta_l} b_l^{\hat{\Phi}} \int d^d \mathbf{x} \langle \mathcal{O}_l(\mathbf{x}) \cdots \rangle + \text{finite as } \delta \rightarrow 0. \quad (7.1)$$

These divergences can be removed by adding a boundary action with appropriate counterterms involving these relevant operators. Physically, this corresponds to considering a fine tuned RG flow in which conformal symmetry on the boundary is preserved.

Analytically continuing the scaling dimensions in our flow equations precisely corresponds to throwing away the divergences in (7.1) when deriving the integrals of blocks \mathcal{I} and \mathcal{J} appearing in (1.3). Since, as was shown in [59], the AdS isometries prevent us from turning on relevant operators on the boundary independently of the bulk deformation, we are led to state that our flow equations also describe these types of fine-tuned flows in AdS¹⁸.

7.1.2 Bulk relevant operators beyond assumption (3.41)

When deriving the BOE flow equation, in order to avoid extra UV divergences we made the assumption

$$\Delta_{\hat{\Phi}}^{\text{UV}} < \frac{1}{2} \left(d + 1 + \min_{\hat{\mathcal{O}} \in \hat{\Phi} \times \hat{\Phi}} \Delta_{\hat{\mathcal{O}}}^{\text{UV}} \right). \quad (7.2)$$

¹⁸Examples of fine-tuned flows with relevant boundary operators are free theories with Neumann boundary conditions and more in general the flows defined by the prolongation of QFT data curves beyond merger-annihilation (like the dashed lines in figure 17). A physically interesting example would be the so-called “Dirichlet*” boundary theory which merges and annihilates with the Dirichlet boundary conditions of Yang-Mills in four dimensions. [60, 61]

We can give up this assumption by introducing a UV cutoff δ in the integral in (3.37) and carefully renormalizing the bulk operators. This would lead to flow equations involving the UV cutoff.

$$\frac{db_i^{\hat{\Phi}}}{d\lambda} = \lim_{\delta \rightarrow 0} \left[\sum_{l,j} b_l^{\hat{\Phi}} b_j^{\hat{\Phi}} C_{lji} \mathcal{J}_{\Delta_i}^{(\delta)}(\Delta_l, \Delta_j) - \sum_{\hat{\mathcal{O}}} b_i^{\hat{\mathcal{O}}} C_{\hat{\Phi}\hat{\Phi}\hat{\mathcal{O}}}^{\text{UV}} \sum_{n=0}^{\infty} \frac{a_n}{\delta^{2\Delta_{\hat{\Phi}} - \Delta_{\hat{\mathcal{O}}} - d - 1 - 2n}} \right] \quad (7.3)$$

where the sum over $\hat{\mathcal{O}}$ runs over bulk operators violating (7.2), a_n are some kinematic coefficients and $\mathcal{J}^{(\delta)}$ is a regulated version of \mathcal{J} with a UV cutoff $(z - z_2)^2 + (\mathbf{x} - \mathbf{x}_2)^2 > \delta^2$.

Notice that now the flow equations do not close anymore. One would in fact need to flow the BOE coefficients of the bulk operators $\hat{\mathcal{O}}$ appearing in the sum in (7.3). This can be remedied quickly, by running again our arguments in section 3, to obtain

$$\frac{db_i^{\hat{\mathcal{O}}}}{d\lambda} = \sum_l \sum_j b_l^{\hat{\Phi}} b_j^{\hat{\mathcal{O}}} C_{lji} \mathcal{J}_{\Delta_i}(\Delta_l, \Delta_j) \quad (7.4)$$

where this time UV convergence is ensured if the lightest operator in the UV OPE of $\hat{\Phi} \times \hat{\mathcal{O}}$ is not lighter than $\hat{\mathcal{O}}$.

In 2D [1], another possibility was presented, which would avoid the appearance of the UV cutoff in the flow equations. The prescription is explicitly presented in section 5.3 there, we summarize it here and refer the reader to that section for a detailed justification.

The reasoning starts by observing that only a finite set of bulk operators $\hat{\mathcal{O}}$ will violate (7.2), and will thus appear in the sum in (7.3). We can choose a basis of bulk operators $\hat{\mathcal{O}}_a$ that are ordered by their UV scaling dimensions $\Delta_a^{\text{UV}} \leq \Delta_{a+1}^{\text{UV}}$ and one for boundary operators such that they are ordered by boundary scaling dimensions $\Delta_i \leq \Delta_{i+1}$. Moreover, we are free to fix $b_i^{\hat{\mathcal{O}}_a} = 0$ if $i < a$ and $b_i^{\hat{\mathcal{O}}_i} = 1$. Now, the prescription is to shift the variations of the BOE coefficients iteratively as follows

$$\delta b_i^{\hat{\mathcal{O}}_a} \rightarrow \delta b_i^{\hat{\mathcal{O}}_a} - \delta b_j^{\hat{\mathcal{O}}_a} b_i^{\hat{\mathcal{O}}_j}, \quad \forall a \geq j, \quad \forall j. \quad (7.5)$$

To give a concrete example, consider the case $a = 1$, the lightest operator:

$$\frac{db_i^{\hat{\mathcal{O}}_1}}{d\lambda} \rightarrow \frac{db_i^{\hat{\mathcal{O}}_1}}{d\lambda} - \frac{db_1^{\hat{\mathcal{O}}_1}}{d\lambda} b_i^{\hat{\mathcal{O}}_1} \quad (7.6)$$

Using the flow equation (7.3) for $\frac{db_1^{\hat{\mathcal{O}}_1}}{d\lambda}$ and the renormalization condition $b_1^{\hat{\mathcal{O}}_1} = 1$ we obtain

$$\frac{db_i^{\hat{\mathcal{O}}_1}}{d\lambda} = \sum_l \sum_j b_l^{\hat{\Phi}} b_j^{\hat{\mathcal{O}}_1} \left[C_{lij} \mathcal{J}_{\Delta_i}(\Delta_l, \Delta_j) - b_i^{\hat{\mathcal{O}}_1} C_{l j 1} \mathcal{J}_{\Delta_1}(\Delta_l, \Delta_j) \right] \quad (7.7)$$

which is now finite and does not involve the UV cutoff.

For the second lightest bulk operator, we must do

$$\frac{db_i^{\hat{\mathcal{O}}_2}}{d\lambda} \rightarrow \frac{db_i^{\hat{\mathcal{O}}_2}}{d\lambda} - \frac{db_2^{\hat{\mathcal{O}}_2}}{d\lambda} b_i^{\hat{\mathcal{O}}_2} \rightarrow \frac{db_i^{\hat{\mathcal{O}}_2}}{d\lambda} - \frac{db_2^{\hat{\mathcal{O}}_2}}{d\lambda} b_i^{\hat{\mathcal{O}}_2} - \frac{db_1^{\hat{\mathcal{O}}_2}}{d\lambda} b_i^{\hat{\mathcal{O}}_1} + \frac{db_1^{\hat{\mathcal{O}}_2}}{d\lambda} b_2^{\hat{\mathcal{O}}_1} b_i^{\hat{\mathcal{O}}_2} \quad (7.8)$$

obtaining again a finite flow equation

$$\begin{aligned} \frac{db_i^{\hat{\mathcal{O}}_2}}{d\lambda} = \sum_l \sum_j b_l^{\hat{\mathcal{O}}_1} b_j^{\hat{\mathcal{O}}_2} & \left[C_{lij} \mathcal{J}_{\Delta_i}(\Delta_l, \Delta_j) - b_i^{\hat{\mathcal{O}}_2} C_{lj2} \mathcal{J}_{\Delta_2}(\Delta_l, \Delta_j) \right. \\ & \left. - (b_i^{\hat{\mathcal{O}}_1} - b_2^{\hat{\mathcal{O}}_1} b_i^{\hat{\mathcal{O}}_2}) C_{lj1} \mathcal{J}_{\Delta_1}(\Delta_l, \Delta_j) \right] \end{aligned} \quad (7.9)$$

This procedure can be applied to any bulk operator which violates assumption (7.2), and leads to finite flow equations free of the UV cutoff.

7.1.3 Marginally relevant bulk deformation

Many interesting QFTs, such as the $O(N)$ model in 2D or Yang-Mills and QCD in 4D, have a deforming operator which is classically marginal $\Delta_{\hat{\Phi}}^{\text{UV}} = d + 1$. In particular, in these examples the deforming operator is the lightest relevant scalar in the UV theory¹⁹. Such theories violate assumption (3.41), leading to logarithmic UV divergences in the BOE flow equations. These can be cured with the same methods discussed in section 7.1.2, but this time we need to apply the iterative procedure (7.5) only once. We normalize $\hat{\Phi}$ by the condition $b_1^{\hat{\Phi}} = 1$ where \mathcal{O}_1 is the lightest boundary operator in the BOE of $\hat{\Phi}$ (remember that $b_1^{\hat{\Phi}} = 0$). Then, the flow equations for the BOE coefficients of $\hat{\Phi}$ can be written as

$$\frac{db_i^{\hat{\Phi}}}{d\lambda} = \sum_l \sum_j b_l^{\hat{\Phi}} b_j^{\hat{\Phi}} \left[C_{lij} \mathcal{J}_{\Delta_i}(\Delta_l, \Delta_j) - b_i^{\hat{\Phi}} C_{lj1} \mathcal{J}_{\Delta_1}(\Delta_l, \Delta_j) \right], \quad i \geq 2. \quad (7.10)$$

once again giving finite flow equations with no need to introduce a UV cutoff.

7.2 Flow equations with no coupling

The coupling λ appearing in our flow equations is not a physical observable. To phrase our framework in a more scheme-independent way, we could express all the QFT data as curves parametrized by the lightest scaling dimension above the identity

$$\{\Delta_i(\Delta_1), \rho_i, C_{ijk}^{(n)}(\Delta_1), b_i^{\hat{\Phi}^{(n)}}(\Delta_1)\} \quad (7.11)$$

The flow equations can then be rephrased by a simple use of the chain rule

$$\begin{aligned} \frac{d\Delta_i}{d\Delta_1} &= \frac{\sum_l b_l^{\hat{\Phi}} C_{lii} \mathcal{I}(\Delta_l)}{\sum_l b_l^{\hat{\Phi}} C_{l11} \mathcal{I}(\Delta_l)} \\ \frac{db_i^{\hat{\Phi}}}{d\Delta_1} &= \frac{\sum_l \sum_j b_l^{\hat{\Phi}} b_j^{\hat{\Phi}} C_{lij} \mathcal{J}_{\Delta_i}(\Delta_l, \Delta_j)}{\sum_l b_l^{\hat{\Phi}} C_{l11} \mathcal{I}(\Delta_l)} \end{aligned} \quad (7.12)$$

while the crossing equations are already independent of λ and implicitly dependent on Δ_1 .

¹⁹For QCD, this is true for the specific case of exactly massless quarks.

7.3 Open questions

- What is the minimal set of QFT data? The locality sum rules of [25] imply nontrivial constraints among the BOE and OPE coefficients

$$\sum_l b_l^{\hat{\Phi}} C_{lij} \theta_{\Delta_l \Delta_i \Delta_j}^{\alpha, n} = 0, \quad \forall \mathcal{O}_i, \mathcal{O}_j, \alpha > \frac{\Delta_i + \Delta_j + \Delta_{\hat{\Phi}}^{\text{UV}}}{2}, n \in \mathbb{N}_0 \quad (7.13)$$

where $\theta_{\Delta_l \Delta_i \Delta_j}^{\alpha, n}$ is a kinematic coefficient which may be found explicitly in [25, 28]. Can these sum rules be used to, for example, express all BOE coefficients in terms of OPE coefficients and scaling dimensions?

- Can we prove that a generic interacting QFT in AdS has QFT data with an asymptotically ordered sign modulation for large scaling dimensions, as discussed in section 5.3? That would ensure that Padé approximants are a useful tool to provide good convergence of the sums in the flow equations also for interacting examples.
- To get a closed set of flow equations and crossing equations for AdS_{d+1} with $d+1 \geq 5$, one has to derive the ODE involving $\frac{d\Delta_i}{d\lambda}$ for operators \mathcal{O}_i carrying mixed symmetry representations ρ_i of $SO(d)$. This may not be too hard, and as in the $SO(2)$ and $SO(3)$ case one may hope to get flow equations which have the same form for any representation ρ_i .
- How do errors propagate when one evolves approximate data with the flow equations? Are these ODEs chaotic? Can we find efficient and controlled numerical algorithms to solve them numerically in interacting examples? For preliminary work in this direction, see [62].
- Is it possible to derive the ODE for the OPE coefficients in closed form? For AdS_4 , it should read

$$\frac{dC_{ijk}^{(c)}}{d\lambda} = \sum_l b_l^{\hat{\Phi}} \sum_m \sum_{a,b} C_{lim}^{(a)} C_{mjk}^{(b)} \mathcal{K}_{ijk}^{(a,b,c)}(\Delta_l, \Delta_m, J_m) + \text{perms.} \quad (7.14)$$

where “perms.” stands for cyclic (ijk) permutations, \mathcal{K} would be integrated bulk-boundary-boundary-boundary blocks and $\mathcal{O}_i, \mathcal{O}_j$ and \mathcal{O}_k would generically need to be spinning operators in order to close the system of equations. Computing \mathcal{K} is quite difficult: the blocks on the 3D boundary are not known in closed form, deriving the bulk-boundary-boundary-boundary block and its integral over AdS thus seems like a very hard task. For AdS_3 , instead, 2D boundary blocks are known in closed form for all spins [40]. The main bottleneck, which also affects the 2D case [1], is the fact that one can at best only derive an integral representation of \mathcal{K} rather than a closed form expression. This slows down the implementation of the flow equations greatly, as one has to evaluate multivariable numerical integrals for each summand in (7.14) at each step in the integration of the flow equations.

- It should be possible to derive flow equations describing the QFT data on a defect inserted on the boundary of AdS. This setup is most naturally realized when studying a Yang-Mills flux tube stretched between Wilson lines inserted at the boundary of AdS [63, 64]. In that case, there exists a displacement operator at the boundary, which has been recently proved to be protected under the bulk RG flow even if there is no stress tensor in the boundary theory [65, 66].

7.4 Possible applications

There are many QFTs of interest which we would like to attack with the flow equations. Let us list a few examples in 3D and 4D

- Yang-Mills in 3D. Following the theory with Neumann boundary conditions, we could try to extract the masses of the lightest glueballs from the asymptotics of $\Delta_i(\lambda)$ and compare with the lattice results [67].
- QCD in 3D. The masses of the resonances are again interesting targets. Moreover, one can study the conformal window and the values of the number of colors N_c and fermions N_f for which the transition between a gapped and gapless IR phase happens [68] (which would be signaled by the $\Delta_i(\lambda)$ growing vs. asymptoting to constants respectively).
- $\lambda\phi^4$ (and more generally $O(N)$ model) in 3D. In the strictly massless case, the IR fixed point is the 3D critical Ising (respectively, $O(N)$) model. Flat space perturbation theory fails in this case, but our flow equations should hold. Since the IR fixed point is a nontrivial BCFT, we would expect the curves $\Delta_i(\lambda)$ to asymptote to the values of the flat space BCFT [69–71]. In principle, one can then extract estimates for the bulk critical exponents by fitting the asymptotic behavior of the BOE coefficients $b_l^{\hat{\mathcal{O}}}$ for large Δ_l . It would be great to compare them to the islands obtained through the conformal bootstrap [72]. For recent perturbative and large N work on this theory in AdS, see [73, 74].
- Similarly to the $O(N)$ case, the 3D Gross-Neveu model has a strongly coupled gapless IR phase, which would be interesting to study with the flow equations. Its data could be compared to [75–77].
- QED in 3D. Depending on the number of fermions N_f , the IR of this theory is either gapped or flows to a CFT with global symmetry $SU(N_f) \times U(1)$ [78–80]. Determining the critical value of N_f for which this transition happens, is an open problem. It would be great to study this issue with the flow equations, and observe a transition of the $\Delta_i(\lambda)$ curves from constant (in the BCFT phase) to growing (in the gapped phase). The BCFT data thus obtained could be matched with the upcoming ϵ -expansion results from [81].²⁰

Other interesting QFTs, but which require treating the classically marginal relevant deformation as discussed in 7.1.3, are

²⁰For other recent studies of QED in AdS, see [82–84].

- Yang-Mills and QCD in 4D. When the gauge fields in these theories have Dirichlet boundary conditions, the QFT data is expected to undergo merger-annihilation at some value of $R\Lambda_{\text{YM/QCD}}$ due to color confinement in the flat space theory [23, 24, 60, 61, 85]. Current estimates of the critical value of $R\Lambda_{\text{YM/QCD}}$ are obtained through perturbation theory. It would be interesting to study the explicit curves of the QFT data in these theories with the flow equations. With Neumann boundary conditions, we could in principle extract estimates of the masses of the resonances in both theories. The conformal window of QCD is also an interesting problem to study.

Acknowledgments

We would like to thank Tomas Reis, Lorenzo Quintavalle, Marco Serone, Jiaxin Qiao, Gregoire Mathys, Xiang Zhao, the participants and organizers of the conference ‘‘QFT in AdS 2026’’ and especially Marco Meineri and Joao Penedones for useful conversations that helped overcome some of the challenges encountered in this work.

Our research is supported by the Italian Ministry of University and Research (MUR) under the FIS grant BootBeyond (CUP: D53C24005470001) and by the INFN ‘‘Iniziativa Specifica’’ ST&FI.

A Derivation of blocks

Here we derive the various conformal blocks introduced in the main text.

A.1 Bulk-bulk

AdS invariance forces the two-point function of bulk operators to take the form

$$\langle \hat{\Phi}_1(X_1)\hat{\Phi}_2(X_2) \rangle = \mathcal{G}_{\hat{\Phi}_1\hat{\Phi}_2}(X_1 \cdot X_2). \quad (\text{A.1})$$

At the same time, we can fix to the conformal frame

$$(z_1, \mathbf{x}_1) = (z, 0), \quad (z_2, \mathbf{x}_2) = (1, 0) \quad (\text{A.2})$$

and then perform the BOE (2.39) of $\hat{\Phi}_1$

$$\begin{aligned} \langle \hat{\Phi}_1(z, 0)\hat{\Phi}_2(1, 0) \rangle &= \sum_l b_l^{\hat{\Phi}_1} z^{\Delta_l} \sum_{n=0}^{\infty} \frac{(-1)^n}{n!2^{2n}(\Delta_l - \frac{d-2}{2})_n} z^{2n} \square^n \langle \mathcal{O}_l(\mathbf{x})\hat{\Phi}_2(1, 0) \rangle \Big|_{\mathbf{x}=0} \\ &= \sum_l b_l^{\hat{\Phi}_1} b_l^{\hat{\Phi}_2} z^{\Delta_l} \sum_{n=0}^{\infty} \frac{(-1)^n}{n!2^{2n}(\Delta_l - \frac{d-2}{2})_n} z^{2n} \square^n \left(\frac{1}{1 + \mathbf{x}^2} \right)^{\Delta_l} \Big|_{\mathbf{x}=0} \\ &= \sum_l b_l^{\hat{\Phi}_1} b_l^{\hat{\Phi}_2} z^{\Delta_l} \sum_{n=0}^{\infty} \frac{(\Delta_l)_n (\frac{d}{2})_n}{n!(\Delta_l - \frac{d-2}{2})_n} z^{2n} \\ &= \sum_l b_l^{\hat{\Phi}_1} b_l^{\hat{\Phi}_2} z^{\Delta_l} {}_2F_1 \left(\begin{matrix} \Delta_l, & \frac{d}{2}, \\ \Delta_l - \frac{d-2}{2}, \end{matrix}; z^2 \right) \\ &= \sum_l b_l^{\hat{\Phi}_1} b_l^{\hat{\Phi}_2} \frac{z^{\Delta_l}}{(1-z)^{2\Delta_l}} {}_2F_1 \left(\begin{matrix} \Delta_l, & \Delta_l - \frac{d-1}{2}, \\ 2\Delta_l - d + 1; \end{matrix} -\frac{4z}{(1-z)^2} \right) \end{aligned} \quad (\text{A.3})$$

where in the last step we used Kummer's quadratic transformation identity

$${}_2F_1\left(\begin{matrix} a & b \\ a-b+1 \end{matrix}; z^2\right) = \frac{1}{(1-z)^{2a}} {}_2F_1\left(\begin{matrix} a & a-b+\frac{1}{2} \\ 2a-2b+1 \end{matrix}; -\frac{4z}{(1-z)^2}\right) \quad (\text{A.4})$$

Now consider the fact that, in frame (A.2), $\sigma \equiv X_1 \cdot X_2 = -\frac{1+z^2}{2z}$. Inverting this relation and using (A.1) we find

$$\langle \hat{\Phi}_1(X_1) \hat{\Phi}_2(X_2) \rangle = \sum_l b_l^{\hat{\Phi}_1} b_l^{\hat{\Phi}_2} \frac{1}{(-2-2\sigma)^{\Delta_l}} {}_2F_1\left(\begin{matrix} \Delta_l, & \Delta_l - \frac{d-1}{2} \\ 2\Delta_l - d + 1 \end{matrix}; \frac{2}{1+\sigma}\right). \quad (\text{A.5})$$

A.2 Bulk-boundary-boundary

Scalars The three-point function of a bulk field with two boundary operators is also fixed up to a function of a single cross ratio

$$\langle \mathcal{O}_i(P_1) \mathcal{O}_j(P_2) \hat{\Phi}(X) \rangle = \frac{1}{P_{12}^{\frac{\Delta_i+\Delta_j}{2}}} \left(\frac{P_1 \cdot X}{P_2 \cdot X} \right)^{\frac{\Delta_j-\Delta_i}{2}} \mathcal{G}_{\hat{\Phi}_{ij}}(\chi), \quad (\text{A.6})$$

where we choose

$$\chi \equiv -\frac{1}{2} \frac{P_1 \cdot P_2}{(P_1 \cdot X)(P_2 \cdot X)}. \quad (\text{A.7})$$

For simplicity, let us fix to the frame

$$(z_1, \mathbf{x}_1) = (0, 0), \quad (z_2, \mathbf{x}_2) = (0, \infty), \quad (z_3, \mathbf{x}_3) = (z, \hat{\mathbf{x}}^1), \quad (\text{A.8})$$

where (z_3, \mathbf{x}_3) is X in Poincaré coordinates, $\hat{\mathbf{x}}^1$ is the unit vector pointing in the 1 direction and we take operators to infinity as follows

$$\mathcal{O}_i(\infty) \equiv \lim_{\mathbf{x}^2 \rightarrow \infty} (\mathbf{x}^2)^{\Delta_i} \mathcal{O}_i(\mathbf{x}) \quad (\text{A.9})$$

Performing the BOE of $\hat{\Phi}$, and using (2.29), we get

$$\begin{aligned} \langle \mathcal{O}_i(0) \mathcal{O}_j(\infty) \hat{\Phi}(z, \hat{\mathbf{x}}^1) \rangle &= \sum_l b_l^{\hat{\Phi}} z^{\Delta_l} \sum_{n=0}^{\infty} \frac{(-1)^n}{n! 2^{2n} (\Delta_l - \frac{d-2}{2})_n} z^{2n} \square^n \langle \mathcal{O}_i(0) \mathcal{O}_j(\infty) \mathcal{O}_l(\mathbf{x}) \rangle \Big|_{\mathbf{x} \rightarrow \hat{\mathbf{x}}^1} \\ &= \sum_l b_l^{\hat{\Phi}} C_{lij} z^{\Delta_l} \sum_{n=0}^{\infty} \frac{(-1)^n (\frac{\Delta_{lij}}{2})_n (\frac{\Delta_{lij}}{2} - \frac{d-2}{2})_n}{n! (\Delta_l - \frac{d-2}{2})_n} z^{2n} \\ &= \sum_l b_l^{\hat{\Phi}} C_{lij} z^{\Delta_l} {}_2F_1\left(\begin{matrix} \frac{\Delta_{lij}}{2} & \frac{\Delta_{lij}}{2} - \frac{d-2}{2} \\ \Delta_l - \frac{d-2}{2} \end{matrix}; -z^2\right) \\ &= \sum_l b_l^{\hat{\Phi}} C_{lij} \frac{z^{\Delta_l}}{(z^2+1)^{\frac{\Delta_{lij}}{2}}} {}_2F_1\left(\begin{matrix} \frac{\Delta_{lij}}{2} & \frac{\Delta_{lij}}{2} \\ \Delta_l - \frac{d-2}{2} \end{matrix}; \frac{z^2}{z^2+1}\right). \end{aligned} \quad (\text{A.10})$$

where in the last step we used the Pfaff transformation

$${}_2F_1\left(\begin{matrix} a & b \\ c \end{matrix}; z\right) = \frac{1}{(1-z)^a} {}_2F_1\left(\begin{matrix} a & c-b \\ c \end{matrix}; \frac{z}{z-1}\right) \quad (\text{A.11})$$

In frame (A.8), we have that $\chi = \frac{z^2}{z^2+1}$. Inverting this relation and matching with (A.6), we can thus write

$$\langle \mathcal{O}_i(P_1)\mathcal{O}_j(P_2)\hat{\Phi}(X) \rangle = \frac{1}{P_{12}^{\frac{\Delta_i+\Delta_j}{2}}} \left(\frac{P_1 \cdot X}{P_2 \cdot X} \right)^{\frac{\Delta_j-\Delta_i}{2}} \sum_l b_l^{\hat{\Phi}} C_{lij} G_{\text{Bbb}}^{\Delta_l, \Delta_i, \Delta_j}(\chi) \quad (\text{A.12})$$

with

$$G_{\text{Bbb}}^{\Delta_l, \Delta_i, \Delta_j}(\chi) = \chi^{\frac{\Delta_l}{2}} {}_2F_1 \left(\frac{\Delta_{lij}}{2}, \frac{\Delta_{lji}}{2}; \Delta_l - \frac{d-2}{2}; \chi \right). \quad (\text{A.13})$$

AdS₃ When spin is involved in AdS₃, it is best to express boundary operators in the complex coordinates discussed in the main text. We will specifically need the case where the two boundary operators are identical, and have spin J .

When we fix the position of the two boundary operators and the bulk operator in a non-degenerate way, the leftover stabilizer group is $SO(d-1) = SO(1)$, hence we have no independent spin cross-ratio in this case, and the three-point function can be fixed up to a function of a single cross-ratio

$$\langle \mathcal{O}_i(\mathbf{z}_1, \bar{\mathbf{z}}_1)\mathcal{O}_i(\mathbf{z}_2, \bar{\mathbf{z}}_2)\hat{\Phi}(z, \mathbf{z}_3, \bar{\mathbf{z}}_3) \rangle = \frac{1}{z_{12}^{2h_i} \bar{z}_{12}^{2\bar{h}_i}} \mathcal{G}_{ii\hat{\Phi}}(\chi) \quad (\text{A.14})$$

where we take χ to be the same cross-ratio as in (A.7). We fix the frame

$$(\mathbf{z}_1, \bar{\mathbf{z}}_1) = (0, 0), \quad (\mathbf{z}_2, \bar{\mathbf{z}}_2) = (\infty, \infty), \quad (\mathbf{z}_3, \bar{\mathbf{z}}_3) = (\mathbf{z}, \bar{\mathbf{z}}), \quad (\text{A.15})$$

where taking an operator to infinity in these coordinates means

$$\mathcal{O}_i(\infty, \infty) \equiv \lim_{\mathbf{z} \rightarrow \infty} \lim_{\bar{\mathbf{z}} \rightarrow \infty} \mathbf{z}^{2h} \bar{\mathbf{z}}^{2\bar{h}} \mathcal{O}_i(\mathbf{z}, \bar{\mathbf{z}}). \quad (\text{A.16})$$

We expand $\hat{\Phi}$ to the boundary with the BOE (2.39). Using the form of the three-point function (2.30) and the laplacian in complex coordinates $\square = 2\partial_z \partial_{\bar{z}}$, we get

$$\begin{aligned} \langle \mathcal{O}_i(0, 0)\mathcal{O}_i(\infty, \infty)\hat{\Phi}(z, \mathbf{z}, \bar{\mathbf{z}}) \rangle &= \sum_l b_l^{\hat{\Phi}} C_{lii} z^{\Delta_l} \sum_{n=0}^{\infty} \frac{(-1)^n z^{2n}}{n! 2^{2n} (\Delta_l)_n} \square^n \frac{1}{(\mathbf{z}\bar{\mathbf{z}})^{\frac{\Delta_l}{2}}} \\ &= \sum_l b_l^{\hat{\Phi}} C_{lii} z^{\Delta_l} \frac{1}{(\mathbf{z}\bar{\mathbf{z}})^{\frac{\Delta_l}{2}}} {}_2F_1 \left(\frac{\Delta_l}{2}, \frac{\Delta_l}{2}; -\frac{z^2}{\mathbf{z}\bar{\mathbf{z}}} \right) \\ &= \sum_l b_l^{\hat{\Phi}} C_{lii} \left(\frac{z^2}{z^2 + \mathbf{z}\bar{\mathbf{z}}} \right)^{\frac{\Delta_l}{2}} {}_2F_1 \left(\frac{\Delta_l}{2}, \frac{\Delta_l}{2}; \frac{z^2}{z^2 + \mathbf{z}\bar{\mathbf{z}}} \right) \end{aligned} \quad (\text{A.17})$$

where we used the Pfaff transform (A.11). Now we recognize the cross ratio in this frame $\chi = \frac{z^2}{z^2+\mathbf{z}\bar{\mathbf{z}}}$. We thus can write

$$\mathcal{G}_{ii\hat{\Phi}}(\chi) = \sum_l b_l^{\hat{\Phi}} C_{lii} \chi^{\frac{\Delta_l}{2}} {}_2F_1 \left(\frac{\Delta_l}{2}, \frac{\Delta_l}{2}; \chi \right), \quad (\text{A.18})$$

just like in the scalar case.

AdS₄ Now let us discuss the analogous case in 4D. In this case, fixing the position of all operators leaves the residual stabilizer group $SO(d-1) = SO(2)$ which allows for the three-point function to be fixed up to a function of a position cross-ratio and a spin cross-ratio

$$\langle \mathcal{O}_i^{(J)}(P_1, Z_1) \mathcal{O}_i^{(J)}(P_2, Z_2) \hat{\Phi}(X) \rangle = \frac{H_{1,2}^J}{P_{1,2}^{\Delta_i+J}} \mathcal{G}_{ii\hat{\Phi}}(\chi, v) \quad (\text{A.19})$$

where we choose χ as in (A.7) and

$$v \equiv \frac{1}{\chi-1} \frac{V_{1,23} V_{2,31}}{H_{1,2}}, \quad P_3 \rightarrow X \quad (\text{A.20})$$

where $H_{i,j}$ and $V_{i,jk}$ are defined in (2.27) and (2.35) respectively. We choose the frame where one boundary operator is at the origin and one at infinity. In embedding notation, this corresponds to

$$\begin{aligned} P_1 &= \left(\frac{1}{2}, 0, \frac{1}{2} \right), & P_2 &= \left(\frac{1}{2}, 0, -\frac{1}{2} \right), & Z_1 &= (0, \mathbf{z}_1, 0), & Z_2 &= (0, \mathbf{z}_2, 0) \\ X &= \left(\frac{2+z^2}{2z}, \frac{\hat{\mathbf{x}}^1}{z}, -\frac{1}{2z} \right) \end{aligned} \quad (\text{A.21})$$

In this frame, the cross ratios take the form

$$v = \frac{\mathbf{z}_1^1 \mathbf{z}_2^1}{\mathbf{z}_1 \cdot \mathbf{z}_2}, \quad \chi = \frac{z^2}{1+z^2}. \quad (\text{A.22})$$

At the same time, the BOE of the bulk field gives

$$\begin{aligned} &\langle \mathcal{O}_i^{(J)}(0, \mathbf{z}_1) \mathcal{O}_i^{(J)}(\infty, \mathbf{z}_2) \hat{\Phi}(z, \hat{\mathbf{x}}^1) \rangle \\ &= \sum_l b_l^{\hat{\Phi}} z^{\Delta_l} \sum_{n=0}^{\infty} \frac{(-1)^n}{n! 2^{2n} (\Delta_l - \frac{1}{2})_n} z^{2n} \square^n \langle \mathcal{O}_i^{(J)}(0, \mathbf{z}_1) \mathcal{O}_i^{(J)}(\infty, \mathbf{z}_2) \mathcal{O}_l(\mathbf{x}) \rangle \Big|_{\mathbf{x} \rightarrow \hat{\mathbf{x}}^1} \\ &= \sum_l b_l^{\hat{\Phi}} z^{\Delta_l} \sum_{m=0}^J C_{lii}^{(m)} \sum_{n=0}^{\infty} \frac{(-1)^n (\mathbf{z}_1 \cdot \mathbf{z}_2)^J}{n! 2^{2n} (\Delta_l - \frac{1}{2})_n} z^{2n} \square^n \frac{\mathcal{H}_m \left(\frac{(\mathbf{z}_1 \cdot \mathbf{x})(\mathbf{z}_2 \cdot \mathbf{x})}{\mathbf{x}^2 (\mathbf{z}_1 \cdot \mathbf{z}_2)} \right)}{(\mathbf{x}^2)^{\frac{\Delta_l}{2}}} \Big|_{\mathbf{x} \rightarrow \hat{\mathbf{x}}^1} \end{aligned} \quad (\text{A.23})$$

where we used the basis decomposition of the boundary three-point function (2.36).

To proceed, we use the following property of the \mathcal{H}_m polynomials, the reason why we chose them as a basis of our tensor structures in the first place: the action of the Laplacian on the basis elements in this frame is diagonal

$$\square \frac{1}{(\mathbf{x}^2)^{\frac{\Delta_l}{2}}} \mathcal{H}_m \left(\frac{(\mathbf{z}_1 \cdot \mathbf{x})(\mathbf{z}_2 \cdot \mathbf{x})}{\mathbf{x}^2 (\mathbf{z}_1 \cdot \mathbf{z}_2)} \right) = \frac{(\Delta_l + 2m)(\Delta_l - 2m - 1)}{(\mathbf{x}^2)^{\frac{\Delta_l}{2}+1}} \mathcal{H}_m \left(\frac{(\mathbf{z}_1 \cdot \mathbf{x})(\mathbf{z}_2 \cdot \mathbf{x})}{\mathbf{x}^2 (\mathbf{z}_1 \cdot \mathbf{z}_2)} \right) \quad (\text{A.24})$$

Using this fact, we have

$$\begin{aligned}
& \langle \mathcal{O}_i^{(J)}(0, \mathbf{z}_1) \mathcal{O}_i^{(J)}(\infty, \mathbf{z}_2) \hat{\Phi}(z, \hat{\mathbf{x}}^1) \rangle \\
&= (\mathbf{z}_1 \cdot \mathbf{z}_2)^J \sum_l b_l^{\hat{\Phi}} z^{\Delta_l} \sum_{m=0}^J C_{l\hat{i}\hat{i}}^{(m)} \mathcal{H}_m \left(\frac{\mathbf{z}_1^1 \mathbf{z}_2^1}{\mathbf{z}_1 \cdot \mathbf{z}_2} \right) \sum_{n=0}^{\infty} \frac{(-1)^n z^{2n} \left(\frac{\Delta_l}{2} + m\right)_n \left(\frac{\Delta_l - 1 - 2m}{2}\right)_n}{n! (\Delta_l - \frac{1}{2})_n} \\
&= (\mathbf{z}_1 \cdot \mathbf{z}_2)^J \sum_l b_l^{\hat{\Phi}} z^{\Delta_l} \sum_{m=0}^J C_{l\hat{i}\hat{i}}^{(m)} \mathcal{H}_m \left(\frac{\mathbf{z}_1^1 \mathbf{z}_2^1}{\mathbf{z}_1 \cdot \mathbf{z}_2} \right) {}_2F_1 \left(\frac{\Delta_l}{2} + m, \frac{\Delta_l - 1 - 2m}{2}; \Delta_l - \frac{1}{2}; -z^2 \right) \quad (\text{A.25}) \\
&= (\mathbf{z}_1 \cdot \mathbf{z}_2)^J \sum_l b_l^{\hat{\Phi}} \frac{z^{\Delta_l}}{(1+z^2)^{\frac{\Delta_l}{2}+m}} \sum_{m=0}^J C_{l\hat{i}\hat{i}}^{(m)} \mathcal{H}_m \left(\frac{\mathbf{z}_1^1 \mathbf{z}_2^1}{\mathbf{z}_1 \cdot \mathbf{z}_2} \right) {}_2F_1 \left(\frac{\Delta_l}{2} + m, \frac{\Delta_l}{2} + m; \Delta_l - \frac{1}{2}; \frac{z^2}{z^2 + 1} \right)
\end{aligned}$$

Comparing with (A.19) and noticing that $H_{1,2} = \mathbf{z}_1 \cdot \mathbf{z}_2$ in this frame, we get

$$\mathcal{G}_{i\hat{i}\hat{\Phi}}(\chi, v) = \sum_l b_l^{\hat{\Phi}} \sum_{n=0}^J C_{l\hat{i}\hat{i}}^{(n)} \mathcal{H}_n(v) G_{\text{Bbb}}^{\Delta_l, n}(\chi) \quad (\text{A.26})$$

where

$$G_{\text{Bbb}}^{\Delta_l, n}(\chi) = \chi^{\frac{\Delta_l}{2}} (1-\chi)^n {}_2F_1 \left(\frac{\Delta_l}{2} + n, \frac{\Delta_l}{2} + n; \Delta_l - \frac{1}{2}; \chi \right) \quad (\text{A.27})$$

Another interesting property of this basis decomposition is the behavior under cross-traces:

$$(D_{\mathbf{z}_1} \cdot D_{\mathbf{z}_2})^m \left[(\mathbf{z}_1 \cdot \mathbf{z}_2)^J \mathcal{H}_n \left(\frac{(\mathbf{z}_1 \cdot \mathbf{x})(\mathbf{z}_2 \cdot \mathbf{x})}{\mathbf{x}^2 (\mathbf{z}_1 \cdot \mathbf{z}_2)} \right) \right] = 0, \quad \forall m > J - n, \quad (\text{A.28})$$

where $D_{\mathbf{z}}$ was defined in (2.22). In other words, elements of this basis have a number of vanishing cross-traces which increases with n , and if in particular we take $m = J$, the only nonvanishing term is the one with $n = 0$.

A.3 Bulk-bulk-boundary

AdS invariance fixes bulk-bulk-boundary three-point functions up to two cross ratios

$$\langle \hat{\Phi}_1(X_1) \hat{\Phi}_2(X_2) \mathcal{O}_i(P_3) \rangle = \frac{1}{(-2P_3 \cdot X_2)^{\Delta_i}} \mathcal{G}_{\hat{\Phi}_1 \hat{\Phi}_2 i}(\xi, \rho). \quad (\text{A.29})$$

We choose

$$\xi = \left(\frac{P_3 \cdot X_1}{P_3 \cdot X_2} \right)^2, \quad \rho = -1 - \xi - 2(X_1 \cdot X_2) \sqrt{\xi} \quad (\text{A.30})$$

At the same time, we can expand both bulk operators to the boundary. We do that in the following frame

$$(z_1, \mathbf{x}_1) = (z, r\hat{\mathbf{x}}^1), \quad (z_2, \mathbf{x}_2) = (1, 0), \quad (z_3, \mathbf{x}_3) = (0, \infty). \quad (\text{A.31})$$

We get

$$\begin{aligned}
& \langle \hat{\Phi}_1(z, r\hat{\mathbf{x}}^1) \hat{\Phi}_2(1, 0) \mathcal{O}_i(\infty) \rangle = \sum_j \sum_l b_l^{\hat{\Phi}_1} b_j^{\hat{\Phi}_2} z^{\Delta_l} \\
& \sum_{n=0}^{\infty} \sum_{m=0}^{\infty} \frac{(-1)^{n+m} 2^{-2(n+m)} z^{2n}}{n! m! (\Delta_l - \frac{d-2}{2})_n (\Delta_j - \frac{d-2}{2})_m} \square^n \square_2^m \langle \mathcal{O}_l(\mathbf{x}) \mathcal{O}_j(\mathbf{x}_2) \mathcal{O}_i(\infty) \rangle \Big|_{\mathbf{x}_2 \rightarrow 0, \mathbf{x} \rightarrow r\hat{\mathbf{x}}^1} \quad (\text{A.32})
\end{aligned}$$

We will eventually want to match this to a block decomposition, which we expect to take the form

$$\langle \hat{\Phi}_1(X_1) \hat{\Phi}_2(X_2) \mathcal{O}_i(P_3) \rangle = \frac{1}{(-2P_3 \cdot X_2)^{\Delta_i}} \sum_j \sum_l b_l^{\hat{\Phi}_1} b_j^{\hat{\Phi}_2} C_{lij} G_{\text{BBb}}^{\Delta_l, \Delta_j, \Delta_i}(\xi, \rho). \quad (\text{A.33})$$

Moreover, in frame (A.31), the cross ratios take the values $\xi = \frac{1}{z^2}$ and $\rho = \frac{r^2}{z^2}$ and the scale factor is $\frac{1}{(-2P_3 \cdot X_2)^{\Delta_i}} \rightarrow \frac{1}{(x_3^2)^{\Delta_i}}$, which gets canceled when we take operator \mathcal{O}_i to infinity as in (A.9).

Continuing from (A.32), we thus have

$$\begin{aligned} G_{\text{BBb}}^{\Delta_l, \Delta_j, \Delta_i} \left(\frac{1}{z^2}, \frac{r^2}{z^2} \right) &= \sum_{n, m=0}^{\infty} \frac{(-1)^{n+m} \left(\frac{\Delta_{lji}}{2}\right)_n \left(\frac{\Delta_{lji}}{2} - \frac{d-2}{2}\right)_n \left(\frac{\Delta_{lji}}{2} + n\right)_m \left(\frac{\Delta_{lji}}{2} - \frac{d-2}{2} + n\right)_m z^{\Delta_l + 2n}}{n! m! (\Delta_l - \frac{d-2}{2})_n (\Delta_j - \frac{d-2}{2})_m r^{\Delta_{lji} + 2n + 2m}} \\ &= \sum_{n, m=0}^{\infty} \frac{(-1)^{n+m} \left(\frac{\Delta_{lji}}{2}\right)_{n+m} \left(\frac{\Delta_{lji}}{2} - \frac{d-2}{2}\right)_{n+m} z^{\Delta_l + 2n}}{n! m! (\Delta_l - \frac{d-2}{2})_n (\Delta_j - \frac{d-2}{2})_m r^{\Delta_{lji} + 2n + 2m}} \\ &= \frac{z^{\Delta_l}}{r^{\Delta_{lji}}} F_4 \left(\begin{matrix} \frac{\Delta_{lji}}{2}, & \frac{\Delta_{lji}}{2} - \frac{d-2}{2} \\ \Delta_l - \frac{d-2}{2}, & \Delta_j - \frac{d-2}{2} \end{matrix}; -\frac{z^2}{r^2}, -\frac{1}{r^2} \right) \end{aligned} \quad (\text{A.34})$$

Matching with (A.33), we get

$$G_{\text{BBb}}^{\Delta_l, \Delta_j, \Delta_i}(\xi, \rho) = \frac{\xi^{\frac{\Delta_j - \Delta_i}{2}}}{\rho^{\frac{\Delta_{lji}}{2}}} F_4 \left(\begin{matrix} \frac{\Delta_{lji}}{2}, & \frac{\Delta_{lji}}{2} - \frac{d-2}{2} \\ \Delta_l - \frac{d-2}{2}, & \Delta_j - \frac{d-2}{2} \end{matrix}; -\frac{1}{\rho}, -\frac{\xi}{\rho} \right). \quad (\text{A.35})$$

This representation of the conformal block is not analytic for all possible values of the cross-ratios. If we instead expand the Appell F_4 as in (2.56) and resum over one of the variables, we can write

$$\begin{aligned} G_{\text{BBb}}^{\Delta_l, \Delta_j, \Delta_i}(\xi, \rho) &= \frac{\xi^{\frac{\Delta_j - \Delta_i}{2}}}{\rho^{\frac{\Delta_{lji}}{2}}} \sum_{m=0}^{\infty} \frac{(-1)^m \left(\frac{\Delta_{lji}}{2} - \frac{d-2}{2}\right)_m \left(\frac{\Delta_{lji}}{2}\right)_m \xi^m}{m! (\Delta_j - \frac{d-2}{2})_m \rho^m} {}_2F_1 \left(\begin{matrix} \frac{\Delta_{lji}}{2} + m, & \frac{\Delta_{lji}}{2} - \frac{d-2}{2} + m \\ \Delta_l - \frac{d-2}{2} \end{matrix}; -\frac{1}{\rho} \right) \\ &= \frac{\xi^{\frac{\Delta_j - \Delta_i}{2}}}{(1 + \rho)^{\frac{\Delta_{lji}}{2}}} \sum_{m=0}^{\infty} \frac{(-1)^m \left(\frac{\Delta_{lji}}{2} - \frac{d-2}{2}\right)_m \left(\frac{\Delta_{lji}}{2}\right)_m}{m! (\Delta_j - \frac{d-2}{2})_m (1 + \rho)^m} {}_2F_1 \left(\begin{matrix} \frac{\Delta_{lji}}{2} - m, & \frac{\Delta_{lji}}{2} + m \\ \Delta_l - \frac{d-2}{2} \end{matrix}; \frac{1}{1 + \rho} \right) \end{aligned} \quad (\text{A.36})$$

The final step is to open up the hypergeometric function with its series representation and resum over m . We obtain

$$\begin{aligned} G_{\text{BBb}}^{\Delta_l, \Delta_j, \Delta_i}(\xi, \rho) &= \frac{\xi^{\frac{\Delta_j - \Delta_i}{2}} \Gamma(\Delta_j - \frac{d-2}{2}) \Gamma(1 - \frac{\Delta_{lji}}{2})}{(1 + \rho)^{\frac{\Delta_{lji}}{2}}} \sum_{n=0}^{\infty} \left(\frac{-1}{1 + \rho} \right)^n \frac{\left(\frac{\Delta_{lji}}{2}\right)_n}{n! (\Delta_l - \frac{d-2}{2})_n} \\ &\quad \times {}_3\tilde{F}_2 \left(\begin{matrix} 1 - \frac{\Delta_{lji}}{2}, & \frac{\Delta_{lji}}{2} - \frac{d-2}{2}, & \frac{\Delta_{lji}}{2} + n \\ 1 - n - \frac{\Delta_{lji}}{2}, & \Delta_j - \frac{d-2}{2} \end{matrix}; -\frac{\xi}{1 + \rho} \right) \end{aligned} \quad (\text{A.37})$$

The advantage of this representation is that it is analytic for all $\xi > 0$ and $\rho > -1$, which in particular includes all configurations in AdS.

B Details about the derivation of the flow equations

We present here some technical details used to derive the flow equations.

B.1 Flow of scaling dimensions

In this section, we derive the structural form of the integral

$$I_{\text{Bbb}}^{\Delta_l, \Delta_i, \Delta_j}(\mathbf{x}_1, \mathbf{x}_2, \epsilon) = \int_{\mathcal{M}_\epsilon} \frac{dz d^d \mathbf{x}}{z^{d+1}} \frac{1}{|\mathbf{x}_{12}|^{\Delta_i + \Delta_j}} \left(\frac{|\mathbf{x} - \mathbf{x}_1|^2 + z^2}{|\mathbf{x} - \mathbf{x}_2|^2 + z^2} \right)^{\frac{\Delta_j - \Delta_i}{2}} G_{\text{Bbb}}^{\Delta_l, \Delta_i, \Delta_j}(\chi). \quad (\text{B.1})$$

To evaluate this expression, we decompose the integral, separating the integration over the entire AdS space from the contributions of the subtracted regions near the boundary points, as in

$$I_{\text{Bbb}}^{\Delta_l, \Delta_i, \Delta_j}(\mathbf{x}_1, \mathbf{x}_2, \epsilon) = I_{\text{Bbb}}^{\Delta_l, \Delta_i, \Delta_j}(\mathbf{x}_1, \mathbf{x}_2, 0) - I_{\text{Bbb, in}}^{\Delta_l, \Delta_i, \Delta_j}(\mathbf{x}_1, \mathbf{x}_2, \epsilon), \quad (\text{B.2})$$

where $I_{\text{Bbb, in}}^{\Delta_l, \Delta_i, \Delta_j}$ represents the integral over the two subtracted half-balls, represented in figure 6. This term is defined as

$$I_{\text{Bbb, in}}^{\Delta_l, \Delta_i, \Delta_j} := \int_{|\mathbf{x} - \mathbf{x}_k|^2 + z^2 < \epsilon^2} \frac{dz d^d \mathbf{x}}{z^{d+1}} \frac{1}{|\mathbf{x}_{12}|^{\Delta_i + \Delta_j}} \left(\frac{|\mathbf{x} - \mathbf{x}_1|^2 + z^2}{|\mathbf{x} - \mathbf{x}_2|^2 + z^2} \right)^{\frac{\Delta_j - \Delta_i}{2}} G_{\text{Bbb}}^{\Delta_l, \Delta_i, \Delta_j}(\chi). \quad (\text{B.3})$$

We note that, if $I_{\text{Bbb}}^{\Delta_l, \Delta_i, \Delta_j}(\mathbf{x}_1, \mathbf{x}_2, 0)$ were a convergent integral, conformal invariance would imply that it vanishes whenever $\Delta_i \neq \Delta_j$. Consequently, one would obtain

$$I_{\text{Bbb}}^{\Delta_l, \Delta_i, \Delta_j}(\mathbf{x}_1, \mathbf{x}_2, \epsilon) = -I_{\text{Bbb, in}}^{\Delta_l, \Delta_i, \Delta_j}(\mathbf{x}_1, \mathbf{x}_2, \epsilon). \quad (\text{B.4})$$

Since the integral in the right-hand side is divergent for all values of the scaling dimensions, this relation must be intended as an analytic continuation, in the following sense: when considering the half-ball centered at \mathbf{x}_1 , we take $\Delta_j > \Delta_i$, and the converse when integrating instead around \mathbf{x}_2 . A justification of this extension is provided in appendix D of [1], and we will assume its validity in the following. We are thus left to evaluate the integration within the subtracted half-balls. Let us focus on the half-ball centered at \mathbf{x}_2 , which is finite in the regime $\Delta_i > \Delta_j$. To compute it, we adopt spherical coordinates centered at \mathbf{x}_2 for the boundary directions, combined with polar coordinates for the half-plane spanned by the boundary radial distance \mathbf{r} and the bulk coordinate z . We then parametrize the bulk coordinates for small distances $R < \epsilon$ as

$$\mathbf{x} = \mathbf{x}_2 + \mathbf{r} \quad \text{with} \quad |\mathbf{r}| = R \cos \theta, \quad z = R \sin \theta. \quad (\text{B.5})$$

where $\theta \in (0, \pi/2)$. Let us now write the conformal block as a power series

$$G_{\text{Bbb}}^{\Delta_l, \Delta_i, \Delta_j}(\chi) = \sum_{n \geq 0} a_n \chi^{\Delta_l/2 + n} \quad (\text{B.6})$$

and expand the integrand in $I_{\text{Bbb,in}}^{\Delta_l, \Delta_i, \Delta_j}$ for small R . In this setup, the cross-ratio limits to $\chi \approx \sin^2 \theta + \mathcal{O}(R)$, and $I_{\text{Bbb,in}}^{\Delta_l, \Delta_i, \Delta_j}$ becomes

$$\begin{aligned} I_{\text{Bbb,in}}^{\Delta_l, \Delta_i, \Delta_j}(\mathbf{x}_1, \mathbf{x}_2, \epsilon) &= \sum_{n \geq 0} a_n \int_{|\mathbf{x}-\mathbf{x}_2|^2+z^2 < \epsilon^2} \frac{dz d^d \mathbf{x}}{z^{d+1}} \frac{1}{|\mathbf{x}_{12}|^{\Delta_i + \Delta_j}} \left(\frac{|\mathbf{x}-\mathbf{x}_1|^2+z^2}{|\mathbf{x}-\mathbf{x}_2|^2+z^2} \right)^{\frac{\Delta_{ji}}{2}} \chi^{\Delta_l/2+n} \\ &= \int d\Omega_d \int_0^{\pi/2} d\theta \frac{\cos^{d-1} \theta}{\sin^{d+1} \theta} \int_0^\epsilon \frac{dR}{R} \sum_{p \geq 0} d_p(\theta, \phi, \Delta_i, \Delta_j, \Delta_k) \left(\frac{R}{|\mathbf{x}_{12}|} \right)^{\Delta_{ij}+p} \end{aligned} \quad (\text{B.7})$$

where ϕ is the polar angle between \mathbf{r} and \mathbf{x}_{12} . The explicit expression for d_p is unimportant here, but it is sufficient to know that the radial integral for a fixed p gives

$$\int_0^\epsilon \frac{dR}{R} \left(\frac{R}{|\mathbf{x}_{12}|} \right)^{\Delta_{ij}+p} = \frac{1}{\Delta_{ij}+p} \left(\frac{\epsilon}{|\mathbf{x}_{12}|} \right)^{\Delta_{ij}+p}. \quad (\text{B.8})$$

We note that, as anticipated, this integral is generically finite only in the regime that we are considering, $\Delta_i > \Delta_j$. Naturally, the converse is true when integrating over the half-ball centered at \mathbf{x}_1 . Furthermore, the integral in (B.7) vanishes for odd values of p . This can be shown via a straightforward generalization of the arguments presented in appendix D of [1].²¹ This constraint, together with (B.4), dictates the following structural form for the total result of $I_{\text{Bbb}}^{\Delta_l, \Delta_i, \Delta_j}$:

$$I_{\text{Bbb}}^{\Delta_l, \Delta_i, \Delta_j}(\mathbf{x}_1, \mathbf{x}_2, \epsilon) = \frac{1}{|\mathbf{x}_{12}|^{\Delta_i + \Delta_j}} \sum_{p=0}^{\infty} \frac{a_{2p}(\Delta_{ij}, \Delta_l)}{\Delta_{ij} - 2p} \left(\frac{\epsilon}{|\mathbf{x}_{12}|} \right)^{2p - \Delta_{ij}} + (\Delta_i \leftrightarrow \Delta_j), \quad (\text{B.9})$$

where the coefficients a_{2p} are generically not needed. The only exception comes from the coefficient a_0 , which can be computed explicitly. By focusing on the $p = 0$ term in (B.7), comparing with the definition in (B.9), and being careful to the fact that $I_{\text{Bbb,in}}^{\Delta_l, \Delta_i, \Delta_j}(\mathbf{x}_1, \mathbf{x}_2, \epsilon)$ and $I_{\text{Bbb}}^{\Delta_l, \Delta_i, \Delta_j}(\mathbf{x}_1, \mathbf{x}_2, \epsilon)$ have opposite signs, we obtain

$$a_0(\Delta_{ij}, \Delta_l) = -\text{Vol}(S^{d-1}) \int_0^{\pi/2} d\theta \frac{\cos^{d-1} \theta}{\sin^{d+1} \theta} (\sin \theta)^{\Delta_j - \Delta_i} G_{\text{Bbb}}^{\Delta_l, \Delta_i, \Delta_j}(\sin^2 \theta). \quad (\text{B.10})$$

The integral can be performed by expanding the hypergeometric using its series definition,

$${}_2F_1(a, b; c; z) = \sum_{k=0}^{\infty} \frac{(a)_k (b)_k}{(c)_k k!} z^k, \quad (\text{B.11})$$

integrating term by term and resumming the result. This gives

$$a_0(\Delta_{ij}, \Delta_l) = \frac{\pi^{\frac{d}{2}} \Gamma\left(\frac{\Delta_l - d}{2}\right)}{2\Gamma\left(\frac{\Delta_l}{2}\right)} {}_3F_2\left(\frac{\Delta_{lij}}{2}, \frac{\Delta_{lji}}{2}, \frac{\Delta_l - d}{2}; \Delta_l + 1 - \frac{d}{2}, \frac{\Delta_l}{2}; 1\right). \quad (\text{B.12})$$

²¹Alternatively, one can see this by inserting the result for $I_{\text{Bbb,in}}^{\Delta_l, \Delta_i, \Delta_j}$ into (3.9) and subsequently into (3.7). The resulting expression must match (3.5), which only contains powers of $\epsilon^{\pm \Delta_{ij} - 2p}$ for non-negative integers p . Consequently, powers of the form $\epsilon^{\pm \Delta_{ij} - 2p + 1}$ must vanish in the final result for $I_{\text{Bbb,in}}^{\Delta_l, \Delta_i, \Delta_j}$.

For the extraction of the flow equation, we require the value of a_0 when the boundary operators are identical, i.e., $\Delta_i = \Delta_j$. In this limit, the ${}_3F_2$ function simplifies dramatically into a ratio of gamma functions, yielding:

$$a_0(0, \Delta_l) = -\frac{2\pi^{d/2}\Gamma(-\frac{d}{2} + \Delta_l + 1)}{\Gamma(\frac{\Delta_l}{2})\Gamma(\frac{\Delta_l+2}{2})(d - \Delta_l)}. \quad (\text{B.13})$$

Furthermore, the derivative of this coefficient with respect to Δ_{ij} evaluates to zero at the origin:

$$\left. \frac{da_0(\Delta_{ij}, \Delta_l)}{d\Delta_{ij}} \right|_{\Delta_{ij}=0} = 0. \quad (\text{B.14})$$

B.2 Flow of BOE coefficients

We want to compute the following quantity:

$$I_i^{\hat{\Phi}\hat{\Phi}}(\mathbf{x}_1, \mathbf{x}_2, z_2, \epsilon) = \left(\frac{z_2}{\mathbf{x}_{12}^2 + z_2^2} \right)^{\Delta_i} \sum_{j,l} b_l^{\hat{\Phi}} b_j^{\hat{\Phi}} C_{lij} I_{\text{BBb}}^{\Delta_l, \Delta_j, \Delta_i}(\mathbf{x}_1, \mathbf{x}_2, z_2, \epsilon), \quad (\text{B.15})$$

by first computing the integrated bulk-bulk-boundary block, defined as

$$I_{\text{BBb}}^{\Delta_l, \Delta_j, \Delta_i}(\mathbf{x}_1, \mathbf{x}_2, z_2, \epsilon) = \int_{|\mathbf{x}-\mathbf{x}_1|^2 + z^2 \geq \epsilon^2} \frac{dz d^d \mathbf{x}}{z^{d+1}} G_{\text{BBb}}^{\Delta_l, \Delta_j, \Delta_i}(\xi, \rho). \quad (\text{B.16})$$

The above integral is finite for $\Delta_j > \Delta_i$, and can be re-expressed as the difference of two contributions, both finite in this regime: the integral in the whole AdS and the integral inside the subtracted half-ball around \mathbf{x}_1 , as in

$$I_{\text{BBb}}^{\Delta_l, \Delta_j, \Delta_i}(\mathbf{x}_1, \mathbf{x}_2, z_2, \epsilon) = I_{\text{BBb}}^{\Delta_l, \Delta_j, \Delta_i}(\mathbf{x}_1, \mathbf{x}_2, z_2, 0) - I_{\text{BBb, in}}^{\Delta_l, \Delta_j, \Delta_i}(\mathbf{x}_1, \mathbf{x}_2, z_2, \epsilon), \quad (\text{B.17})$$

where

$$I_{\text{BBb, in}}^{\Delta_l, \Delta_j, \Delta_i}(\mathbf{x}_1, \mathbf{x}_2, z_2, \epsilon) := \int_{|\mathbf{x}-\mathbf{x}_1|^2 + z^2 < \epsilon^2} \frac{dz d^d \mathbf{x}}{z^{d+1}} G_{\text{BBb}}^{\Delta_l, \Delta_j, \Delta_i}(\xi, \rho). \quad (\text{B.18})$$

Our strategy is to compute both terms separately, analytically continue them to arbitrary Δ_i and Δ_j , and substitute the results back into (B.15). This gives

$$I_i^{\hat{\Phi}\hat{\Phi}}(\mathbf{x}_1, \mathbf{x}_2, z_2, \epsilon) = \left(\frac{z_2}{\mathbf{x}_{12}^2 + z_2^2} \right)^{\Delta_i} \sum_{j,l} b_l^{\hat{\Phi}} b_j^{\hat{\Phi}} C_{lij} \left(I_{\text{BBb}}^{\Delta_l, \Delta_j, \Delta_i}(\mathbf{x}_1, \mathbf{x}_2, z_2, 0) - I_{\text{BBb, in}}^{\Delta_l, \Delta_j, \Delta_i}(\mathbf{x}_1, \mathbf{x}_2, z_2, \epsilon) \right). \quad (\text{B.19})$$

We begin by evaluating $I_{\text{BBb}}^{\Delta_l, \Delta_j, \Delta_i}(\mathbf{x}_1, \mathbf{x}_2, z_2, 0)$. Because this integral is independent of the configuration of points that we choose, it depends exclusively on the scaling dimensions Δ_i , Δ_l , and Δ_j . We can therefore define a new quantity $\mathcal{J}_{\Delta_i}(\Delta_l, \Delta_j)$, that for convenience absorbs an overall minus sign,

$$\mathcal{J}_{\Delta_i}(\Delta_l, \Delta_j) \equiv -I_{\text{BBb}}^{\Delta_l, \Delta_j, \Delta_i}(\mathbf{x}_1, \mathbf{x}_2, z_2, 0). \quad (\text{B.20})$$

To compute $\mathcal{J}_{\Delta_i}(\Delta_l, \Delta_j)$, we select the specific points

$$\mathbf{x}_1 = \infty, \quad (z_2, \mathbf{x}_2) = (1, 0), \quad (z, \mathbf{x}) = (z, r\hat{\mathbf{x}}^1), \quad (\text{B.21})$$

for which the cross ratios remarkably simplify: $\xi = 1/z^2$, $\rho = r^2/z^2$. The integral then becomes

$$\mathcal{J}_{\Delta_i}(\Delta_l, \Delta_j) = -\text{Vol}(S^{d-1}) \int \frac{dzdr}{z^{d+1}} r^{d-1} G_{\text{BBb}}^{\Delta_l, \Delta_j, \Delta_i} \left(-\frac{z^2}{r^2}, -\frac{1}{r^2} \right), \quad (\text{B.22})$$

which, using (A.37), is

$$\begin{aligned} \mathcal{J}_{\Delta_i}(\Delta_l, \Delta_j) &= -\text{Vol}(S^{d-1}) \sum_{n=0}^{\infty} \frac{\left(\frac{\Delta_{lj}}{2}\right)_n \left(\frac{\Delta_{lji}}{2}\right)_n}{n! \left(1 - \frac{d}{2} + \Delta_l\right)_n} \int_0^{\infty} dr \int_0^{\infty} dz \frac{r^{d-1+\Delta_{ij}-\Delta_l}}{z^{d+1-2n-\Delta_l}} \\ &\quad (r^2 + z^2)^{\frac{\Delta_{ij}-\Delta_l}{2}-n} {}_3F_2 \left(\begin{matrix} \frac{2-d}{2} + \frac{\Delta_{lji}}{2}, & n + \frac{\Delta_{lji}}{2}, & 1 - \frac{\Delta_{lj}}{2} \\ \frac{2-d}{2} + \Delta_j, & 1 - n - \frac{\Delta_{lj}}{2} \end{matrix}; -\frac{1}{r^2 + z^2} \right). \end{aligned} \quad (\text{B.23})$$

This ${}_3F_2$ admits a representation as a finite sum of ${}_2F_1$, through the following identity

$${}_2F_2 \left(\begin{matrix} a_1, & a_2, & c \\ b, & c-n \end{matrix}; z \right) = \sum_{l=0}^n \binom{n}{l} \frac{z^l}{(c-n)_l} \frac{(a_1)_l (a_2)_l}{(b)_l} {}_2F_1(a_1 + l, a_2 + l, b + l, z). \quad (\text{B.24})$$

Opening up the ${}_2F_1$ as well, we can carry out the integral over z . This results into

$$\begin{aligned} \mathcal{J}_{\Delta_i}(\Delta_l, \Delta_j) &= -\text{Vol}(S^{d-1}) \sum_{m,n=0}^{\infty} \sum_{l=0}^n \frac{(-1)^{l+m} \binom{n}{l} \Gamma\left(\frac{d+2l+2m-\Delta_{ij}}{2}\right) \Gamma\left(\frac{-d+2n+\Delta_l}{2}\right) \left(\frac{\Delta_{lj}}{2}\right)_n}{2m!n! \Gamma\left(l+m+n+\frac{\Delta_{lji}}{2}\right) \left(1 - \frac{d}{2} + \Delta_l\right)_n} \\ &\quad \frac{\left(\frac{\Delta_{lji}}{2}\right)_n \left(\frac{2-d+\Delta_{lji}}{2}\right)_l \left(\frac{2n+\Delta_{lji}}{2}\right)_l \left(\frac{2-d+2l+\Delta_{lji}}{2}\right)_m \left(\frac{2l+2n+\Delta_{lji}}{2}\right)_m}{\left(1 - \frac{d}{2} + \Delta_j\right)_l \left(1 - n - \frac{\Delta_{lj}}{2}\right)_l \left(1 - \frac{d}{2} + l + \Delta_j\right)_m} \int_0^{\infty} dr r^{\Delta_{ij}-1-2l-2m}. \end{aligned} \quad (\text{B.25})$$

The remaining integral does not converge, but we can improve the situation by resumming over m and integrating over r after that. The result reads

$$\mathcal{J}_{\Delta_i}(\Delta_l, \Delta_j) = -\frac{\pi^{d/2} \Gamma\left(\frac{\Delta_{ji}}{2}\right) \Gamma\left(\Delta_l - \frac{d-2}{2}\right) \Gamma\left(\Delta_j - \frac{d-2}{2}\right) \Gamma\left(\frac{\Delta_l-d}{2}\right)}{\Delta_l \Gamma\left(\frac{\Delta_l}{2}\right) \Gamma\left(\frac{\Delta_{lji}}{2}\right) \Gamma\left(\frac{\Delta_i+\Delta_j-d+2}{2}\right) \Gamma\left(\frac{\Delta_{lji}-d+2}{2}\right)}. \quad (\text{B.26})$$

We note that in the limit $\Delta_j \rightarrow \Delta_i$ this quantity diverges, and we get

$$\mathcal{J}_{\Delta_i}(\Delta_l, \Delta_j) = \frac{2\pi^{d/2} \Gamma\left(-\frac{d}{2} + \Delta_l + 1\right)}{\Delta_{ji} \Gamma\left(\frac{\Delta_l}{2}\right) \Gamma\left(\frac{\Delta_l+2}{2}\right) (d - \Delta_l)} + [\mathcal{J}_{\Delta_i}(\Delta_l, \Delta_j)]_0 + \mathcal{O}(\Delta_{ji}), \quad (\text{B.27})$$

where

$$[\mathcal{J}_{\Delta_i}(\Delta_l, \Delta_j)]_0 = \frac{2\pi^{d/2} \Gamma\left(1 - \frac{d}{2} + \Delta_l\right) \left(\gamma_E - H_{-\frac{d}{2}+\Delta_i} + H_{\frac{\Delta_l-d}{2}} + \psi\left(\frac{\Delta_l}{2}\right)\right)}{\Delta_l (\Delta_l - d) \Gamma\left(\frac{\Delta_l}{2}\right)^2}. \quad (\text{B.28})$$

We are now left with the computation of $I_{\text{BBb, in}}^{\Delta_l, \Delta_j, \Delta_i}$ in (B.18). The first step is to rewrite the bulk-bulk-boundary blocks in terms of bulk-boundary-boundary blocks. This can be

done by starting from the three point function in (2.54) and replacing one of the bulk operator with its BOE expansion. Replacing then equation (2.45) and imposing that this decomposition has to match with the expansion in bulk-bulk-boundary blocks, one gets

$$G_{\text{BBb}}^{\Delta_l, \Delta_j, \Delta_i}(\xi, \rho) = \left(\frac{\mathbf{x}_{12}^2 + z_2^2}{z_2} \right)^{\Delta_i} z_2^{\Delta_j} \sum_n \frac{(-1)^n}{n! 2^{2n} (\Delta_j - \frac{d-2}{2})_n} z_2^{2n} \times \square_{\mathbf{x}_2}^n \left(\frac{1}{|\mathbf{x}_{12}|^{\Delta_i + \Delta_j}} \left(\frac{|\mathbf{x} - \mathbf{x}_1|^2 + z^2}{|\mathbf{x} - \mathbf{x}_2|^2 + z^2} \right)^{\frac{\Delta_j - \Delta_i}{2}} G_{\text{BBb}}^{\Delta_l, \Delta_i, \Delta_j}(\chi) \right). \quad (\text{B.29})$$

This implies that we can rewrite the integral in (B.18) in terms of the bulk-boundary-boundary integrated block $I_{\text{BBb, in}}^{\Delta_l, \Delta_i, \Delta_j}$ defined in (B.3). We then obtain

$$I_{\text{BBb, in}}^{\Delta_l, \Delta_j, \Delta_i} = \left(\frac{\mathbf{x}_{12}^2 + z_2^2}{z_2} \right)^{\Delta_i} z_2^{\Delta_j} \sum_n \frac{(-1)^n}{n! 2^{2n} (\Delta_j - \frac{d-2}{2})_n} z_2^{2n} \square_{\mathbf{x}_2}^n I_{\text{BBb, in}}^{\Delta_l, \Delta_i, \Delta_j}. \quad (\text{B.30})$$

Matching with (B.9) and (B.4), we get

$$\begin{aligned} I_{\text{BBb, in}}^{\Delta_l, \Delta_j, \Delta_i} &= \left(\frac{\mathbf{x}_{12}^2 + z_2^2}{z_2} \right)^{\Delta_i} \sum_{n,p} \frac{(-1)^{n+1}}{n! 2^{2n} (\Delta_j - \frac{d-2}{2})_n} z_2^{2n + \Delta_j} \square_{\mathbf{x}_2}^n \frac{a_{2p}(\Delta_{ij}, \Delta_l)}{\Delta_{ij} - 2p} \frac{\epsilon^{2p - \Delta_{ij}}}{|\mathbf{x}_{12}|^{2\Delta_j + 2p}} \\ &= \left(\frac{\mathbf{x}_{12}^2 + z_2^2}{z_2} \right)^{\Delta_i} \sum_{n,p} \frac{(-1)^{n+1} z_2^{2n + \Delta_j} a_{2p}(\Delta_{ij}, \Delta_l) \epsilon^{2p - \Delta_{ij}} \square_{\mathbf{x}_2}^n \square_{\mathbf{x}_1}^p \langle \mathcal{O}_j(\mathbf{x}_1) \mathcal{O}_j(\mathbf{x}_2) \rangle}{n! 2^{2n} (\Delta_j - \frac{d-2}{2})_n 2^{2p} (\Delta_j - \frac{d-2}{2})_p (\Delta_j)_p (\Delta_{ij} - 2p)} \\ &= - \sum_p \frac{a_{2p}(\Delta_{ij}, \Delta_l) \epsilon^{2p - \Delta_{ij}}}{2^{2p} (\Delta_j - \frac{d-2}{2})_p (\Delta_j)_p (\Delta_{ij} - 2p)} \square_{\mathbf{x}_2}^p \left(\frac{\mathbf{x}_{12}^2 + z_2^2}{z_2} \right)^{\Delta_j + \Delta_i} \end{aligned} \quad (\text{B.31})$$

Having in mind equation (B.19), we can insert this result in the sum

$$\begin{aligned} &\left(\frac{z_2}{\mathbf{x}_{12}^2 + z_2^2} \right)^{\Delta_i} \sum_{j,l} b_l^{\hat{\Phi}} b_j^{\hat{\Phi}} C_{lij} I_{\text{BBb, in}}^{\Delta_l, \Delta_j, \Delta_i} \\ &= - \sum_{p,j,l} b_l^{\hat{\Phi}} b_j^{\hat{\Phi}} C_{lij} \frac{a_{2p}(\Delta_{ij}, \Delta_l) \epsilon^{2p - \Delta_{ij}}}{2^{2p} (\Delta_i - \frac{d-2}{2})_p (\Delta_i)_p (\Delta_{ij} - 2p)} \square_{\mathbf{x}_1}^p \left(\frac{\mathbf{x}_{12}^2 + z_2^2}{z_2} \right)^{\Delta_j} \end{aligned} \quad (\text{B.32})$$

First, consider the case $j \neq i$. Using the counterterm expressions found in (3.14), we recover

$$\sum_{j \neq i, p} b_j^{\hat{\Phi}} \frac{\delta \mathcal{Z}_{ij;p}}{\delta \lambda} \square_{\mathbf{x}_1}^p \left(\frac{\mathbf{x}_{12}^2 + z_2^2}{z_2} \right)^{\Delta_j}. \quad (\text{B.33})$$

To see what happens as $\Delta_j \rightarrow \Delta_i$ in the sum, we observe that the only non-vanishing contribution comes from the $p = 0$ term, which reads:

$$\left(\frac{\mathbf{x}_{12}^2 + z_2^2}{z_2} \right)^{\Delta_i} b_i^{\hat{\Phi}} \sum_l b_l^{\hat{\Phi}} C_{jil} a_0(0, \Delta_l) \left(\frac{1}{\Delta_{ji}} + \log \epsilon + \log \left(\frac{z_2}{\mathbf{x}_{12}^2 + z_2^2} \right) \right) + \mathcal{O}(\Delta_{ji}), \quad (\text{B.34})$$

where we used $\partial_{\Delta_{ji}} a_0(0, \Delta_l) = 0$, as obtained in (B.14). Matching with the expression for a_0 found in (B.13), and replacing in (B.19), we find that the pole in Δ_{ji} cancels in the total result and we get

$$\begin{aligned}
I_i^{\hat{\Phi}\hat{\Phi}}(\mathbf{x}_1, \mathbf{x}_2, z_2, \epsilon) &= - \left(\frac{z_2}{\mathbf{x}_{12}^2 + z_2^2} \right)^{\Delta_i} \sum_{j,l} b_l^{\hat{\Phi}} b_j^{\hat{\Phi}} C_{lij} [\mathcal{J}_{\Delta_i}(\Delta_l, \Delta_j)]_{\text{reg}} \\
&\quad - b_i^{\hat{\Phi}} \left(\frac{z_2}{\mathbf{x}_{12}^2 + z_2^2} \right)^{\Delta_i} \sum_l b_l^{\hat{\Phi}} C_{iil} \mathcal{I}(\Delta_l) \log \left(\frac{z_2 \epsilon}{\mathbf{x}_{12}^2 + z_2^2} \right) \\
&\quad - \sum_{j \neq i} \sum_{n=0}^{\infty} b_j^{\hat{\Phi}} \frac{\delta \mathcal{Z}_{ij;n}}{\delta \lambda} \square_{\mathbf{x}_2}^n \left(\frac{z_2}{\mathbf{x}_{12}^2 + z_2^2} \right)^{\Delta_j(\lambda)}.
\end{aligned} \tag{B.35}$$

C Some properties of $\frac{dC_{ijk}}{d\lambda}$

In this work, we have not derived the higher dimensional analogue of the flow equation involving the derivative of the OPE coefficients [1], instead arguing that the crossing equation is a more efficient substitute. Nevertheless, we can prove certain properties of $\frac{dC_{ijk}}{d\lambda}$ without computing the required conformal integrals explicitly. These properties are important in the derivations of the merger-annihilation and level repulsion scenarios in section 6. We will focus on OPE coefficients of scalar operators for simplicity.

The variation of the OPE coefficients is captured by the correction to the boundary three-point function in perturbation theory. The renormalized operators have three-point function

$$\langle \mathcal{O}_i^{(\text{ren})}(\mathbf{x}_1) \mathcal{O}_j^{(\text{ren})}(\mathbf{x}_2) \mathcal{O}_k^{(\text{ren})}(\mathbf{x}_3) \rangle_{\lambda+\delta\lambda} = \frac{C_{ijk} + \delta C_{ijk}}{(\mathbf{x}_{12}^2)^{\frac{\Delta_{ijk}}{2} + \frac{\delta\Delta_{ijk}}{2}} (\mathbf{x}_{23}^2)^{\frac{\Delta_{jki}}{2} + \frac{\delta\Delta_{jki}}{2}} (\mathbf{x}_{13}^2)^{\frac{\Delta_{ikj}}{2} + \frac{\delta\Delta_{ikj}}{2}}} \tag{C.1}$$

Using (3.2), the bare operators have instead

$$\begin{aligned}
\langle \mathcal{O}_i^{(\text{bare})}(\mathbf{x}_1) \mathcal{O}_j^{(\text{bare})}(\mathbf{x}_2) \mathcal{O}_k^{(\text{bare})}(\mathbf{x}_3) \rangle_{\lambda+\delta\lambda} &= \frac{1}{(\mathbf{x}_{12}^2)^{\frac{\Delta_{ijk}}{2}} (\mathbf{x}_{23}^2)^{\frac{\Delta_{jki}}{2}} (\mathbf{x}_{13}^2)^{\frac{\Delta_{ikj}}{2}}} \\
&\times \left[C_{ijk} + \delta C_{ijk} + \frac{\delta\Delta_i}{2} \log \left(\frac{\mathbf{x}_{23}^2}{\mathbf{x}_{12}^2 \mathbf{x}_{13}^2} \right) + \frac{\delta\Delta_j}{2} \log \left(\frac{\mathbf{x}_{13}^2}{\mathbf{x}_{12}^2 \mathbf{x}_{23}^2} \right) + \frac{\delta\Delta_k}{2} \log \left(\frac{\mathbf{x}_{12}^2}{\mathbf{x}_{23}^2 \mathbf{x}_{13}^2} \right) \right] \\
&+ \sum_m \sum_{p=0}^{\infty} \delta \mathcal{Z}_{im,p} \square_1^p \frac{1}{(\mathbf{x}_{12}^2)^{\frac{\Delta_{mjk}}{2}} (\mathbf{x}_{23}^2)^{\frac{\Delta_{jkm}}{2}} (\mathbf{x}_{13}^2)^{\frac{\Delta_{mkj}}{2}}} \\
&+ \sum_m \sum_{p=0}^{\infty} \delta \mathcal{Z}_{jm,p} \square_1^p \frac{1}{(\mathbf{x}_{12}^2)^{\frac{\Delta_{imk}}{2}} (\mathbf{x}_{23}^2)^{\frac{\Delta_{mki}}{2}} (\mathbf{x}_{13}^2)^{\frac{\Delta_{ikm}}{2}}} \\
&+ \sum_m \sum_{p=0}^{\infty} \delta \mathcal{Z}_{km,p} \square_1^p \frac{1}{(\mathbf{x}_{12}^2)^{\frac{\Delta_{ijm}}{2}} (\mathbf{x}_{23}^2)^{\frac{\Delta_{jmi}}{2}} (\mathbf{x}_{13}^2)^{\frac{\Delta_{imj}}{2}}}
\end{aligned} \tag{C.2}$$

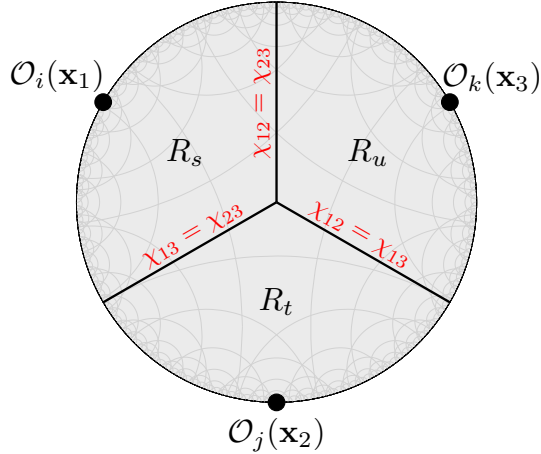


Figure 19. The three regions in which we split integral (C.4). In region R_s we use the s -channel OPE pairing (jk) , in region R_t we pair (ik) and in region R_u we pair (ij) .

At the same time

$$\begin{aligned} \langle \mathcal{O}_i^{(\text{bare})}(\mathbf{x}_1) \mathcal{O}_j^{(\text{bare})}(\mathbf{x}_2) \mathcal{O}_k^{(\text{bare})}(\mathbf{x}_3) \rangle_{\lambda+\delta\lambda} &= \langle \mathcal{O}_i(\mathbf{x}_1) \mathcal{O}_j(\mathbf{x}_2) \mathcal{O}_k(\mathbf{x}_3) \rangle_{\lambda} \\ &\quad - \delta\lambda \int_{\epsilon} \frac{dz d^d \mathbf{x}}{z^{d+1}} \langle \hat{\Phi}(z, \mathbf{x}) \mathcal{O}_i(\mathbf{x}_1) \mathcal{O}_j(\mathbf{x}_2) \mathcal{O}_k(\mathbf{x}_3) \rangle_{\lambda} \end{aligned} \quad (\text{C.3})$$

where the subscript ϵ is the usual regularization in which we integrate everywhere in AdS except semicircles of radius ϵ in half-plane coordinates centered around the insertions of the boundary operators.

Let us thus focus on

$$I_{Bbbb}^{\hat{\Phi}ijk}(\mathbf{x}_1, \mathbf{x}_2, \mathbf{x}_3; \epsilon) \equiv \int_{(\mathbf{x}-\mathbf{x}_i)^2+z^2 \geq \epsilon^2} \frac{dz d^d \mathbf{x}}{z^{d+1}} \langle \hat{\Phi}(z, \mathbf{x}) \mathcal{O}_i(\mathbf{x}_1) \mathcal{O}_j(\mathbf{x}_2) \mathcal{O}_k(\mathbf{x}_3) \rangle_{\lambda}. \quad (\text{C.4})$$

We would like to carry out this integral universally in terms of the QFT data, hence to use a block decomposition. In this case, we would need to use the BOE of the bulk field $\hat{\Phi}$ and an OPE among the boundary operators. The crucial difference with the previous cases is that there is no OPE that converges in all AdS. Instead, we divide AdS in three regions which will be delimited by co-dimension 1 surfaces defined by the equations

$$\chi_{12} = \chi_{23}, \quad \chi_{13} = \chi_{23}, \quad \chi_{13} = \chi_{12}, \quad \chi_{ij} \equiv -\frac{1}{2} \frac{P_i \cdot P_j}{(X \cdot P_i)(X \cdot P_j)}. \quad (\text{C.5})$$

We will split the integral in these three regions and use different OPEs in each. We give a pictorial representation in figure 19. Let us focus on the s -channel region, corresponding to the OPE pairing (jk) .

$$I_{Bbbb,s}^{\hat{\Phi}ijk}(\mathbf{x}_1, \mathbf{x}_2, \mathbf{x}_3; \epsilon) \equiv \int_{R_s | (\mathbf{x}-\mathbf{x}_1)^2+z^2 \geq \epsilon^2} \frac{dz d^d \mathbf{x}}{z^{d+1}} \langle \hat{\Phi}(z, \mathbf{x}) \mathcal{O}_i(\mathbf{x}_1) \mathcal{O}_j(\mathbf{x}_2) \mathcal{O}_k(\mathbf{x}_3) \rangle_{\lambda}. \quad (\text{C.6})$$

Now we perform the OPE (jk) using (2.28)

$$\langle \hat{\Phi}(z, \mathbf{x}) \mathcal{O}_i(\mathbf{x}_1) \mathcal{O}_j(\mathbf{x}_2) \mathcal{O}_k(\mathbf{x}_3) \rangle = \sum_m \frac{C_{jkm}}{(\mathbf{x}_{23}^2)^{\frac{\Delta_{jkm}}{2}}} \mathcal{C}_{a_1 \dots a_{J_m}}(\mathbf{x}_{23}, \partial_3) \langle \hat{\Phi}(z, \mathbf{x}) \mathcal{O}_i(\mathbf{x}_1) \mathcal{O}_m^{a_1 \dots a_{J_m}}(\mathbf{x}_3) \rangle \quad (\text{C.7})$$

For the remaining bulk-boundary-boundary three-point function, we use the block decomposition (2.51)

$$\begin{aligned} & \langle \hat{\Phi}(z, \mathbf{x}) \mathcal{O}_i(\mathbf{x}_1) \mathcal{O}_j(\mathbf{x}_2) \mathcal{O}_k(\mathbf{x}_3) \rangle \\ &= \sum_l b_l^{\hat{\Phi}} \sum_m \frac{C_{lim} C_{jkm}}{(\mathbf{x}_{23}^2)^{\frac{\Delta_{jkm}}{2}}} \mathcal{C}_{a_1 \dots a_{J_m}}(\mathbf{x}_{23}, \partial_3) \frac{V_{3,1X}^{a_1 \dots a_{J_m}}}{(\mathbf{x}_{13}^2)^{\frac{\Delta_i + \Delta_m + J_m}{2}}} \left(\frac{z^2 + (\mathbf{x} - \mathbf{x}_1)^2}{z^2 + (\mathbf{x} - \mathbf{x}_3)^2} \right)^{\frac{\Delta_m + J_m - \Delta_i}{2}} G_{\text{Bbb}, J_m}^{\Delta_l, \Delta_i, \Delta_m}(\chi_{13}) \\ &\equiv \frac{\sum_l b_l^{\hat{\Phi}} \sum_m C_{lim} C_{jkm} G_{\text{Bbbb}, s, J_m}^{\Delta_l, \Delta_m, \Delta_i, \Delta_j, \Delta_k}(\chi_{12}, \chi_{13}, \chi_{23})}{(\mathbf{x}_{12}^2)^{\frac{\Delta_{ijk}}{2}} (\mathbf{x}_{23}^2)^{\frac{\Delta_{jki}}{2}} (\mathbf{x}_{13}^2)^{\frac{\Delta_{ikj}}{2}}} \quad (\text{C.8}) \end{aligned}$$

where in the second line

$$V_{3,1X}^{a_1 \dots a_{J_m}} \equiv \frac{1}{\left(\frac{d-2}{2}\right)_{J_m}!} D_{\mathbf{z}_{a_1}} \dots D_{\mathbf{z}_{a_{J_m}}} V_{3,12}, \quad P_2 \rightarrow X \quad (\text{C.9})$$

and $V_{3,12}$ here is the pullback to local coordinates of (2.35). In the third line of (C.8), we used χ_{ij} defined in (C.5) to form the three independent conformal cross ratios of this correlation function.

Using this in (C.6), we obtain

$$I_{\text{Bbbb}, s}^{\hat{\Phi}ijk}(\mathbf{x}_1, \mathbf{x}_2, \mathbf{x}_3; \epsilon) = \frac{\sum_l b_l^{\hat{\Phi}} \sum_m C_{lim} C_{mjk} I_{\text{Bbbb}, s, J_m}^{\Delta_l \Delta_m \Delta_i \Delta_j \Delta_k}(\epsilon)}{(\mathbf{x}_{12}^2)^{\frac{\Delta_{ijk}}{2}} (\mathbf{x}_{23}^2)^{\frac{\Delta_{jki}}{2}} (\mathbf{x}_{13}^2)^{\frac{\Delta_{ikj}}{2}}} \quad (\text{C.10})$$

where

$$I_{\text{Bbbb}, s, J_m}^{\Delta_l \Delta_m \Delta_i \Delta_j \Delta_k}(\epsilon) \equiv \int_{R_s | (\mathbf{x} - \mathbf{x}_1)^2 + z^2 \geq \epsilon^2} \frac{dz d^d \mathbf{x}}{z^{d+1}} G_{\text{Bbbb}, s, J_m}^{\Delta_l, \Delta_m, \Delta_i, \Delta_j, \Delta_k}(\chi_{12}, \chi_{13}, \chi_{23}). \quad (\text{C.11})$$

This integral will generically diverge when $\epsilon \rightarrow 0$. To study this divergence, let us consider the integral *inside* the half-ball. For simplicity, we will only focus on the scalar contribution $J_m = 0$. We will find that it is finite when $\Delta_m > \Delta_i$, while it diverges when $\Delta_m \leq \Delta_i$. In the regime where it is finite, we find

$$\begin{aligned} I_{\text{Bbbb}, s, \text{in}, 0}^{\Delta_l \Delta_m \Delta_i \Delta_j \Delta_k}(\epsilon) &= \int_{(\mathbf{x} - \mathbf{x}_1)^2 + z^2 < \epsilon^2} \frac{dz d^d \mathbf{x}}{z^{d+1}} G_{\text{Bbbb}, s, 0}^{\Delta_l, \Delta_m, \Delta_i, \Delta_j, \Delta_k}(\chi_{12}, \chi_{13}, \chi_{23}) \\ &= \frac{1}{(\mathbf{x}_{23}^2)^{\frac{\Delta_{jkm}}{2}}} \mathcal{C}(\mathbf{x}_{23}, \partial_3) \frac{1}{(\mathbf{x}_{13}^2)^{\frac{\Delta_i + \Delta_m}{2}}} \int_{(\mathbf{x} - \mathbf{x}_1)^2 + z^2 < \epsilon^2} \frac{dz d^d \mathbf{x}}{z^{d+1}} \left(\frac{z^2 + (\mathbf{x} - \mathbf{x}_1)^2}{z^2 + (\mathbf{x} - \mathbf{x}_3)^2} \right)^{\frac{\Delta_m - \Delta_i}{2}} G_{\text{Bbb}}^{\Delta_l, \Delta_i, \Delta_m}(\chi_{13}) \\ &= - \frac{1}{(\mathbf{x}_{23}^2)^{\frac{\Delta_{jkm}}{2}}} \sum_{p=0}^{\infty} \frac{a_{2p}(\Delta_{im}, \Delta_l)}{\Delta_{im} - 2p} \frac{\epsilon^{2p - \Delta_{im}}}{2^{2p} (\Delta_m)_p (\Delta_m - \frac{d-2}{2})_p} \mathcal{C}(\mathbf{x}_{23}, \partial_3) \square_1^p \frac{1}{(\mathbf{x}_{13}^2)^{\Delta_m}} \\ &= - \sum_{p=0}^{\infty} \frac{a_{2p}(\Delta_{im}, \Delta_l)}{\Delta_{im} - 2p} \frac{\epsilon^{2p - \Delta_{im}}}{2^{2p} (\Delta_m)_p (\Delta_m - \frac{d-2}{2})_p} \square_1^p \frac{1}{(\mathbf{x}_{12}^2)^{\frac{\Delta_{mjk}}{2}} (\mathbf{x}_{23}^2)^{\frac{\Delta_{jkm}}{2}} (\mathbf{x}_{13}^2)^{\frac{\Delta_{mkj}}{2}}} \quad (\text{C.12}) \end{aligned}$$

where to go from the second to the third line we recognized (B.3), and from the third to the fourth we used that

$$\langle \mathcal{O}_m(\mathbf{x}_1) \mathcal{O}_j(\mathbf{x}_2) \mathcal{O}_k(\mathbf{x}_3) \rangle = \frac{C_{jkm}}{(\mathbf{x}_{23}^2)^{\frac{\Delta_{jkm}}{2}}} \mathcal{C}(\mathbf{x}_{23}, \partial_3) \langle \mathcal{O}_m(\mathbf{x}_1) \mathcal{O}_m(\mathbf{x}_3) \rangle \quad (\text{C.13})$$

by virtue of the OPE (2.28). In the final expression in (C.12) we recognize the counterterms (3.14). If we thus split the finite integral (C.11) as

$$I_{\text{Bbbb},s,0}^{\Delta_l \Delta_m \Delta_i \Delta_j \Delta_k}(\epsilon) = \mathcal{K}_{\Delta_i \Delta_j \Delta_k}(\Delta_l, \Delta_m, 0) - I_{\text{Bbbb},s,\text{in},0}^{\Delta_l \Delta_m \Delta_i \Delta_j \Delta_k}(\epsilon) \quad (\text{C.14})$$

where \mathcal{K} is the integral over the full region R_s with no subtraction, plugging things back into (C.2) the counterterms and the logarithms when $\Delta_m = \Delta_i$ all cancel, leading to the following differential equation:

$$\frac{dC_{ijk}}{d\lambda} = \sum_l b_l^{\hat{\Phi}} \sum_m C_{lim} C_{mjk} \mathcal{K}_{\Delta_i \Delta_j \Delta_k}(\Delta_l, \Delta_m, 0) + \text{perms.} + \text{spin} \quad (\text{C.15})$$

where ‘‘perms.’’ stands for the cyclic permutations of i, j, k and ‘‘spin’’ stands for contributions from exchanged spinning operators.

We do not determine the explicit form of $\mathcal{K}_{\Delta_i \Delta_j \Delta_k}(\Delta_l, \Delta_m, 0)$. For the purposes of section 6, we need the following statements:

Pole at $\Delta_l = d$ The block G_{Bbbb} is obtained by performing the BOE of $\hat{\Phi}$, which goes as $\hat{\Phi} \sim b_l^{\hat{\Phi}} z^{\Delta_l} \mathcal{O}_l + \dots$. As such, the integral near the boundary goes like

$$\int_0 \frac{dz}{z^{d+1}} G_{\text{Bbbb},s}^{\Delta_l, \Delta_m, \Delta_i, \Delta_j, \Delta_k}(\chi_{12}, \chi_{13}, \chi_{23}) \sim \int_0 \frac{dz}{z^{d+1}} z^{\Delta_l} \sim \frac{1}{(\Delta_l - d)} (\dots) \quad (\text{C.16})$$

hence we expect

$$\mathcal{K}_{\Delta_i \Delta_j \Delta_k}(\Delta_l, \Delta_m) \stackrel{\Delta_l \rightarrow d}{\sim} \frac{1}{\Delta_l - d} \times O(1) \quad (\text{C.17})$$

Pole at $\Delta_m = \Delta_i$ Consider expression (C.14). The integral outside the half-sphere is finite even when $\Delta_m = \Delta_i$, while the integral inside diverges logarithmically in that case. This immediately tells us that $\mathcal{K}_{\Delta_i \Delta_j \Delta_k}(\Delta_l, \Delta_m)$ has a pole at $\Delta_m = \Delta_i$ with residue that has to match the one of (C.12). This pole comes from the $p = 0$ term in (C.12). By explicitly matching the residue, we find

$$\text{Res}_{\Delta_m = \Delta_i} \mathcal{K}_{\Delta_i \Delta_j \Delta_k}(\Delta_l, \Delta_m) = -a_0(0, \Delta_l) = -\mathcal{I}(\Delta_l) \quad (\text{C.18})$$

D Universal asymptotics of QFT data

Here we estimate the universal large Δ_l behavior of the BOE and OPE coefficients using Tauberian theorems. Some recent more refined results on OPE coefficients can be found in [86].

D.1 Asymptotics of BOE coefficients

Consider a relevant bulk operator $\hat{\Phi}$ with $\frac{d-1}{2} < \Delta_{\hat{\Phi}}^{\text{UV}} < d+1$. Its two-point function in the coincident points limit goes like

$$\lim_{X_1 \rightarrow X_2} \langle \hat{\Phi}(X_1) \hat{\Phi}(X_2) \rangle \sim \frac{1}{(-2 - 2X_1 \cdot X_2)^{\Delta_{\hat{\Phi}}^{\text{UV}}}} \quad (\text{D.1})$$

At the same time, this singularity should be reproduced by the sum over the BOE coefficients of the bulk-bulk block ($\sigma \equiv X_1 \cdot X_2$)

$$\sum_l \left(b_l^{\hat{\Phi}} \right)^2 \frac{1}{(-2 - 2\sigma)^{\Delta_l}} {}_2F_1 \left(\begin{matrix} \Delta_l & \Delta_l - \frac{d-1}{2} \\ & 2\Delta_l - d + 1 \end{matrix}; \frac{2}{1 + \sigma} \right) \sim \frac{1}{(-2 - 2\sigma)^{\Delta_{\hat{\Phi}}^{\text{UV}}}} \quad (\text{D.2})$$

A more convenient expression to study this limit is the following equivalent one

$$\sum_l \left(b_l^{\hat{\Phi}} \right)^2 \frac{1}{(2 - 2\sigma)^{\Delta_l}} {}_2F_1 \left(\begin{matrix} \Delta_l & \Delta_l - \frac{d-1}{2} \\ & 2\Delta_l - d + 1 \end{matrix}; \frac{2}{1 - \sigma} \right) \sim \frac{1}{(-2 - 2\sigma)^{\Delta_{\hat{\Phi}}^{\text{UV}}}} \quad (\text{D.3})$$

obtained by doing a Pfaff transformation on the previous one.

Now to take the limit correctly, seeing how the singularity at $\sigma = -1$ is reproduced, we need to scale $(1 - \sigma)^{-1}$ with Δ_l^2 . We extract the asymptotics using the integral representation of the hypergeometric function

$$\begin{aligned} {}_2F_1 \left(\begin{matrix} \Delta_l & \Delta_l - \frac{d-1}{2} \\ & 2\Delta_l - d + 1 \end{matrix}; \frac{2}{1 - \sigma} \right) &= \frac{\Gamma(2\Delta_l - d + 1)}{2\pi\Gamma(\Delta_l)\Gamma(\Delta_l - d + 1)\Gamma(\frac{1-d}{2} + \Delta_l)^2} \\ &\times \int_C dt \Gamma\left(\frac{1-d}{2} - t\right) \Gamma(\Delta_l + t) \Gamma\left(\frac{1-d}{2} + \Delta_l + t\right) \Gamma(-t) \left(\frac{\sigma+1}{\sigma-1}\right)^t \end{aligned} \quad (\text{D.4})$$

where the contour is vertical in the complex t plane and such that $-\Delta_l + \frac{d-1}{2} < \text{Re}(t) < -\frac{d-1}{2}$.

Using the Stirling approximation for the gamma functions involving Δ_l , we get

$${}_2F_1 \left(\begin{matrix} \Delta_l & \Delta_l - \frac{d-1}{2} \\ & 2\Delta_l - d + 1 \end{matrix}; \frac{2}{1 - \sigma} \right) \approx \frac{2^{2\Delta_l} \Delta_l^{\frac{d}{2}}}{2^{d+1} \pi^{\frac{3}{2}}} \int_C dt \Gamma\left(\frac{1-d}{2} - t\right) \Gamma(-t) \left(\Delta_l^2 \frac{\sigma+1}{\sigma-1}\right)^t \quad (\text{D.5})$$

Now we use the integral representation of the remaining gamma functions

$${}_2F_1 \left(\begin{matrix} \Delta_l & \Delta_l - \frac{d-1}{2} \\ & 2\Delta_l - d + 1 \end{matrix}; \frac{2}{1 - \sigma} \right) \approx \frac{2^{2\Delta_l} \Delta_l^{\frac{d}{2}}}{2^{d+1} \pi^{\frac{3}{2}}} \int_0^\infty \frac{du}{u} e^{-u} u^{\frac{1-d}{2}} \int_0^\infty \frac{dv}{v} e^{-v} \int_{\mathbb{R}} dt \left(\Delta_l^2 \frac{\sigma+1}{\sigma-1} \frac{1}{uv}\right)^{it} \quad (\text{D.6})$$

The integral over t is now a delta function supported on $uv = \Delta_l^2 \frac{\sigma+1}{\sigma-1}$.

$${}_2F_1 \left(\begin{matrix} \Delta_l & \Delta_l - \frac{d-1}{2} \\ & 2\Delta_l - d + 1 \end{matrix}; \frac{2}{1 - \sigma} \right) \approx \frac{2^{2\Delta_l} \Delta_l^{\frac{d}{2}}}{2^d \pi^{\frac{1}{2}}} \int_0^\infty \frac{du}{u} e^{-u} u^{\frac{1-d}{2}} \int_0^\infty \frac{dv}{v} e^{-v} \delta\left(\Delta_l^2 \frac{\sigma+1}{\sigma-1} \frac{1}{uv} - 1\right) \quad (\text{D.7})$$

Applying the Dirac delta, the remaining integral is the representation of a Bessel function of the second kind:

$${}_2F_1\left(\begin{matrix} \Delta_l & \Delta_l - \frac{d-1}{2} \\ & 2\Delta_l - d + 1 \end{matrix}; \frac{2}{1-\sigma}\right) \approx \frac{2^{2\Delta_l-d+1}\sqrt{\Delta_l}}{\sqrt{\pi}} \left(\frac{\sigma-1}{\sigma+1}\right)^{\frac{d-1}{4}} K_{\frac{d-1}{2}}\left(2\Delta_l\sqrt{\frac{\sigma+1}{\sigma-1}}\right) \quad (\text{D.8})$$

The result is not surprising: we have obtained the flat space propagator with mass $m^2 R^2 = \Delta_l^2$. We are zooming in on the coincident point singularity while scaling the mass appropriately, which means we still see the mass but we do not see the AdS curvature.

Now let us change variables to $\sigma = 1 - \frac{1}{2x^2}$. The relation (D.1) has become

$$\sum_l \left(b_l^{\hat{\Phi}}\right)^2 \sqrt{\frac{\Delta_l}{\pi}} \left(\frac{x}{2}\right)^{\frac{d-1}{2}} K_{\frac{d-1}{2}}\left(\frac{\Delta_l}{x}\right) \sim x^{2\Delta_{\hat{\Phi}}^{\text{UV}}}, \quad x \rightarrow \infty \quad (\text{D.9})$$

To bound the coefficients, we use the Tauberian theorem in [87] equation (4.7). It states that, given any two functions w_1 and w_2 with unit integrals

$$\int_0^\infty dt w_i(t) = 1 \quad (\text{D.10})$$

and a nonnegative function $\rho(\Delta)$, if

$$\frac{1}{x} \int_0^\infty d\Delta \rho(\Delta) w_1\left(\frac{\Delta}{x}\right) \sim 1, \quad x \rightarrow \infty, \quad (\text{D.11})$$

then

$$\frac{1}{x} \int_0^\infty d\Delta \rho(\Delta) w_2\left(\frac{\Delta}{x}\right) \sim 1, \quad x \rightarrow \infty. \quad (\text{D.12})$$

The trick is then to identify

$$\begin{aligned} \rho(\Delta) &= \sum_l \left(b_l^{\hat{\Phi}}\right)^2 \frac{\Gamma(\Delta_{\hat{\Phi}}^{\text{UV}})\Gamma(\Delta_{\hat{\Phi}}^{\text{UV}} - \frac{d-1}{2})}{\sqrt{\pi}2^{d+1-2\Delta_{\hat{\Phi}}^{\text{UV}}}} \Delta_l^{1+\frac{d}{2}-2\Delta_{\hat{\Phi}}^{\text{UV}}} \delta(\Delta - \Delta_l), \\ w_1(t) &= \frac{2}{\Gamma(\Delta_{\hat{\Phi}}^{\text{UV}})\Gamma(\Delta_{\hat{\Phi}}^{\text{UV}} - \frac{d-1}{2})} \left(\frac{t}{2}\right)^{2\Delta_{\hat{\Phi}}^{\text{UV}}-1-\frac{d-1}{2}} K_{\frac{d-1}{2}}(t) \\ w_2(t) &= 2\Delta_{\hat{\Phi}}^{\text{UV}} t^{2\Delta_{\hat{\Phi}}^{\text{UV}}-1} \Theta(0 < t < 1) \end{aligned} \quad (\text{D.13})$$

notice that the integral over w_1 only converges if $\Delta_{\hat{\Phi}}^{\text{UV}} > \frac{d-1}{2}$, which is the UV unitarity bound. We thus get

$$\sum_{l|\Delta_l < x} \left(b_l^{\hat{\Phi}}\right)^2 \frac{\Gamma(\Delta_{\hat{\Phi}} + 1)\Gamma(\Delta_{\hat{\Phi}}^{\text{UV}} - \frac{d-1}{2})}{2^{d-2\Delta_{\hat{\Phi}}^{\text{UV}}}\sqrt{\pi}} \Delta_l^{\frac{d}{2}} \sim x^{2\Delta_{\hat{\Phi}}^{\text{UV}}}, \quad x \rightarrow \infty, \quad (\text{D.14})$$

where the step function effectively truncated the sum at $x \equiv \Delta_{\text{max}}$. If we assume that the BOE coefficients have an asymptotic power law behavior $b_l^{\hat{\Phi}} \sim c\Delta_l^a$, and we treat the sum as an integral, we find

$$a = \Delta_{\hat{\Phi}}^{\text{UV}} - \frac{d+2}{4}. \quad (\text{D.15})$$

This generalizes equation (F.13) from [1] to $d+1$ dimensions.

D.2 Asymptotics of OPE coefficients

To compute the asymptotics of the OPE coefficients, we need to apply a similar procedure to that of the previous section, now to the four-point function of boundary operators. To this purpose, we need the expression for the associated conformal blocks, which is known in closed form only for $d = 1$ and $d = 2$. The first case was studied in appendix F of [1]. We review here the main steps as they will be useful for the case $d = 2$. The starting point is the four-point function of four identical boundary operators in the specific configuration:

$$\begin{aligned} \langle \mathcal{O}_i(0) \mathcal{O}_j(z) \mathcal{O}_j(1) \mathcal{O}_i(\infty) \rangle &= z^{-\Delta_i - \Delta_j} G(z) \\ G(z) &= \sum_k C_{ijk}^2 z^{\Delta_k} {}_2F_1(\Delta_{kji}, \Delta_{kji}, 2\Delta_k; z), \end{aligned} \quad (\text{D.16})$$

which satisfies

$$\lim_{z \rightarrow 1^-} \langle \mathcal{O}_i(0) \mathcal{O}_j(z) \mathcal{O}_j(1) \mathcal{O}_i(\infty) \rangle \sim (1-z)^{-2\Delta_j}. \quad (\text{D.17})$$

The right-hand side can be approximated by Bessel functions in the large Δ_k limit. One way to obtain that is by expressing the hypergeometric with the Euler representation

$${}_2F_1(\Delta_{kji}, \Delta_{kji}, 2\Delta_k; z) = \int_0^1 dt \frac{(1-t)^{-1+\Delta_{ikj}} t^{-1-\Delta_{jki}} z^{-\Delta_{ijk}} (1-tz)^{-\Delta_{jki}} \Gamma(2\Delta_k)}{\Gamma(\Delta_{ikj}) \Gamma(\Delta_{jki})} \quad (\text{D.18})$$

and to perform a change of variable $t = s/(1+s)$. Using the saddle-point approximation one can see that the resulting integral over s is dominated by large s , and therefore one can expand the integral for large s and large Δ_k . Using $\lim_{t \rightarrow \infty} (1+1/t)^t = e$, this gives

$${}_2F_1(\Delta_{kji}, \Delta_{kji}, 2\Delta_k; z) \sim \int_0^\infty ds \frac{e^{-\frac{\Delta_k}{s} + s(z-1)\Delta_k} s^{-1-2\Delta_i+2\Delta_j} \Gamma(2\Delta_k)}{\Gamma(\Delta_{ikj}) \Gamma(\Delta_{jki})}, \quad (\text{D.19})$$

which once integrated over s gives a Bessel function. Putting everything together and expanding the overall factor for large values of Δ_k , one gets

$$\sum_k C_{ijk}^2 4^{\Delta_k} \sqrt{\frac{\Delta_k}{\pi}} K_{2\Delta_{ij}}(2\Delta_k \sqrt{1-z}) \sim (1-z)^{-\Delta_i - \Delta_j}, \quad (\text{D.20})$$

Then, using the Tauberian theorem from the previous section with

$$\begin{aligned} \rho(\Delta) &= \sum_k C_{ijk}^2 4^{\Delta_k - 1} \Delta_k^{\frac{3}{2} - 2\Delta_i - 2\Delta_j} \delta(\Delta - \Delta_l), \\ w_1(t) &= \frac{2}{\Gamma(2\Delta_i) \Gamma(2\Delta_j)} \left(\frac{t}{2}\right)^{2\Delta_i + 2\Delta_j - 1} K_{2\Delta_{ij}}(t) \\ w_2(t) &= 2\Delta_{ij} t^{2\Delta_{ij} - 1} \Theta(0 < x < 1), \end{aligned} \quad (\text{D.21})$$

we get

$$\sum_{\Delta_k \leq \Delta_{\max}} C_{ijk}^2 4^{\Delta_k} \sqrt{\frac{\Delta_k}{\pi}} \sim \frac{2}{(\Delta_i + \Delta_j) \Gamma(2\Delta_i) \Gamma(2\Delta_j)} \Delta_{\max}^{2\Delta_i + 2\Delta_j}. \quad (\text{D.22})$$

Assuming again a power law behavior, this gives the asymptotics of C_{ijk}

$$C_{ijk} \sim 2^{-\Delta_k} \Delta_k^{\Delta_i + \Delta_j - 3/4}, \quad (\text{D.23})$$

which is consistent with the large order behaviour that we find with GFF OPE coefficients.

Let us now focus on the case $d = 2$. In this case, the blocks factorize into a product of two one-dimensional blocks, which allows us to apply the logic that we used for $d = 1$ to the two sectors separately. Consider the four-point function of two sets of identical primary operators in the specific $d = 2$ configuration $\mathbf{x}_1 \rightarrow 0$, $\mathbf{x}_2 \rightarrow (\eta, \bar{\eta})$, $\mathbf{x}_3 \rightarrow (1, 1)$, and $\mathbf{x}_4 \rightarrow \infty$. This reads

$$\langle \mathcal{O}_i(0) \mathcal{O}_j(\eta, \bar{\eta}) \mathcal{O}_j(1) \mathcal{O}_i(\infty) \rangle = (\eta \bar{\eta})^{-\Delta_i - \Delta_j} \mathcal{G}(\eta, \bar{\eta}), \quad (\text{D.24})$$

with

$$\mathcal{G}(\eta, \bar{\eta}) = \sum_m C_{ijm}^2 G_{h_m, \bar{h}_m}^{ijji}(\eta, \bar{\eta}), \quad (\text{D.25})$$

and $G_{h_m, \bar{h}_m}^{ijkl}$ is defined in equation (2.63). Notably, this factorizes into holomorphic and anti-holomorphic one-dimensional blocks depending on the intermediate weights $h_m = \frac{\Delta_m + J_m}{2}$ and $\bar{h}_m = \frac{\Delta_m - J_m}{2}$. When $\eta, \bar{\eta} \rightarrow 1^-$, the expansion yields

$$\lim_{|1-\eta| \rightarrow 0^+} \langle \mathcal{O}_i(0) \mathcal{O}_j(\eta, \bar{\eta}) \mathcal{O}_j(1) \mathcal{O}_i(\infty) \rangle \sim ((1-\eta)(1-\bar{\eta}))^{-\Delta_j} \quad (\text{D.26})$$

At large Δ_m , the hypergeometric functions inside the block can be approximated by Bessel functions. To see this, we apply the approximation from equation (D.20) to both the h_m and \bar{h}_m parts. Substituting this into the expansion, we get

$$\sum_m C_{ijm}^2 \frac{4^{\Delta_m}}{(1 + \delta_{J_m, 0})} \frac{\sqrt{h_m \bar{h}_m}}{\pi} \left[K_{2\Delta_{ij}}(2h_m \sqrt{1-\eta}) K_{2\Delta_{ij}}(2\bar{h}_m \sqrt{1-\bar{\eta}}) + (\eta \leftrightarrow \bar{\eta}) \right] \sim ((1-\eta)(1-\bar{\eta}))^{-\frac{\Delta_i - \Delta_j}{2}} \quad (\text{D.27})$$

Next, we use the Tauberian theorem to relate the divergence as $\eta, \bar{\eta} \rightarrow 1$ to the asymptotic sum over the large weights $h_m, \bar{h}_m \rightarrow \infty$. Let us consider explicitly the double sum over the holomorphic and anti-holomorphic weights up to cutoffs h_{\max} and \bar{h}_{\max} :

$$\sum_{h_m \leq h_{\max}, \bar{h}_m \leq \bar{h}_{\max}} C_{ijm}^2 4^{\Delta_m} \frac{\sqrt{h_m \bar{h}_m}}{\pi} \sim \left(\frac{2}{(\Delta_i + \Delta_j) \Gamma(2\Delta_i) \Gamma(2\Delta_j)} \right)^2 h_{\max}^{\Delta_i + \Delta_j} \bar{h}_{\max}^{\Delta_i + \Delta_j}. \quad (\text{D.28})$$

Assuming again a power law behavior for the squared OPE coefficients C_{ijm}^2 , we can deduce the asymptotic behavior of C_{ijm} in the case $d = 2$:

$$C_{ijm} \sim \# 2^{-\Delta_m} (h_m \bar{h}_m)^{\frac{\Delta_i + \Delta_j}{2} - \frac{3}{4}}. \quad (\text{D.29})$$

Focusing specifically at the scalar sector, where $h_m = \bar{h}_m = \Delta_m/2$, this gives

$$C_{ijm} \sim \# 2^{-\Delta_m} \Delta_m^{\Delta_i + \Delta_j - \frac{3}{2}}, \quad (\text{D.30})$$

which matches with the asymptotic behavior of the GFF OPE coefficients in $d = 2$.

Given the results obtained for $d = 1$ and $d = 2$, we can guess the asymptotic behavior of the OPE coefficients in generic dimension to be

$$C_{ijm} \sim \# 2^{-\Delta_m} \Delta_m^{\Delta_i + \Delta_j - \frac{3d}{4}}, \quad (\text{D.31})$$

which matches with the GFF result for any value of d .

E QFT data of free scalar and free tensor

In section 4, we present checks of the flow equations in the theories of a free scalar and a free tensor. In such theories, the coupling of the deformation is the mass in units of the AdS radius, $\lambda = \frac{1}{2}m^2R^2$. Since the theories are free, we know the QFT data for any value of λ . For simplicity, we parametrize the QFT data in terms of the scaling dimension of the elementary boundary primary.

E.1 Free scalar theory

E.1.1 Scaling dimensions

For the free scalar, with action (4.6), the dimension of the elementary boundary primary ϕ is

$$\Delta_\phi(\lambda) = \frac{d}{2} \pm \sqrt{\frac{d^2}{4} + 2\lambda} \quad (\text{E.1})$$

and double trace operators have dimensions

$$\Delta_{[\phi^2]_{n,l}} = 2\Delta_\phi + 2n + l \quad (\text{E.2})$$

E.1.2 BOE coefficients

We use two types of BOE coefficients in our checks: the one which appears in the expansion of the bulk elementary field $\hat{\phi}$ into the boundary primary ϕ

$$b_\phi^{\hat{\phi}} = \sqrt{\frac{\Gamma(\Delta_\phi)}{2\pi^{\frac{d}{2}}\Gamma(\Delta_\phi - \frac{d-1}{2})}}, \quad (\text{E.3})$$

which can be for example fixed by decomposing the canonically normalized massive bulk-bulk propagator into the bulk-bulk blocks (2.42); and the coefficients appearing in the expansion of $\hat{\phi}^2$ into boundary scalar double trace primaries [88]

$$b_{[\phi^2]_{n,0}}^{\hat{\phi}^2} = \sqrt{\frac{(2(\Delta_\phi + n) - \frac{d}{2})\Gamma(\Delta_\phi + n)\Gamma(2(\Delta_\phi + n))\Gamma(\Delta_\phi - \frac{d-1}{2} + n)\Gamma(2\Delta_\phi - \frac{d}{2} + n)(\frac{d}{2})_n}{(2\pi)^d n! \Gamma(\Delta_\phi + \frac{1}{2} + n)\Gamma(\Delta_\phi - \frac{d-2}{2} + n)\Gamma(2\Delta_\phi - d + 1 + n)\Gamma(2(\Delta_\phi + n) - \frac{d-2}{2})}}, \quad (\text{E.4})$$

which can be extracted from the spectral decomposition of the bulk two-point function of $\hat{\phi}^2$.

E.1.3 OPE coefficients

Some OPE coefficients of free scalar theory are available in the literature. For example, [89]

$$C_{\phi\phi[\phi^2]_{n,s}} = \frac{(-1)^n 2^{\frac{s+1}{2}} (\Delta_\phi)_{n+s} (\Delta_\phi - \frac{d-2}{2})_n}{\sqrt{n!s! (\frac{d}{2} + s)_n (2\Delta_\phi + n - d + 1)_n (2\Delta_\phi - \frac{d}{2} + n + s)_n (2\Delta_\phi + 2n + s - 1)_s}}. \quad (\text{E.5})$$

In AdS₃, we are using the normalization of Osborn [40], hence we have

$$\left(C_{\phi\phi[\phi^2]_{n,s}}^{(\text{AdS}_3)}\right)^2 = \left(-\frac{1}{2}\right)^s \times (\text{E.5}). \quad (\text{E.6})$$

We also needed the OPE coefficients $C_{\phi^2[\phi^2]_n[\phi^2]_m}$. To compute them, we started from the three-point function $\langle \hat{\phi}^2(X_1)\hat{\phi}^2(X_2)\phi(P_3) \rangle$ in terms of Wick contractions and compared its expansion near the boundary to the expansion into bulk-bulk-boundary blocks (2.55). Using the knowledge of $b_{[\phi^2]_n}^{\hat{\phi}^2}$ (E.4), we obtained

$$\begin{aligned} & C_{\phi^2[\phi^2]_{n,0}[\phi^2]_{m,0}} \\ &= \frac{\left(b_{[\phi^2]_n}^{\hat{\phi}^2} b_{[\phi^2]_m}^{\hat{\phi}^2}\right)^{-1} (-1)^{n+m} \sqrt{2}\Gamma(\Delta_\phi)^2 (\Delta_\phi)_m (\Delta_\phi)_n (\Delta_\phi)_{n+m} (\Delta_\phi - \frac{d-2}{2})_{m+n}}{m!n!\pi^d \Gamma(\Delta_\phi - \frac{d-2}{2})^2 (\Delta_\phi - \frac{d-2}{2})_m (\Delta_\phi - \frac{d-2}{2})_n (2\Delta_\phi - \frac{d}{2} + m)_m (2\Delta_\phi - \frac{d}{2} + n)_n} \end{aligned} \quad (\text{E.7})$$

Some more checks we performed in free theories involved $\frac{d\Delta_\phi^m}{d\lambda}$ for various values of $m \in \mathbb{N}$. The required OPE coefficients can be computed easily in terms of $C_{\phi\phi[\phi^2]_n}$ as follows: consider the three-point function

$$\frac{1}{m!} \langle \phi^m(P_1)\phi^m(P_2)\hat{\phi}^2(X) \rangle = m \langle \phi(P_1)\phi(P_2) \rangle^{m-1} \langle \phi(P_1)\phi(P_2)\hat{\phi}^2(X) \rangle, \quad (\text{E.8})$$

where the $(m!)^{-1}$ is there to ensure proper normalization of the boundary operators, such that the two-point function is unit normalized

$$\frac{1}{m!} \langle \phi^m(P_1)\phi^m(P_2) \rangle = \langle \phi(P_1)\phi(P_2) \rangle^m = \frac{1}{P_{12}^{m\Delta_\phi}}. \quad (\text{E.9})$$

Then, comparing the bulk-boundary-boundary expansion of the two sides (2.45), we find

$$C_{\phi^m\phi^m[\phi^2]_n} = m C_{\phi\phi[\phi^2]_n}. \quad (\text{E.10})$$

E.2 Free tensor theory

E.2.1 Scaling dimensions

In the free traceless symmetric tensor theory, with action (4.11), the boundary elementary field h_{ab} has dimensions related to the mass $\lambda = \frac{1}{2}m^2R^2$ as

$$\Delta_h(\lambda) = \frac{d}{2} \pm \sqrt{\frac{d^2}{4} + 2\lambda}. \quad (\text{E.11})$$

The bulk field implementing the mass deformation, $\hat{h}^2 \equiv \hat{h}^{\mu\nu}\hat{h}_{\mu\nu}$, has in its BOE an infinite set of scalar double trace primaries $[h^2]_{n,0}$ with dimensions

$$\Delta_{[h^2]_{n,0}} = 2\Delta_h + 2n \quad (\text{E.12})$$

We will focus on the case of $d = 3$.

E.2.2 BOE×OPE coefficients

In this case we will only ever need a product of BOE coefficients and OPE coefficients, $b_{[h^2]_{n,0}}^{\hat{h}^2} C_{hh[h^2]_{n,0}}^{(m)}$ where $m = 0, 1, 2$ labels the different tensor structures in the boundary three-point function $\langle h^{(2)}(P_1, Z_1)h^{(2)}(P_2, Z_2)[h^2]_{n,0}(P_3) \rangle$, where $h^{(2)}$ is the boundary elementary tensor with indices contracted by polarization tensors

$$h^{(2)}(P, Z) \equiv Z_A Z_B h^{AB}(P). \quad (\text{E.13})$$

To get this QFT data, we compute the three-point function $\langle h^{(2)}(P_1, Z_1)h^{(2)}(P_2, Z_2)\hat{h}^2(X) \rangle$ from Wick contractions in the special frame

$$\begin{aligned} P_1 &= \left(\frac{1}{2}, \mathbf{0}, \frac{1}{2} \right), & P_2 &= \left(\frac{1}{2}, \mathbf{0}, -\frac{1}{2} \right), & Z_1 &= (0, \mathbf{z}_1, 0), & Z_2 &= (0, \mathbf{z}_2, 0) \\ X &= \left(\frac{2+z^2}{2z}, \frac{\hat{\mathbf{x}}^1}{z}, -\frac{1}{2z} \right) \end{aligned} \quad (\text{E.14})$$

Using the bulk-boundary propagators of a free massive spin 2 field from [90], we get

$$\begin{aligned} &\langle h^{(2)}(0, \mathbf{z}_1)h^{(2)}(\infty, \mathbf{z}_2)\hat{h}^2(z, \hat{\mathbf{x}}^1) \rangle \\ &= \frac{(\Delta_h + 1)\Gamma(\Delta_h - 1)}{\Gamma(\Delta_h - \frac{1}{2})\pi^{\frac{3}{2}}} \left(\frac{z^2}{1+z^2} \right)^{\Delta_h} \left(\mathbf{z}_1 \cdot \mathbf{z}_2 - 2\frac{\mathbf{z}_1^1 \mathbf{z}_2^1}{z^2 + 1} \right)^2 \end{aligned} \quad (\text{E.15})$$

We compare the $z \rightarrow 0$ expansion of this expression to the same expansion applied to the basis decomposition (2.48) in the same frame, and extract the product of BOE and OPE coefficients:

$$\begin{aligned} b_{[h^2]_{n,0}}^{\hat{h}^2} C_{hh[h^2]_{n,0}}^{(0)} &= \frac{f_n(\Delta_h)}{24(n + \Delta_h)^2(n + 1 + \Delta_h)^2} b_{[h^2]_{n,0}}^{\hat{h}^2} C_{hh[h^2]_{n,0}}^{(2)}, \\ b_{[h^2]_{n,0}}^{\hat{h}^2} C_{hh[h^2]_{n,0}}^{(1)} &= \frac{5(3(\Delta_h + 1)^2 + n(6 - 8\Delta_h) - 4n^2)}{6(\Delta_h + n + 1)^2} b_{[h^2]_{n,0}}^{\hat{h}^2} C_{hh[h^2]_{n,0}}^{(2)}, \\ b_{[h^2]_{n,0}}^{\hat{h}^2} C_{hh[h^2]_{n,0}}^{(2)} &= \frac{8(-1)^n \Gamma(\Delta_h - 1) ((\Delta_h + 1)_{n+1})^2}{35\pi^{\frac{3}{2}} (\Delta_h + 1)n! \Gamma(\Delta_h - \frac{1}{2})(2\Delta_h + n - \frac{3}{2})_n}, \end{aligned} \quad (\text{E.16})$$

where

$$\begin{aligned} f_n(\Delta_h) &= 7 \left(8n^4 + 3\Delta_h^2(\Delta_h + 1)^2 + 8n^3(4\Delta_h - 3) \right. \\ &\quad \left. - 2n\Delta_h(6 + \Delta_h)(4\Delta_h - 3) + 2n^2(9 + 2\Delta_h(7\Delta_h - 18)) \right), \end{aligned} \quad (\text{E.17})$$

and we isolated each contribution by taking traces using (A.28).

References

- [1] M. Loparco, G. Mathys, J. Penedones, J. Qiao, and X. Zhao, “QFT as a set of ODEs,” [arXiv:2601.04310 \[hep-th\]](#).
- [2] Z. Davoudi, E. T. Neil, *et al.*, “Report of the Snowmass 2021 Topical Group on Lattice Gauge Theory,” [arXiv:2209.10758 \[hep-lat\]](#).
- [3] A. L. Fitzpatrick and E. Katz, “Snowmass White Paper: Hamiltonian Truncation,” [arXiv:2201.11696 \[hep-th\]](#).
- [4] M. Kruczenski, J. Penedones, and B. C. van Rees, “Snowmass White Paper: S-matrix Bootstrap,” [arXiv:2203.02421 \[hep-th\]](#).
- [5] Y. He and M. Kruczenski, “The Gauge Theory Bootstrap: Computing Pion amplitudes and low energy parameters from QCD,” *PoS CD2024* (2026) 040.
- [6] Y. He and M. Kruczenski, “The Gauge Theory Bootstrap: Predicting pion dynamics from QCD,” [arXiv:2505.19332 \[hep-th\]](#).
- [7] Y. He and M. Kruczenski, “Bootstrapping gauge theories,” *Phys. Rev. Lett.* **133** (2024) 191601, [arXiv:2309.12402 \[hep-th\]](#).
- [8] Y. He and M. Kruczenski, “Gauge Theory Bootstrap: Pion amplitudes and low energy parameters,” [arXiv:2403.10772 \[hep-th\]](#).
- [9] A. Guerrieri, K. Häring, and N. Su, “From data to the analytic S-matrix: A Bootstrap fit of the pion scattering amplitude,” *SciPost Phys.* **20** no. 2, (2026) 034, [arXiv:2410.23333 \[hep-th\]](#).
- [10] J. Albert and L. Rastelli, “Bootstrapping pions at large N,” *JHEP* **08** (2022) 151, [arXiv:2203.11950 \[hep-th\]](#).
- [11] J. Albert and L. Rastelli, “Bootstrapping pions at large N. Part II. Background gauge fields and the chiral anomaly,” *JHEP* **09** (2024) 039, [arXiv:2307.01246 \[hep-th\]](#).
- [12] J. Albert, D. Kosva, and L. Rastelli, “Bootstrapping Pion Form Factors at Large N ,” [arXiv:2606.19420 \[hep-th\]](#).
- [13] C. Behan, “Conformal manifolds: ODEs from OPEs,” *JHEP* **03** (2018) 127, [arXiv:1709.03967 \[hep-th\]](#).
- [14] S. Hollands and R. M. Wald, “The Operator Product Expansion in Quantum Field Theory,” [arXiv:2312.01096 \[hep-th\]](#).
- [15] C. G. Callan, Jr. and F. Wilczek, “INFRARED BEHAVIOR AT NEGATIVE CURVATURE,” *Nucl. Phys. B* **340** (1990) 366–386.
- [16] D. Mazac and M. F. Paulos, “The analytic functional bootstrap. Part I: 1D CFTs and 2D S-matrices,” *JHEP* **02** (2019) 162, [arXiv:1803.10233 \[hep-th\]](#).
- [17] M. Hogervorst, M. Meineri, J. Penedones, and K. S. Vaziri, “Hamiltonian truncation in Anti-de Sitter spacetime,” *JHEP* **08** (2021) 063, [arXiv:2104.10689 \[hep-th\]](#).
- [18] A. Antunes, M. S. Costa, J. Penedones, A. Salgarkar, and B. C. van Rees, “Towards bootstrapping RG flows: sine-Gordon in AdS,” *JHEP* **12** (2021) 094, [arXiv:2109.13261 \[hep-th\]](#).
- [19] A. Antunes, E. Lauria, and B. C. van Rees, “A bootstrap study of minimal model deformations,” *JHEP* **05** (2024) 027, [arXiv:2401.06818 \[hep-th\]](#).

- [20] A. Antunes, N. Levine, and M. Meineri, “Demystifying integrable QFTs in AdS: No-go theorems for higher-spin charges,” [arXiv:2502.06937 \[hep-th\]](#).
- [21] D. Bason, C. Copetti, L. Di Pietro, Z. Ji, and S. Komatsu, “F-theorem for Quantum Field Theories in Anti-de Sitter Space,” [arXiv:2512.18392 \[hep-th\]](#).
- [22] D. Carmi, L. Di Pietro, and S. Komatsu, “A Study of Quantum Field Theories in AdS at Finite Coupling,” *JHEP* **01** (2019) 200, [arXiv:1810.04185 \[hep-th\]](#).
- [23] C. Copetti, L. Di Pietro, Z. Ji, and S. Komatsu, “Taming Mass Gaps with Anti-de Sitter Space,” *Phys. Rev. Lett.* **133** no. 8, (2024) 081601, [arXiv:2312.09277 \[hep-th\]](#).
- [24] O. Aharony, M. Berkooz, D. Tong, and S. Yankielowicz, “Confinement in Anti-de Sitter Space,” *JHEP* **02** (2013) 076, [arXiv:1210.5195 \[hep-th\]](#).
- [25] N. Levine and M. F. Paulos, “Bootstrapping bulk locality. Part I: Sum rules for AdS form factors,” *JHEP* **01** (2024) 049, [arXiv:2305.07078 \[hep-th\]](#).
- [26] M. Meineri, J. Penedones, and T. Spirig, “Renormalization group flows in AdS and the bootstrap program,” [arXiv:2305.11209 \[hep-th\]](#).
- [27] N. Levine and M. F. Paulos, “Bootstrapping bulk locality. Part II: Interacting functionals,” [arXiv:2408.00572 \[hep-th\]](#).
- [28] M. Loparco, G. Mathys, J. Penedones, J. Qiao, and X. Zhao, “Locality constraints in AdS₂ without parity,” [arXiv:2511.20749 \[hep-th\]](#).
- [29] M. F. Paulos, J. Penedones, J. Toledo, B. C. van Rees, and P. Vieira, “The S-matrix bootstrap. Part I: QFT in AdS,” *JHEP* **11** (2017) 133, [arXiv:1607.06109 \[hep-th\]](#).
- [30] J. Penedones, “Writing CFT correlation functions as AdS scattering amplitudes,” *JHEP* **03** (2011) 025, [arXiv:1011.1485 \[hep-th\]](#).
- [31] L. Susskind, “Holography in the flat space limit,” *AIP Conf. Proc.* **493** no. 1, (1999) 98–112, [arXiv:hep-th/9901079](#).
- [32] J. Polchinski, “S matrices from AdS space-time,” [arXiv:hep-th/9901076](#).
- [33] E. Hijano, “Flat space physics from AdS/CFT,” *JHEP* **07** (2019) 132, [arXiv:1905.02729 \[hep-th\]](#).
- [34] S. Komatsu, M. F. Paulos, B. C. Van Rees, and X. Zhao, “Landau diagrams in AdS and S-matrices from conformal correlators,” *JHEP* **11** (2020) 046, [arXiv:2007.13745 \[hep-th\]](#).
- [35] Y.-Z. Li, “Notes on flat-space limit of AdS/CFT,” *JHEP* **09** (2021) 027, [arXiv:2106.04606 \[hep-th\]](#).
- [36] L. Córdova, Y. He, and M. F. Paulos, “From conformal correlators to analytic S-matrices: CFT₁/QFT₂,” *JHEP* **08** (2022) 186, [arXiv:2203.10840 \[hep-th\]](#).
- [37] B. C. van Rees and X. Zhao, “Quantum Field Theory in AdS Space instead of Lehmann-Symanzik-Zimmerman Axioms,” *Phys. Rev. Lett.* **130** no. 19, (2023) 191601, [arXiv:2210.15683 \[hep-th\]](#).
- [38] B. C. van Rees and X. Zhao, “Flat-space Partial Waves From Conformal OPE Densities,” [arXiv:2312.02273 \[hep-th\]](#).
- [39] M. S. Costa, J. Penedones, D. Poland, and S. Rychkov, “Spinning Conformal Correlators,” *JHEP* **11** (2011) 071, [arXiv:1107.3554 \[hep-th\]](#).

- [40] H. Osborn, “Conformal Blocks for Arbitrary Spins in Two Dimensions,” *Phys. Lett. B* **718** (2012) 169–172, [arXiv:1205.1941 \[hep-th\]](#).
- [41] P. Kravchuk and D. Simmons-Duffin, “Counting Conformal Correlators,” *JHEP* **02** (2018) 096, [arXiv:1612.08987 \[hep-th\]](#).
- [42] J. Penedones, E. Trevisani, and M. Yamazaki, “Recursion Relations for Conformal Blocks,” *JHEP* **09** (2016) 070, [arXiv:1509.00428 \[hep-th\]](#).
- [43] M. S. Costa, T. Hansen, J. Penedones, and E. Trevisani, “Radial expansion for spinning conformal blocks,” *JHEP* **07** (2016) 057, [arXiv:1603.05552 \[hep-th\]](#).
- [44] R. S. Erramilli, L. V. Iliesiu, and P. Kravchuk, “Recursion relation for general 3d blocks,” *JHEP* **12** (2019) 116, [arXiv:1907.11247 \[hep-th\]](#).
- [45] R. S. Erramilli, L. V. Iliesiu, P. Kravchuk, W. Landry, D. Poland, and D. Simmons-Duffin, “blocks_3d: software for general 3d conformal blocks,” *JHEP* **11** (2021) 006, [arXiv:2011.01959 \[hep-th\]](#).
- [46] D. Poland, S. Rychkov, and A. Vichi, “The Conformal Bootstrap: Theory, Numerical Techniques, and Applications,” *Rev. Mod. Phys.* **91** (2019) 015002, [arXiv:1805.04405 \[hep-th\]](#).
- [47] G. A. Baker and P. Graves-Morris, *Padé Approximants*. Encyclopedia of Mathematics and its Applications. Cambridge University Press, 2 ed., 1996.
- [48] H. Stahl, “Orthogonal polynomials with complex-valued weight function, i,” *Constructive Approximation* **2** (1986) 225–240. <https://api.semanticscholar.org/CorpusID:120504673>.
- [49] H. Stahl, “The convergence of padé approximants to functions with branch points,” *Journal of Approximation Theory* **91** (1997) 139–204. <https://api.semanticscholar.org/CorpusID:122298118>.
- [50] R. E. A. C. Paley and A. Zygmund, “On some series of functions, (1),” *Mathematical Proceedings of the Cambridge Philosophical Society* **26** no. 3, (1930) 337–357.
- [51] R. E. A. C. Paley and A. Zygmund, “On some series of functions, (3),” *Mathematical Proceedings of the Cambridge Philosophical Society* **28** no. 2, (1932) 190–205.
- [52] J. M. Deutsch, “Eigenstate thermalization hypothesis,” *Rept. Prog. Phys.* **81** no. 8, (2018) 082001, [arXiv:1805.01616 \[quant-ph\]](#).
- [53] J. Maldacena, D. Simmons-Duffin, and A. Zhiboedov, “Looking for a bulk point,” *JHEP* **01** (2017) 013, [arXiv:1509.03612 \[hep-th\]](#).
- [54] D. Li, D. Meltzer, and D. Poland, “Conformal Bootstrap in the Regge Limit,” *JHEP* **12** (2017) 013, [arXiv:1705.03453 \[hep-th\]](#).
- [55] D. B. Kaplan, J.-W. Lee, D. T. Son, and M. A. Stephanov, “Conformality Lost,” *Phys. Rev. D* **80** (2009) 125005, [arXiv:0905.4752 \[hep-th\]](#).
- [56] V. Gorbenko, S. Rychkov, and B. Zan, “Walking, Weak first-order transitions, and Complex CFTs,” *JHEP* **10** (2018) 108, [arXiv:1807.11512 \[hep-th\]](#).
- [57] V. Gorbenko, S. Rychkov, and B. Zan, “Walking, Weak first-order transitions, and Complex CFTs II. Two-dimensional Potts model at $Q > 4$,” *SciPost Phys.* **5** no. 5, (2018) 050, [arXiv:1808.04380 \[hep-th\]](#).

- [58] J. von Neuman and E. Wigner, “Über merkwürdige diskrete Eigenwerte. Über das Verhalten von Eigenwerten bei adiabatischen Prozessen,” *Physikalische Zeitschrift* **30** (Jan., 1929) 467–470.
- [59] E. Lauria, M. N. Milam, and B. C. van Rees, “Perturbative RG flows in AdS. An étude,” *JHEP* **03** (2024) 005, [arXiv:2309.10031 \[hep-th\]](#).
- [60] R. Ciccone, F. De Cesare, L. Di Pietro, and M. Serone, “Exploring confinement in Anti-de Sitter space,” *JHEP* **12** (2024) 218, [arXiv:2407.06268 \[hep-th\]](#). [Erratum: *JHEP* **06**, 037 (2025)].
- [61] R. Ciccone, F. De Cesare, L. Di Pietro, and M. Serone, “QCD in AdS,” [arXiv:2511.04752 \[hep-th\]](#).
- [62] R. Xiao, “Quantum Field Theory in Anti-de Sitter Spacetime,” *EPFL Master Thesis* (2026) .
- [63] B. Gabai, V. Gorbenko, and J. Qiao, “Yang-Mills Flux Tube in AdS,” [arXiv:2508.08250 \[hep-th\]](#).
- [64] B. Gabai, V. Gorbenko, and B. Offertaler, “Yang-Mills Flux Tube in AdS II: Effective String Theory,” [arXiv:2602.16694 \[hep-th\]](#).
- [65] J. Qiao, “Protected operators in non-local defect CFTs from AdS,” [arXiv:2605.13975 \[hep-th\]](#).
- [66] L. Bianchi, E. de Sabbata, and M. Meineri, “Conformal defects and Goldstone bosons in Anti-de Sitter space,” [arXiv:2605.13947 \[hep-th\]](#).
- [67] A. Athenodorou and M. Teper, “SU(N) gauge theories in 2+1 dimensions: glueball spectra and k-string tensions,” *JHEP* **02** (2017) 015, [arXiv:1609.03873 \[hep-lat\]](#).
- [68] T. Appelquist and D. Nash, “Critical Behavior in (2+1)-dimensional QCD,” *Phys. Rev. Lett.* **64** (1990) 721.
- [69] S. Giombi and H. Khanchandani, “CFT in AdS and boundary RG flows,” *JHEP* **11** (2020) 118, [arXiv:2007.04955 \[hep-th\]](#).
- [70] S. Giombi and Z. Sun, “Higher loops in AdS: applications to boundary CFT,” *JHEP* **12** (2025) 011, [arXiv:2506.14699 \[hep-th\]](#).
- [71] J. Csipes and P. Vaško, “O(N) BCFT: new data from conformal partial wave expansions,” [arXiv:2606.14733 \[hep-th\]](#).
- [72] F. Kos, D. Poland, D. Simmons-Duffin, and A. Vichi, “Precision Islands in the Ising and O(N) Models,” *JHEP* **08** (2016) 036, [arXiv:1603.04436 \[hep-th\]](#).
- [73] D. Carmi, R. Ciccone, and S. Sukholski, “Closing the loop on Φ^4 in AdS₃,” [arXiv:2606.06589 \[hep-th\]](#).
- [74] J. Dujava and P. Vaško, “Finite-coupling spectrum of O(N) model in AdS,” *JHEP* **12** (2025) 036, [arXiv:2503.16345 \[hep-th\]](#).
- [75] L. Iliesiu, F. Kos, D. Poland, S. S. Pufu, and D. Simmons-Duffin, “Bootstrapping 3D Fermions with Global Symmetries,” *JHEP* **01** (2018) 036, [arXiv:1705.03484 \[hep-th\]](#).
- [76] S. Giombi, C. Sleight, and M. Taronna, “Spinning AdS Loop Diagrams: Two Point Functions,” *JHEP* **06** (2018) 030, [arXiv:1708.08404 \[hep-th\]](#).
- [77] O. Diatlyk, S. Giombi, and Z. Sun, “Boundary criticality in the Gross-Neveu-Yukawa model at higher orders,” [arXiv:2606.07510 \[hep-th\]](#).

- [78] T. W. Appelquist, M. J. Bowick, D. Karabali, and L. C. R. Wijewardhana, “Spontaneous Chiral Symmetry Breaking in Three-Dimensional QED,” *Phys. Rev. D* **33** (1986) 3704.
- [79] L. Di Pietro, Z. Komargodski, I. Shamir, and E. Stamou, “Quantum Electrodynamics in $d=3$ from the ε Expansion,” *Phys. Rev. Lett.* **116** no. 13, (2016) 131601, [arXiv:1508.06278 \[hep-th\]](#).
- [80] N. Karthik and R. Narayanan, “No evidence for bilinear condensate in parity-invariant three-dimensional QED with massless fermions,” *Phys. Rev. D* **93** no. 4, (2016) 045020, [arXiv:1512.02993 \[hep-lat\]](#).
- [81] F. De Cesare and S. Giombi, “Conformal QED in AdS as a BCFT,”.
- [82] Ankur, D. Carmi, and L. Di Pietro, “Scalar QED in AdS,” *JHEP* **10** (2023) 089, [arXiv:2306.05551 \[hep-th\]](#).
- [83] Ankur, L. Di Pietro, V. Gorbenko, S. Komatsu, and V. Sacchi, “Dressing and Screening in Anti-de Sitter,” [arXiv:2601.04321 \[hep-th\]](#).
- [84] L. Di Pietro, S. C. Lanza, and P. Niro, “Symmetry breaking in QED₃ from Anti-de Sitter Space.” Work in progress, 2026.
- [85] L. Di Pietro, S. R. Kousvos, M. Meineri, A. Piazza, M. Serone, and A. Vichi, “A Bootstrap Study of Confinement in AdS,” [arXiv:2512.00150 \[hep-th\]](#).
- [86] I. Burić, F. Mangialardi, F. Russo, V. Schomerus, and A. Vichi, “Thermal One-point Functions and Asymptotic CFT Data: QFT in AdS,” [arXiv:2606.17167 \[hep-th\]](#).
- [87] J. Qiao and S. Rychkov, “A tauberian theorem for the conformal bootstrap,” *JHEP* **12** (2017) 119, [arXiv:1709.00008 \[hep-th\]](#).
- [88] A. L. Fitzpatrick, E. Katz, D. Poland, and D. Simmons-Duffin, “Effective Conformal Theory and the Flat-Space Limit of AdS,” *JHEP* **07** (2011) 023, [arXiv:1007.2412 \[hep-th\]](#).
- [89] A. L. Fitzpatrick and J. Kaplan, “Unitarity and the Holographic S-Matrix,” *JHEP* **10** (2012) 032, [arXiv:1112.4845 \[hep-th\]](#).
- [90] M. S. Costa, V. Gonçalves, and J. Penedones, “Spinning AdS Propagators,” *JHEP* **09** (2014) 064, [arXiv:1404.5625 \[hep-th\]](#).